

## Supporting Information

### **Bioaccumulation, Biotransformation, and Synergistic Effects of Binary Fungicide Mixtures in *Hyalella azteca* and *Gammarus pulex*: How Different/Similar Are the Two Species?**

Qiuguo Fu,<sup>†, #</sup> Andrea Rösch,<sup>†, ‡, #</sup> Davide Fedrizzi,<sup>†, §</sup> Caroline Vignet,<sup>†</sup> and Juliane Hollender<sup>†, ‡, \*</sup>

<sup>†</sup> Eawag, Swiss Federal Institute of Aquatic Science and Technology, 8600 Dübendorf, Switzerland

<sup>‡</sup> Institute of Biogeochemistry and Pollutant Dynamics, ETH Zürich, 8092 Zürich, Switzerland

<sup>§</sup> Department of Plant and Environmental Sciences, University of Copenhagen, 1871 Frederiksberg C, Denmark

<sup>#</sup> Qiuguo Fu and Andrea Rösch contributed equally to this work.

Corresponding author: [juliane.hollender@eawag.ch](mailto:juliane.hollender@eawag.ch)

Total pages: 70

Number of Supplementary Tables: 18

Number of Supplementary Figures: 7

## Contents

SI. A	Chemicals and Solutions .....	3
SI. B	<i>Hyalella azteca</i> and <i>Gammarus pulex</i> Cultivation .....	4
SI. C	Sampling during the <i>H. azteca</i> Kinetic Experiments.....	4
SI. D	Quality Control.....	4
SI. E	Biotransformation Product Identification in <i>H. azteca</i> by Suspect and Nontarget Screening using Compound Discoverer .....	5
SI. F	Modeling Bioaccumulation and Biotransformation Kinetics .....	7
SI. G	Lethal Concentrations of Azoxystrobin (LC50s) in the Presence and .....	11
SI. H	Exposure Medium Concentrations, Internal Concentrations and Bioaccumulation Factors (BAFs) for <i>H. azteca</i> .....	11
SI. I	Determination of IC <sub>50, PRZ, AZS</sub> in <i>H. azteca</i> .....	18
SI. J	Dose-Response Fitting of IC <sub>50, PRZ, AZS</sub> in <i>H. azteca</i> .....	19
SI. K	Distance moved (cm) of the Video-Tracking of <i>G. pulex</i> and <i>H. azteca</i> during 18 h prochloraz exposure .....	21
SI. L	Comparison of different <i>H. azteca</i> Sample Wet Weights for Detection and Quantification of Biotransformation Products .....	21
SI. M	Identified Biotransformation Products for Azoxystrobin and Prochloraz in <i>H. azteca</i> .....	22
	References.....	70

## SI. A Chemicals and Solutions

**Table S1: Fungicides. All standard solutions were prepared in methanol.**

Substance	CAS number	Supplier	Quality
Azoxystrobin	131860-33-8	Dr. Ehrenstorfer	99.5%
Azoxystrobin acid	1185255-09-7	HPC Standards GmbH	99%
Azoxystrobin-d4	1346606-39-0	Sigma-Aldrich	98%
Prochloraz	67747-09-5	Dr. Ehrenstorfer	98.5%
Prochloraz-d7		Dr. Ehrenstorfer	97%

**Table S2: Other chemicals and solvents.**

Substance	CAS number	Supplier	Quality
Acetic acid	64-19-7	Merck	100%
Acetonitrile	75-05-8	Acros Organics	HPLC-grade
Ammonium acetate	631-61-8	Sigma-Aldrich	> 98%
Calcium chloride	10035-04-8	Sigma-Aldrich	> 99%
Ethanol	64-17-5	Merck	Analytical grade
Formic acid	64-18-6	Merck	98-100%
Magnesium sulfate	10034-99-8	Sigma-Aldrich	> 99%
Isopropanol	67-63-0	Fisher Chemicals	> 99%
Methanol	67-56-1	Fisher Chemicals	LC-MS grade
Potassium chloride	7447-40-7	Sigma-Aldrich	> 99%
Sodium acetate trihydrate	6131-90-4	Fluka	> 99.5%
Sodium hydrogen carbonate	144-55-8	Merck	> 99%
Sodium bromide	7647-15-6	Sigma-Aldrich	> 99%

## SI. B *Hyalella azteca* and *Gammarus pulex* Cultivation

*Hyalella azteca* were kept in 1.5 L-glass beakers filled with previously aerated Borgmann water and were fed three times a week with approximately 30 mg ground fish food flasks. Each beaker contained approximately 100 organisms and a piece of cotton gauze as substrate to hold on to and hide. All beakers were placed in a water bath ( $23 \pm 1$  °C) with a 16h light/8h dark cycle. Borgmann water was changed weekly and juvenile *H. azteca* were separated from the adults and kept in separated beakers.

Borgmann water (BW) composition<sup>1</sup>:  $0.03 \text{ g L}^{-1} \text{ MgSO}_4$ ,  $0.084 \text{ g L}^{-1} \text{ NaHCO}_3$ ,  $0.0037 \text{ g L}^{-1} \text{ KCl}$ ,  $0.11 \text{ g L}^{-1} \text{ CaCl}_2$ , and  $0.001 \text{ g L}^{-1} \text{ NaBr}$ .

*Gammarus pulex* were acclimatized in an aquarium with aerated artificial pond water (APW) for 3-5 days at  $11 \pm 2$  °C and 12 h/12 h light/dark conditions. *G. pulex* were fed with horse chestnut leaves inoculated with *Cladosporium herbarum*. Detailed information on the preparation of APW and the inoculation of leaves are found elsewhere.<sup>2</sup>

Artificial pond water (APW) composition<sup>3</sup>:  $0.12 \text{ g L}^{-1} \text{ MgSO}_4 \cdot 7 \text{ H}_2\text{O}$ ,  $0.065 \text{ g L}^{-1} \text{ NaHCO}_3$ ,  $0.0058 \text{ g L}^{-1} \text{ KCl}$ , and  $0.29 \text{ g L}^{-1} \text{ CaCl}_2 \cdot 2\text{H}_2\text{O}$ .

## SI. C Sampling during the *H. azteca* Kinetic Experiments

Table S3: Sampled time-points during the azoxystrobin and prochloraz kinetic experiments.

Uptake (U) / Depuration (D)	Time [h]	Time [d]
U	0.5	0.02
U	1.5	0.06
U	2.5	0.10
U	5.5	0.23
U	9.5	0.40
U	17.5	0.73
U	24	1.00
D	24	1.00
D	25	1.04
D	26	1.08
D	28	1.17
D	31	1.29
D	35	1.46
D	42	1.75
D	50	2.08
D	65	2.71
D	95	3.96
D	119	4.96
D	144	6.00

## SI. D Quality Control

Internal standard calibration was used for quantification using Trace Finder software 3.1, 3.3 and 4.1 (Thermo Scientific). In total, 16 calibration points were prepared in a range of  $0.5\text{-}3000 \text{ ng L}^{-1}$  and the calibration curves were obtained by linear least square regression using a weighing factor of  $1/x$ . All BTPs were quantified based

on the calibration curve of the corresponding parent compound except for azoxystrobin acid (AZ\_M390b), for which a reference standard was available. Reference standards for two prochloraz BTPs (PRZ\_M282 and PRZ\_M325) were obtained after finishing the experiment and were only used for confirming the proposed structures.

Limits of Quantification (LOQ) and matrix factors were calculated according to our previous publications.<sup>2</sup>

**Table S4: Calculated matrix factors for *H. azteca* extracts and limits of quantification (LOQs) for azoxystrobin and prochloraz in *H. azteca* extracts and in the exposure medium. Duplicate samples (prespike 1 and 2) were spiked before *H. azteca* extraction with 25  $\mu\text{g L}^{-1}$  (i.e., 5 ng absolute in 200  $\mu\text{L}$  measured extract) and 50  $\mu\text{g L}^{-1}$  (i.e., 10 ng absolute in 200  $\mu\text{L}$  measured extract) of azoxystrobin and prochloraz, respectively.**

Compound	Matrix factors					LOQ*	LOQ**
	Prespike 1 5 ng	Prespike 2 5 ng	Prespike 1 10 ng	Prespike 2 10 ng	Average	[nmol kg <sub>ww</sub> <sup>-1</sup> ]	[ng L <sup>-1</sup> ]
Azoxystrobin	0.4	0.4	0.4	0.4	0.4	2.4	0.5
Prochloraz	0.6	0.6	0.6	0.6	0.6	1.7	0.5

\*: LOQ for *H. azteca* extract samples

\*\*: LOQ for medium samples

**Table S5: Relative recoveries for the whole sample preparation and analytical procedure. Duplicate samples (prespike 1 and 2) spiked before *H. azteca* extraction with 25  $\mu\text{g L}^{-1}$  (i.e., 5 ng absolute in 200  $\mu\text{L}$  measured extract) and 50  $\mu\text{g L}^{-1}$  (i.e., 10 ng absolute in 200  $\mu\text{L}$  measured extract) of the parent compounds, respectively, were used to determine the recovery of the whole procedure of sample preparation and chemical analysis.**

Compound	Relative recovery [%]			
	Prespike 1 5 ng	Prespike 2 5 ng	Prespike 1 10 ng	Prespike 2 10 ng
Azoxystrobin	101	101	104	98
Prochloraz	115	118	107	99

## SI. E Biotransformation Product Identification in *H. azteca* by Suspect and Nontarget Screening using Compound Discoverer

Compound Discoverer small molecule identification software version 2.0 (Thermo Scientific) was used for suspect and nontarget screening by comparing treatment and control samples. As control samples “exposure medium controls”, “chemical controls” (chemical positive, cotton gauze and organism negative), “organism controls” (chemical negative, organism and food positive) and “standard controls” (calibration standard) were used. “Standard controls” and “chemical controls” were additionally selected as control samples compared to the screening conducted with SIEVE software (Thermo Scientific) in our previous publications.<sup>2,4</sup> “Standard controls” account for impurities of the reference standards, and “chemical controls” provide in addition to the “exposure medium controls” evidence that BTPs are actually formed by the organisms and not due to e.g., abiotic processes in the medium. Due to a high volume to organism ratio (500 mL exposure medium containing

50 organisms) and since no additional enrichment of the exposure medium besides online-SPE was conducted, no BTPs formed by the organisms can be detected in the medium. Thus, the detection of BTPs in the exposure medium would point towards additional formation processes.

For suspect screening, the generated frame list was compared to the mass list of predicted BTPs. BTPs were predicted based on (i) *in silico* pathway prediction (Eawag-PPS, <http://eawag-bbd.ethz.ch/predict/>, Eawag-PPS predicts microbial degradation of chemicals based on biotransformation rules), (ii) *in silico* manual prediction of BTPs considering most common enzymatic biotransformation reactions, and (iii) identified BTPs of azoxystrobin and prochloraz reported in any organism in scientific literature. The mass lists for azoxystrobin and prochloraz contained 1325 and 490 predicted BTPs masses, respectively.

Framing describes the process of building regions in the  $m/z$  versus retention time plane, whereby all peaks above a given threshold are collected.

For nontarget screening, the generated frame list was filtered with (i) an integrated intensity threshold of 0.1% of the parent compound and (ii) an integrated intensity ratio between treatment and control samples of 10 (with the exception of the ratio “treatment / organisms control”, which was adjusted individually, see below).

The workflow was validated with known low concentrated BTPs detected in previous work<sup>2,4</sup> that were also detected in *H. azteca*. With the selected nontarget criteria the filtered frame list should still contain these low concentrated BTPs. The node “Fill Gaps”, included in the applied workflow, fills in areas for missing peaks or for peaks with intensities below the chosen threshold. This is done to avoid dividing by zero to be still able to form ratios with control samples, where no peak was detected. For some of these low concentrated BTPs the ratio “treatment / organisms control” was considerably smaller than 10 due to “Fill Gaps”. Therefore, the ratio “treatment / organisms control” was adopted to the observed conditions and reduced to 4 (AZ) and 3.8 (PRZ), respectively.

For both screening approaches, potential BTPs had to show increasing/decreasing intensities during the uptake/depuration phase. Moreover, Compound Discoverer allows to screen for specific isotopic patterns. Therefore, the presence of the chlorophenyl moiety (chlorine isotopic pattern) in potential BTPs that after biotransformation still contain the chlorophenyl moiety, facilitated BTP screening for prochloraz.

**Table S6: Settings used for suspect and nontarget screening with Compound Discoverer (Thermo Scientific, version 2.0).**

Retention time window	5-20 min
$m/z$ window	100-1000
Minimal number of scans per peak	3
Maximum peak width	1 min
$m/z$ tolerance	5 ppm
Peak intensity threshold	$10^6$

## SI. F Modeling Bioaccumulation and Biotransformation Kinetics

For comparison with the simultaneous fitting approach, we further applied a stepwise fitting approach to determine the uptake and elimination rate of the parent compound by fitting the simplest compartment model (see SI. F) with only two parameters ( $k_u$  and  $k_e$ , total or parent) to the internal concentration of the parent compound.

$$\frac{dC_{in,p}(t)}{dt} = C_{water}(t) \cdot k_u - C_{in,p}(t) \cdot k_e \quad \text{equation S1}$$

where  $C_{in,p}(t)$  [nmol kg<sub>ww</sub><sup>-1</sup>] is whole body internal concentration of azoxystrobin,  $C_{water}(t)$  [nmol L<sup>-1</sup>] is the time course of azoxystrobin in the exposure medium and  $k_u$  [L kg<sub>ww</sub><sup>-1</sup> d<sup>-1</sup>] and  $k_e$  [d<sup>-1</sup>] are the uptake and elimination rate constant, respectively. In this case  $k_e$  covers direct elimination of the parent compound as well as further elimination due to biotransformation.

In general, the simultaneously fitting approach of all rate constants and the stepwise fitting approach showed the same result (Figure S2 and S3) but for *H. azteca*  $k_{m,1st,total}$  seemed to contribute more to the total elimination of the parent compound compared to *G. pulex* (see Figure 2 in the corresponding publication). Although especially for *G. pulex*, elimination of azoxystrobin was overpredicted by either of the models, elimination of azoxystrobin was faster in *G. pulex* compared to *H. azteca* and consequently the smaller  $k_{m,1st,total}$  of *G. pulex* compared to those of *H. azteca* contributed less to the total elimination. Reason for the discrepancy of actual and simulated elimination could be a longer retention of azoxystrobin in any biomass component of aquatic organisms such as lipids, which is not covered by the applied simple one-compartment model assuming well-mixed organisms. However, elimination of azoxystrobin was simulated much better in *H. azteca*, although both species do not significantly deviate in their total lipid content (1.3-1.8% of wet weight),<sup>5,6</sup> indicating that the change to a more complex model such as a two-compartment model does not necessarily improve the match between experimental data and model and might be more important for more lipophilic compounds and more lipid rich organisms.<sup>7</sup>

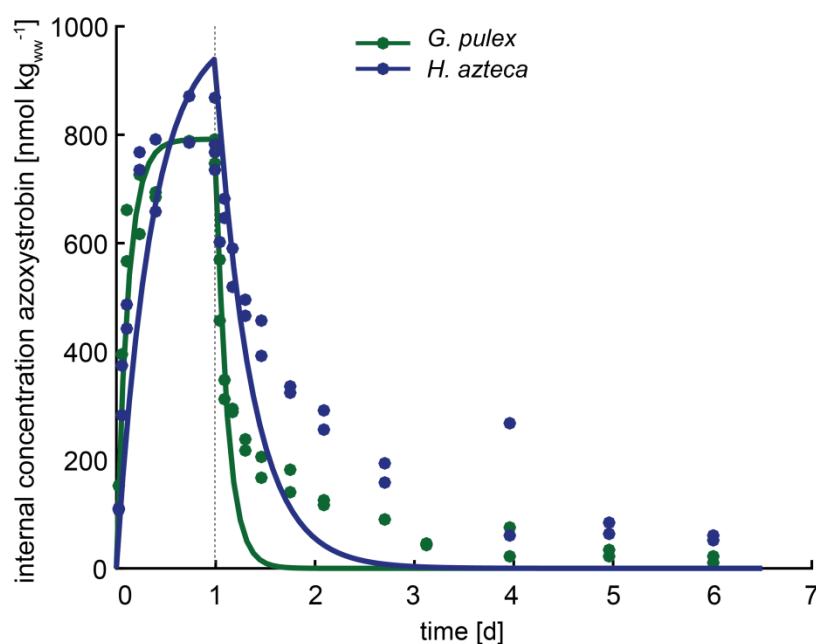


Figure S1: Uptake and depuration kinetic for azoxystrobin in *G. pulex* (green) and *H. azteca* (blue) modeled with the simplest compartment model (see equation S1). Shown are the measured (dots) and modeled (lines) time courses for azoxystrobin in *G. pulex* and *H. azteca*. The dashed vertical line indicates the change from uptake (1 d) to depuration (5 d).

Table S7: Kinetic rate constants for azoxystrobin in the two species *G. pulex* and *H. azteca* (lower and upper 95% confidence internals are given in brackets) and kinetic bioaccumulation factors (BAF<sub>k</sub>s). The simplest compartment model (see equation S1) was used for fitting the kinetic rate constants. Results are rounded to three significant digits. Two replicate internal concentrations were used per time point.

	$k_u$ [L kg <sub>ww</sub> <sup>-1</sup> d <sup>-1</sup> ]	$k_e$ [d <sup>-1</sup> ]
<b>Azoxystrobin</b>		
<i>G. pulex</i>		
BAF <sub>k</sub> AZ: 4.95 [L kg <sub>ww</sub> <sup>-1</sup> ]	42.2 [33.6; 55.7]	8.52 [6.81; 11.4]
<i>H. azteca</i>		
BAF <sub>k</sub> AZ: 5.22 [L kg <sub>ww</sub> <sup>-1</sup> ]	14.7 [9.65; 20.3]	2.82 [1.68; 4.07]

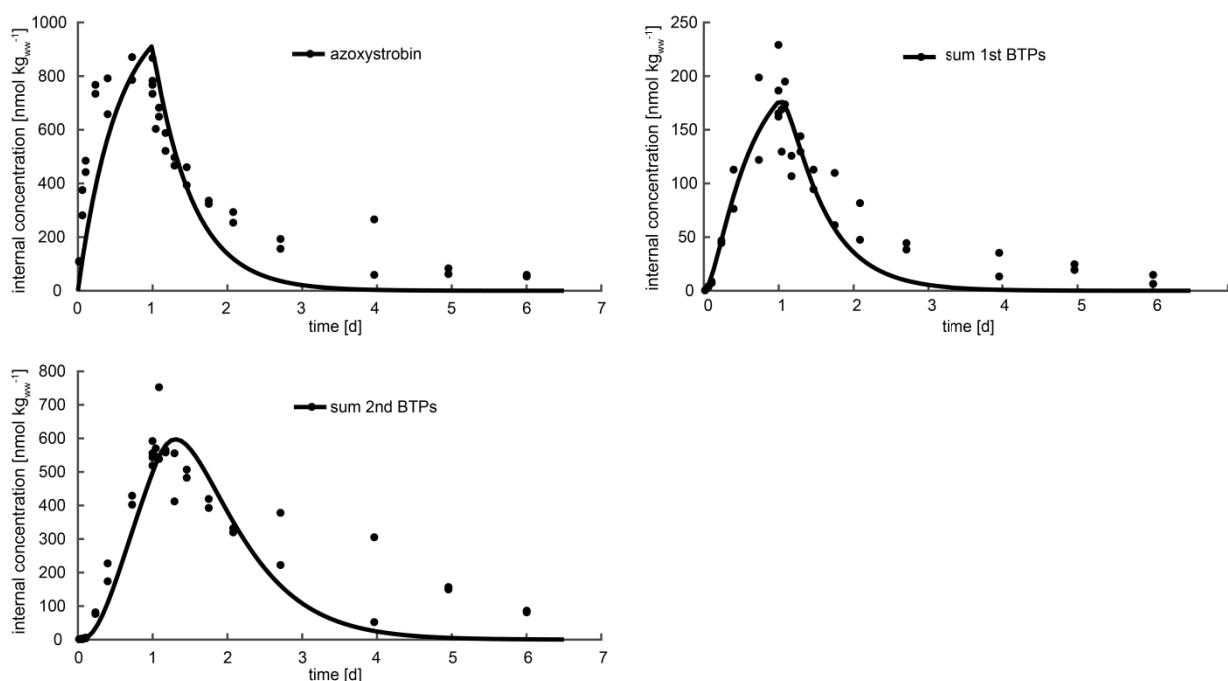
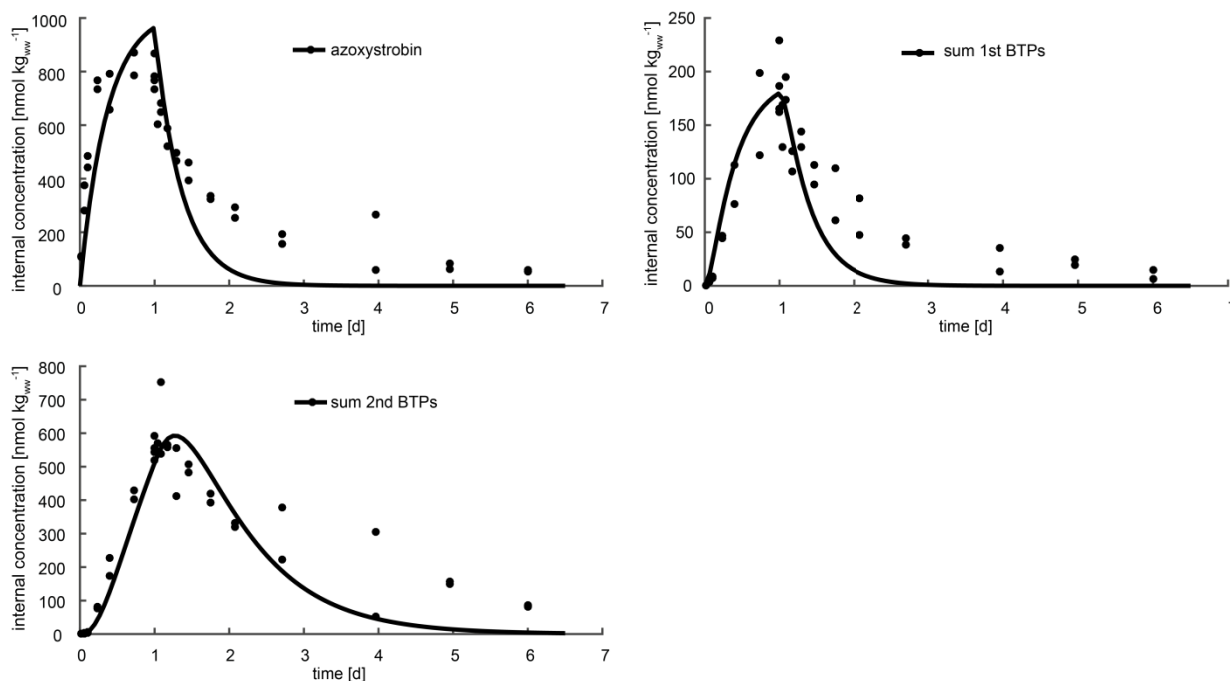


Figure S2: Measured (dots) and modeled (lines) time series of internal concentrations of azoxystrobin, the sum of 1st BTPs and the sum of 2nd BTPs in *H. azteca* in the uptake (1 d) and depuration phase (5 d) shown in separate panels. All parameters were fitted simultaneously.



**Figure S3:** Measured (dots) and modeled (lines) time series of internal concentrations of azoxystrobin, the sum of 1st BTPs and the sum of 2nd BTPs in *H. azteca* in the uptake (1 d) and depuration phase (5 d) shown in separate panels. The uptake rate  $k_u$  [ $\text{L kg}_{\text{ww}}^{-1} \text{d}^{-1}$ ] was determined in a first step by only fitting the azoxystrobin parent compound kinetic with two parameters ( $k_u$  and  $k_e$ , see equation S1) and in a second step fixing  $k_u$  ( $14.7 \text{ L kg}_{\text{ww}}^{-1} \text{d}^{-1}$ , see Table S7) and simultaneously fitting  $k_e$  and the kinetic rate constants of the sum of 1st BTPs and the sum of 2nd BTPs, respectively.

**Table S8:** Comparison of kinetic rate constants of azoxystrobin, the sum of 1st BTPs and the sum of 2nd BTPs in *H. azteca*. Kinetic rate constants were either determined by simultaneously fitting of all kinetic rate constants or with a stepwise approach, by first only fitting the azoxystrobin parent compound kinetic with two parameters ( $k_u$  and  $k_e$ , see equation S1) and in a second step fixing  $k_u$  ( $14.7 \text{ L kg}_{\text{ww}}^{-1} \text{d}^{-1}$ , see Table S7) and simultaneously fitting  $k_e$  and the kinetic rate constants of the sum of 1st BTPs and the sum of 2nd BTPs, respectively.

	simultaneously fitting of all kinetic rate constants	fixed $k_u$ ( $14.7 \text{ L kg}_{\text{ww}}^{-1} \text{d}^{-1}$ , see Table S7) and simultaneously fitting of all remaining kinetic rate constants
$k_e$ [ $\text{d}^{-1}$ ]:	0.131 [0.0001; 0.804]	0.001 [0.001; 1.77]
$k_u$ [ $\text{L kg}_{\text{ww}}^{-1} \text{d}^{-1}$ ]:	10.6 [9.40; 12.2]	-
$k_{m, 1st, total}$ [ $\text{d}^{-1}$ ]:	1.75 [1.46; 1.48]; [1.57; 2.14]	2.74 [2.40; 3.05]
$k_{m, 2nd total}$ [ $\text{d}^{-1}$ ]:	8.62 [7.60; 11.0]	6.42 [4.94; 8.14]
$k_{e, 1st, total}$ [ $\text{d}^{-1}$ ]:	0.0001 [0.0001; 4.92]	7.97 [5.90; 9.78]
$k_{em, 2nd, total}$ [ $\text{d}^{-1}$ ]:	1.85 [1.50; 2.52]	1.14 [0.69; 1.73]
<b>total elimination azoxystrobin</b> <b>[<math>\text{d}^{-1}</math>] (<math>k_e + k_{m, 1st, total}</math>):</b>	1.88	2.74
<b>fraction <math>k_{m, 1st, total}</math> on total</b> <b>elimination [%]:</b>	93.0	100
<b>BAF<sub>k</sub> AZ [<math>\text{L kg}_{\text{ww}}^{-1}</math>]:</b>	5.63	5.37

**Table S9: Internal concentration (nmol kg<sub>ww</sub><sup>-1</sup>) of azoxystrobin, prochloraz, and their BTPs in the two species during the toxicokinetic experiment.**

	<i>G. pulex</i>			<i>H. azteca</i>			<i>G. pulex</i>			<i>H. azteca</i>			
	Time [h]	AZ	AZ <sub>1<sup>st</sup></sub> BTPs	AZ <sub>2<sup>nd</sup></sub> BTPs	AZ	AZ <sub>1<sup>st</sup></sub> BTPs	AZ <sub>2<sup>nd</sup></sub> BTPs	PRZ	PRZ <sub>1<sup>st</sup></sub> BTPs	PRZ <sub>2<sup>nd</sup></sub> BTPs	PRZ	PRZ <sub>1<sup>st</sup></sub> BTPs	PRZ <sub>2<sup>nd</sup></sub> BTPs
Uptake	t0.5_1	154	3	0	110	0	0	1693	7	44	3850	6	65
	t_0.5_2	151	4	0	108	0	0	1433	2	30	3892	8	69
	t1.5_1	375	5	3	281	3	2	2973	35	69	8397	32	335
	t1.5_2	395	4	3	375	4	3	6533	47	219	7386	29	230
	t2.5_1	565	14	16	486	7	4	5998	117	506	11122	78	662
	t2.5_2	662	14	15	443	9	6	9880	142	771	10034	50	502
	t5.5_1	725	46	80	768	44	77	8066	162	1008	21521	316	2314
	t5.5_2	617	45	66	735	47	82	7933	244	1124	18018	173	1832
	t9.5_1	694	69	128	657	77	174	9943	336	2394	21270	446	3237
	t9.5_2	683	105	177	792	113	227	8800	467	2293	24340	432	3728
	t17.5_1	787	132	214	787	122	402	12345	572	5352	23996	899	6676
	t17.5_2	788	208	328	872	198	429	11593	723	5701	22448	870	6371
	t24_1	791	229	435	767	229	555	11519	612	5450	33353	1476	10526
	t24_2	748	165	303	782	162	543	11636	849	6889	22685	1239	8793
Depuration	t0_1	568	168	370	734	186	593	12106	688	7341	27075	1024	9201
	t0_2	456	169	317	868	165	519	11317	810	6631	24108	1090	8836
	t1_1	346	162	339	602	129	546	7587	465	4184	24107	948	8390
	t1_2	312	201	443	1048	169	571	8709	531	5705	20345	1157	9858
	t2_1	293	216	383	683	195	752	3755	654	4972	20931	1142	10465
	t2_2	287	215	318	648	174	538	4720	374	4064	18250	839	8069
	t4_1	238	161	290	589	107	565	2145	474	4041	13888	632	6533
	t4_2	217	102	197	520	126	558	3411	431	3535	22298	1544	12654
	t7_1	166	54	113	466	129	412	803	338	2243	8943	954	9232
	t7_2	206	150	286	496	144	557	676	463	3463	10433	1142	10242
	t11_1	141	89	201	393	113	482	341	377	2705	5112	923	7934
	t11_2	183	94	239	459	94	508	1013	562	3618	7182	807	8479
	t18_1	118	41	122	323	110	419	168	384	2282	3610	1092	9172
	t18_2	126	86	239	336	61	392	155	28	1005	2995	769	6926
	t26_1	91	70	187	255	82	332	113	136	912	1067	558	5574
	t26_2	91	21	51	292	47	320	161	110	898	1160	622	4895
	t41_1	43	63	154	193	39	377	110	112	853	604	437	3818
	t41_2	45	46	138	158	45	223	106	14	488	453	706	5150
	t71_1	77	28	40	267	35	305	139	44	426	492	552	4011
	t71_2	21	7	4	60	13	53	280	60	727	700	518	4022
	t95_1	23	21	27	83	19	149	83	30	374	442	255	2522
	t95_2	34	31	93	63	25	158	58	62	386	304	204	2469
	t120_1	11	0	0	60	6	87	117	43	276	360	182	2110
	t120_2	22	11	22	52	15	82	74	23	333	341	148	1652

## SI. G Lethal Concentrations of Azoxystrobin (LC50s) in the Presence and

**Table S10: Used azoxystrobin concentration [ $\mu\text{g L}^{-1}$ ] for the determination of  $\text{LC}_{50}\text{s}$  of azoxystrobin in the presence and absence of prochloraz based on a range defining test.**

Species	Treatment	azoxystrobin concentration [ $\mu\text{g L}^{-1}$ ]
<i>Gammarus pulex</i>	AZ	50, 100, 150, 200, 250, 300, 350
	AZ + 0.37 $\mu\text{g L}^{-1}$ PRZ	50, 100, 150, 200, 250, 300, 350
	AZ + 74 $\mu\text{g L}^{-1}$ PRZ	5, 15, 25, 35, 45, 55, 65
<i>Hyalella azteca</i>	AZ	50, 100, 150, 200, 250, 300, 400, 500, 600
	AZ + 0.37 $\mu\text{g L}^{-1}$ PRZ	50, 100, 150, 200, 250, 300, 400, 500, 600
	AZ + 74 $\mu\text{g L}^{-1}$ PRZ	25, 35, 45, 55, 65, 75, 85, 95, 105

## SI. H Exposure Medium Concentrations, Internal Concentrations and Bioaccumulation Factors (BAFs) for *H. azteca*

Tables in this section are sorted according to the order of the experiments in the *Materials and Methods*. BAFs reported in this section are based on the ratio of the concentration of the parent compound in the organisms and of the concentration of the parent compound in the exposure medium with the requirement of steady state (see equation 4 in the corresponding publication).  $t_0$  refers to the addition of the substrate and  $t_{24}$  to the end of the exposure phase.

The following abbreviations are valid for all tables located in this section:

m: medium samples

C+ cg-: “chemical controls” (organism and cotton gauze negative, chemical positive)

C+ cg+: “food controls” (organism negative, cotton gauze and chemical positive)

AZ: azoxystrobin

PRZ: prochloraz

**Table S11: Biotransformation screening experiment in *H. azteca*: exposure to 100 µg L<sup>-1</sup> AZ and PRZ, respectively. In the control samples nominal concentrations of 100 µg L<sup>-1</sup> AZ and PRZ, respectively, were used.**

Measured concentration in exposure medium				
	AZ [µg L <sup>-1</sup> ]	AZ [nmol L <sup>-1</sup> ]	PRZ [µg L <sup>-1</sup> ]	PRZ [nmol L <sup>-1</sup> ]
m_C+ cg- t0_1	98		96	
m_C+ cg- t0_2	96		95	
m_C+ cg- t24_1	102		98	
m_C+ cg- t24_2	102		100	
m_C+ cg+ t0_1	92		84	
m_C+ cg+ t0_2	100		93	
m_C+ cg+ t24_1	101		91	
m_C+ cg+ t24_2	98		89	
m_AZ t0_1	101	252		
m_AZ t0_2	96	239		
m_AZ t24_1	97	240		
m_AZ t24_2	89	222		
m_PRZ t0_1			101	269
m_PRZ t0_2			100	265
m_PRZ t24_1			81	216
m_PRZ t24_2			91	243
Whole body internal concentration 24 h after substrate addition and corresponding BAFs				
	AZ [nmol kg <sub>ww</sub> <sup>-1</sup> ]	BAF AZ [L kg <sub>ww</sub> <sup>-1</sup> ]	PRZ [nmol kg <sub>ww</sub> <sup>-1</sup> ]	BAF PRZ [L kg <sub>ww</sub> <sup>-1</sup> ]
AZ_1	890	4		
AZ_2	901	4		
PRZ_1			9413	39
PRZ_2			10793	42

**Table S12: Toxicokinetic experiment in *H. azteca*: exposure to 80 µg L<sup>-1</sup> AZ in the uptake phase. In the control samples nominal concentrations of 80 µg L<sup>-1</sup> AZ were used.**

Measured concentration in exposure medium		
	AZ [µg L <sup>-1</sup> ]	AZ [nmol L <sup>-1</sup> ]
m_C+ cg- t0_1	77	
m_C+ cg- t0_2	77	
m_C+ cg- t24_1	78	
m_C+ cg- t24_2	80	
m_C+ cg+ t0_1	82	
m_C+ cg+ t0_2	78	
m_C+ cg+ t24_1	82	
m_C+ cg+ t24_2	75	
m_AZ t0_1	71	177
m_AZ t0_2	79	195
m_AZ t24_1	77	191
m_AZ t24_2	78	193
m_AZ t0_1 <sup>*)</sup>	76	189
m_AZ t0_2 <sup>*)</sup>	78	194
m_AZ t24_1 <sup>*)</sup>	80	199
m_AZ t24_2 <sup>*)</sup>	81	201

Whole body internal concentrations 24 h after substrate addition and corresponding BAFs		
	AZ [nmol kg <sub>ww</sub> <sup>-1</sup> ]	BAF AZ [L kg <sub>ww</sub> <sup>-1</sup> ]
AZ_Ut24_1	767	4
AZ_Ut24_2	782	4
AZ_Dt0_1	734	4
AZ_Dt0_2	868	5

<sup>\*)</sup> Uptake phase for following depuration experiment.

**Table S13: Toxicokinetic experiment in *H. azteca*: exposure to 80 µg L<sup>-1</sup> PRZ in the uptake phase. In the control samples nominal concentrations of 80 µg L<sup>-1</sup> PRZ were used.**

Measured concentration in exposure medium		
	PRZ [µg L <sup>-1</sup> ]	PRZ [nmol L <sup>-1</sup> ]
m_C+ cg- t0_1	88	
m_C+ cg- t0_2	98	
m_C+ cg- t24_1	89	
m_C+ cg- t24_2	95	
m_C+ cg+ t0_1	94	
m_C+ cg+ t0_2	90	
m_C+ cg+ t24_1	98	
m_C+ cg+ t24_2	96	
m_PRZ t0_1	92	244
m_PRZ t0_2	92	245
m_PRZ t24_1	88	234
m_PRZ t24_2	90	240
m_PRZ t0_1 <sup>*)</sup>	98	262
m_PRZ t0_2 <sup>*)</sup>	90	242
m_PRZ t24_1 <sup>*)</sup>	93	247
m_PRZ t24_2 <sup>*)</sup>	93	249

Whole body internal concentrations 24 h after substrate addition and corresponding BAFs		
	PRZ [nmol kg <sub>ww</sub> <sup>-1</sup> ]	BAF PRZ [L kg <sub>ww</sub> <sup>-1</sup> ]
PRZ_Ut24_1	33353	116
PRZ_Ut24_2	22685	143
PRZ_Dt0_1	27075	100
PRZ_Dt0_2	24108	94

<sup>\*)</sup> Uptake phase for following depuration experiment.

**Table S14: Exposure and whole body concentrations of the experiment on Half-maximal inhibitory concentration of PRZ in *H. azteca* using AZ as a substrate ( $IC_{50, PRZ, AZ}$ ). Exposure to 40  $\mu\text{g L}^{-1}$  AZ and varying PRZ concentrations of c1 = 0.19  $\mu\text{g L}^{-1}$ , c2 = 0.37  $\mu\text{g L}^{-1}$ , c3 = 0.74  $\mu\text{g L}^{-1}$ , c4 = 3.7  $\mu\text{g L}^{-1}$ , c5 = 7.4  $\mu\text{g L}^{-1}$ , c6 = 22  $\mu\text{g L}^{-1}$ , c7 = 37  $\mu\text{g L}^{-1}$ , c8 = 74  $\mu\text{g L}^{-1}$  and c9 = 372  $\mu\text{g L}^{-1}$  (18 h pre-exposure to PRZ). In the control samples nominal concentrations of 40  $\mu\text{g L}^{-1}$  AZ and 37  $\mu\text{g L}^{-1}$  PRZ were used.**

Exposure medium			
	AZ [ $\mu\text{g L}^{-1}$ ]	AZ [nmol L <sup>-1</sup> ]	PRZ [ $\mu\text{g L}^{-1}$ ]
m_C+ cg- _1 (t0 PRZ)			36
m_C+ cg- _2 (t0 PRZ)			36
m_C+ cg- t0 _1	39		35
m_C+ cg- t0 _2	40		36
m_C+ cg- t24 _1	38		34
m_C+ cg- t24 _2	40		35
m_C+ cg+ _1 (t0 PRZ)			37
m_C+ cg+ _2 (t0 PRZ)			36
m_C+ cg+ t0 _1	38		36
m_C+ cg+ t0 _2	39		37
m_C+ cg+ t24 _1	38		34
m_C+ cg+ t24 _2	38		36
m_AZ + PRZ c1 _1 (t0 PRZ)			0.2
m_AZ + PRZ c1 _2 (t0 PRZ)			0.2
m_AZ + PRZ c2 _1 (t0 PRZ)			0.4
m_AZ + PRZ c2 _2 (t0 PRZ)			0.4
m_AZ + PRZ c3 _1 (t0 PRZ)			0.7
m_AZ + PRZ c3 _2 (t0 PRZ)			0.7
m_AZ + PRZ c4 _1 (t0 PRZ)			3
m_AZ + PRZ c4 _2 (t0 PRZ)			3
m_AZ + PRZ c5 _1 (t0 PRZ)			7
m_AZ + PRZ c5 _2 (t0 PRZ)			7
m_AZ + PRZ c6 _1 (t0 PRZ)			20
m_AZ + PRZ c7 _1 (t0 PRZ)			34
m_AZ + PRZ c7 _2 (t0 PRZ)			35
m_AZ + PRZ c8 _1 (t0 PRZ)			68
m_AZ + PRZ c8 _2 (t0 PRZ)			69
m_AZ + PRZ c9 _1 (t0 PRZ)			358
m_AZ + PRZ c9 _2 (t0 PRZ)			339
m_AZ t0 _1	39	97	
m_AZ t0 _2	40	99	
m_AZ + PRZ c1 t0 _1	37	92	0.4
m_AZ + PRZ c1 t0 _2	37	92	0.4
m_AZ + PRZ c2 t0 _1	39	98	0.5
m_AZ + PRZ c2 t0 _2	38	94	0.5
m_AZ + PRZ c3 t0 _1	38	93	0.8
m_AZ + PRZ c3 t0 _2	40	100	0.8

Exposure medium			
	AZ [ $\mu\text{g L}^{-1}$ ]	AZ [ $\text{nmol L}^{-1}$ ]	PRZ [ $\mu\text{g L}^{-1}$ ]
m_AZ + PRZ c4 t0_2	40	98	3
m_AZ + PRZ c5 t0_1	39	97	7
m_AZ + PRZ c5 t0_2	41	101	8
m_AZ + PRZ c6 t0_1	41	102	20
m_AZ + PRZ c6 t0_2	40	100	21
m_AZ + PRZ c7 t0_1	38	95	34
m_AZ + PRZ c7 t0_2	38	95	35
m_AZ + PRZ c8 t0_1	38	94	70
m_AZ + PRZ c8 t0_2	39	98	68
m_AZ + PRZ c9 t0_1	41	103	353
m_AZ + PRZ c9 t0_2	41	102	348
m_AZ t24_1	37	92	
m_AZ t24_2	39	97	
m_AZ + PRZ c1 t24_1	38	94	0.3
m_AZ + PRZ c1 t24_2	38	94	0.3
m_AZ + PRZ c2 t24_1	39	98	0.4
m_AZ + PRZ c2 t24_2	39	96	0.4
m_AZ + PRZ c3 t24_1	38	94	0.8
m_AZ + PRZ c3 t24_2	41	101	0.8
m_AZ + PRZ c4 t24_1	37	91	3
m_AZ + PRZ c4 t24_2	41	101	3
m_AZ + PRZ c5 t24_1	38	95	7
m_AZ + PRZ c5 t24_2	40	99	7
m_AZ + PRZ c6 t24_1	40	100	19
m_AZ + PRZ c6 t24_2	39	98	19
m_AZ + PRZ c7 t24_1	38	95	33
m_AZ + PRZ c7 t24_2	39	97	33
m_AZ + PRZ c8 t24_1	38	93	65
m_AZ + PRZ c8 t24_2	40	98	67
m_AZ + PRZ c9 t24_1	38	94	338
m_AZ + PRZ c9 t24_2	42	104	355
Whole body internal concentrations 24 h after substrate addition and corresponding BAFs			
	AZ [ $\text{nmol kg}_{\text{ww}}^{-1}$ ]	BAF AZ [ $\text{L kg}_{\text{ww}}^{-1}$ ]	PRZ [ $\text{nmol kg}_{\text{ww}}^{-1}$ ]
AZ_1	781	8	
AZ_2	703	7	
AZ_3	792	8	
AZ + PRZ c1_1	710	8	54
AZ + PRZ c1_2	769	8	52
AZ + PRZ c2_1	750	8	127
AZ + PRZ c2_2	743	8	113
AZ + PRZ c3_1	713	7	211

Whole body internal concentrations 24 h after substrate addition and corresponding BAFs			
	AZ [nmol kg <sub>ww</sub> <sup>-1</sup> ]	BAF AZ [L kg <sub>ww</sub> <sup>-1</sup> ]	PRZ [nmol kg <sub>ww</sub> <sup>-1</sup> ]
AZ + PRZ c3_2	834	9	221
AZ + PRZ c4_1	770	8	1107
AZ + PRZ c4_2	838	9	1129
AZ + PRZ c5_1	802	8	3158
AZ + PRZ c5_2	776	8	2243
AZ + PRZ c6_1	888	9	6720
AZ + PRZ c6_2	867	9	6496
AZ + PRZ c7_1	927	10	10937
AZ + PRZ c7_2	887	9	11245
AZ + PRZ c8_1	1095	11	20921
AZ + PRZ c8_2	1149	12	22851
AZ + PRZ c9_1	1183	12	77899
AZ + PRZ c9_2	1151	11	67027

## SI. I Determination of $IC_{50}$ , PRZ, AZS in *H. azteca*

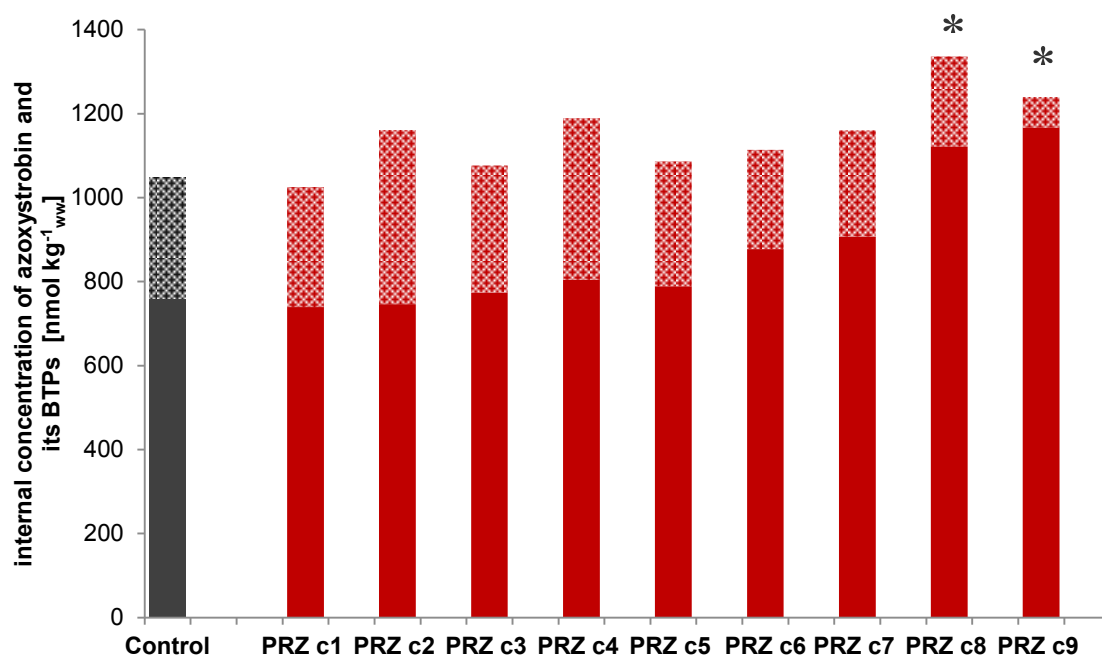


Figure S4: Whole body internal concentration of azoxystrobin and its BTPs after 24 h exposure to  $40 \mu\text{g L}^{-1}$  azoxystrobin: 18 h pre-exposure without chemical in black (sample replicates  $n=3$ ) and 18 h pre-exposure to varying prochloraz (PRZ) concentrations ( $n=2$ ) (c1: 0.19, c2: 0.37, c3: 0.74, c4: 3.7, c5: 7.4, c6: 22, c7: 37, c8: 74 and c9:  $372 \mu\text{g L}^{-1}$ ) in red. The filled areas mark the parent compound azoxystrobin, whereas the hatched areas mark the sum of all detected BTPs. Total internal concentrations in each mixture were compared to those of the controls (single exposure to azoxystrobin) with a t-test (two tailed distribution, two-sample equal variance) and showed statistical difference for treatment PRZ c8 and PRZ c9 ( $p < 0.05$ ) marked with an asterisk.

## SI. J Dose-Response Fitting of $IC_{50, PRZ, AZ}$ in *H. azteca*

The log-logistic four-parameter model (LL.4) used for the fitting of dose-response curves is available in the R<sup>8</sup> package “drc” from Ritz and Streibig (2005)<sup>9</sup> and is described by the following equation:

Log-logistic four-parameter model (LL.4):

$$f(x) = c + \frac{d - c}{1 + \exp(b(\log(x) - \log(e)))} \quad \text{equation S2}$$

where  $d$  and  $c$  are the upper and lower limits of response, respectively,  $b$  denotes the relative slope in the inflection point,  $e$  is the inflection point and thereby the  $EC_{50}$ , and  $x$  is the prochloraz concentration.

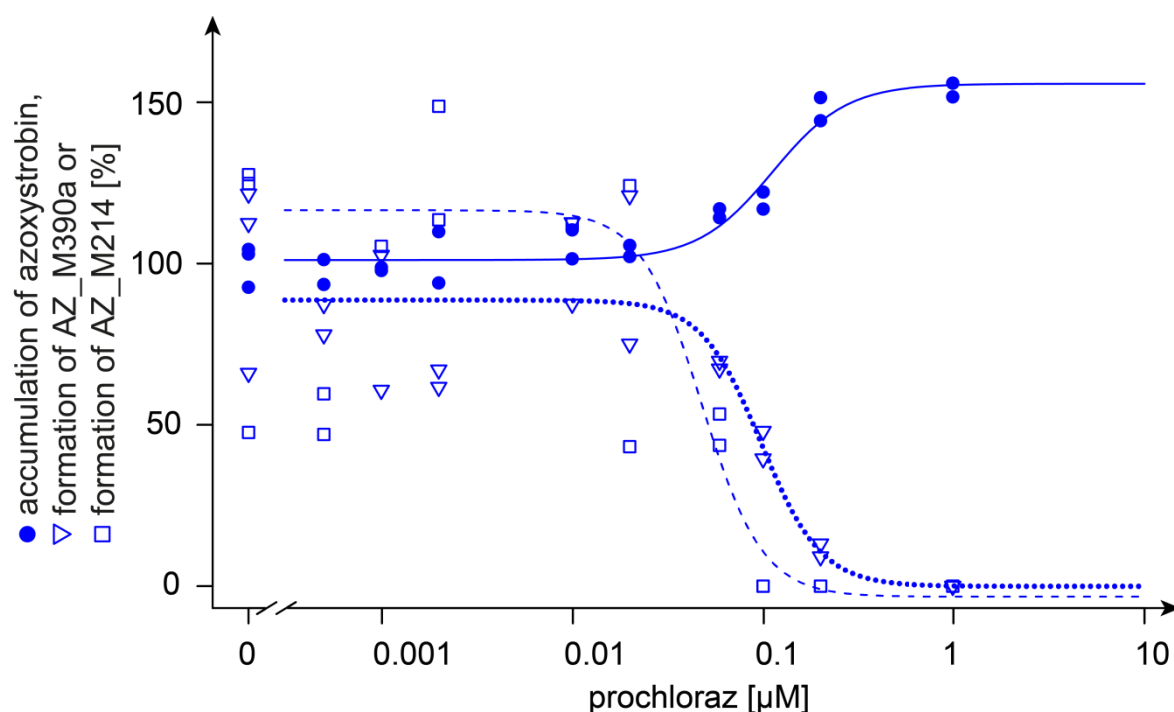


**Figure S5: Dose-response curves for the  $IC_{50/10, PRZ, AZ}$  determination based on whole body internal concentration measurements of azoxystrobin and its BTPs (shown are the two primary BTPs AZ\_M390a and AZ\_M214). Internal concentrations of azoxystrobin and its BTPs were measured after 24 h exposure to  $40 \mu g L^{-1}$  azoxystrobin. Controls were pre-exposed without chemical for 18 h, whereas treatments were pre-exposed for 18 h to varying prochloraz concentrations (c1: 0.19, c2: 0.37, c3: 0.74, c4: 3.7, c5: 7.4, c6: 22, c7: 37, c8: 74 and c9: 372  $\mu g L^{-1}$ ).**

**Table S15: Estimated parameters (d: upper limit of response; c: lower limit of response; b: relative slope in the inflection point; e: inflection point and thereby the  $IC_{50, PRZ, AZ}$ ) and determined  $IC_{50/10, PRZ, AZ}$ s for azoxystrobin and primary BTPs with the four-parameter log-logistic mode in *H. azteca*. Parameters and  $IC_{50/10, PRZ, AZ}$ s are reported with the corresponding standard errors. Measured internal concentrations of AZ\_M214 exhibited large variations (see Figure S5 above). Therefore,  $IC_{50/10, AZ, PRZ}$ s based on the dose response curve of AZ\_M214 have to be treated with care.**

	b	c	d	e, $IC_{50, PRZ, AZ}$ [ $\mu M$ ]	e, $IC_{50, PRZ, AZ}$ [ $\mu g L^{-1}$ ]	$IC_{10, PRZ, AZ}$ [ $\mu M$ ]	$IC_{10, PRZ, AZ}$ [ $\mu g L^{-1}$ ]
<b>Azoxystrobin</b>	-2.24 $\pm 0.686$	101 $\pm 1.73$	156 $\pm 4.09$	0.111 $\pm 0.0144$	41.7 $\pm 5.39$	0.0416 $\pm 0.0134$	15.6 $\pm 5.01$
<b>AZ_M390b</b>	2.78 $\pm 1.41$	-0.0557 $\pm 13.1$	88.7 $\pm 5.43$	0.0970 $\pm 0.0234$	36.4 $\pm 8.76$	0.0440 $\pm 0.0173$	16.5 $\pm 6.47$
<b>AZ_M214</b>	2.73 $\pm 2.28$	-3.29 $\pm 24.1$	117 $\pm 14.7$	0.0472 $\pm 0.0264$	17.7 $\pm 9.92$	0.0211 $\pm 0.0217$	7.91 $\pm 8.15$

A “Lack-of-fit-F-test” with the “anova function” available in the R<sup>8</sup> package “drc” from Ritz and Streibig (2005)<sup>9</sup> was performed to test if there is statistical difference between the dose-response curves fitted to the internal concentrations of azoxystrobin and AZ\_M390b, respectively, in *H. azteca* and *G. pulex*. It was tested if the reduction from a larger to a smaller model is statistically justified. Therefore, first, both datasets (data of azoxystrobin or AZ\_M390b, respectively, of the two test species) are fitted into one model together but with individual parameters for the log-logistic four parameter model for each dataset. Second, both datasets are fitted into one model with similar parameters for the log-logistic four parameter model.

The calculated p-values showed that there is statistical difference between the dose response curves for azoxystrobin ( $p < 0.0059$ ) and AZ\_M390b ( $p < 0.0130$ ), respectively, for the two test species.

**Table S16: The  $LC_{50}$  and benchmark dose ( $BMD_5$ ) of azoxystrobin in the absence and presence of prochloraz observed in *H. azteca* and *G. pulex***

Indicators	Azoxystrobin	Azoxystrobin + 0.2 $\mu M$ prochloraz	Fold change
<i>H. azteca</i>	(nM)	(nM)	
$LC_{50}$	500	200	2.5
$BMD_5$	376	102	3.7
$BMDL_5$	299	19	15.7
$BMDU_5$	689	135	5.1
<i>G. pulex</i>			
$LC_{50}$	400	100	4.0
$BMD_5$	246	55	4.5
$BMDL_5$	136	16	8.5
$BMDU_5$	383	73	5.2

$LC_{50}$ : median lethal concentration. BMD, benchmark dose,  $BMDL$ , lowest benchmark dose lower bound from exponential models;  $BMDU$ , highest benchmark dose upper bound Hill models; The subscripted number means the benchmark response, i.e. 5%, used when calculating BMD.

## SI. K Distance moved (cm) of the Video-Tracking of *G. pulex* and *H. azteca* during 18 h prochloraz exposure

Species	Concentration of prochloraz in exposure medium					
	0 $\mu$ M	0.02 $\mu$ M	0.1 $\mu$ M	0.2 $\mu$ M	1 $\mu$ M	2 $\mu$ M
<i>Hyalella azteca</i>	3545 $\pm$ 4381	2304 $\pm$ 3247	2567 $\pm$ 3237	1910 $\pm$ 1968	4949 $\pm$ 9782	3673 $\pm$ 4950
<i>Gammarus pulex</i>	1159 $\pm$ 835	1668 $\pm$ 883*	2174 $\pm$ 1054*	1381 $\pm$ 998	1841 $\pm$ 1769*	864 $\pm$ 543

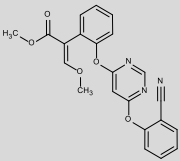
Protocol for *G. pulex* is described in Rösch et al.<sup>4</sup>. *H. azteca* were placed in 6 well plate with 5 ml per well and recorded for 18 hours. Distance moved was calculated for each animal. Asterisks indicate treatment samples that are significantly different from the control.

## SI. L Comparison of different *H. azteca* Sample Wet Weights for Detection and Quantification of Biotransformation Products

Measuring internal concentrations at different time points during the uptake and depuration phase requires the use of plenty of test organisms (~2000 organisms if one sample is composed of 50 organisms). Therefore, reducing the amount of organisms was tried. For the *H. azteca* screening experiment (exposure to 100  $\mu$ g L<sup>-1</sup> azoxystrobin) the same sample wet weight as applied in the *G. pulex* bioaccumulation and biotransformation experiments was used (~130 mg which relate to 4 *G. pulex* or 50 *H. azteca*). Additionally, a reduced wet weight of ~70 mg (30 *H. azteca*) with similar exposure concentrations was tested to evaluate if a decreased wet weight is sufficient in terms of LOQs of BTPs (see SI. B). All BTPs of azoxystrobin were still detected in the extracts of the reduced sample wet weight. However, the sulfate-containing BTPs are more sensitive during negative electrospray ionization but have to be quantified in positive ionization mode since their quantification is based on the parent compound, which is only detectable in positive ionization mode. Therefore, two sulfate-containing BTPs (AZ\_M514 and AZ\_M618) that already displayed very low intensities using ~130 mg wet weight, could no longer be quantified. The loss of two minor BTPs was considered acceptable in the light of reducing the number of test organisms and the kinetic experiment was carried out with the reduced wet weight.

## SI. M Identified Biotransformation Products for Azoxystrobin and Prochloraz in *H. azteca*

Table S17: Overview of azoxystrobin and identified biotransformation products formed in the aquatic invertebrate *H. azteca*. Biotransformation products are listed according to their relative peak intensity. Information about mass error and retention time (RT) are given for both replicate samples. CE stands for collision energy applied for fragmentation in the MS/MS experiment. Below each biotransformation product the abbreviation (S) stands for “identified by suspect screening (S)”, whereas (N) stands for “identified by nontarget” screening. The abbreviation (H) stands for BTPs that were only identified in *H. azteca* and not in *G. pulex*. (H‡) stands for BTPs that were afterward identified in *G. pulex*, but with intensities below the set threshold of 1E6. The mass error of all identified BTPs was < 3ppm.

Compound	Formula [M]	RT [min] <sup>iii)</sup>	Polarity	Elemental change <sup>iv)</sup>	Log D <sub>ow</sub> <sup>v)</sup>	Identification confidence <sup>vi)</sup>	Description	CE [eV]	MS/MS confirmatory ions <sup>viii)</sup>
MassBank ID of displayed MS/MS spectrum	Exact mass of [M+H] <sup>+</sup> / [M-H] <sup>-</sup>					/level according to Schymanski et al. (2014) <sup>6/ vii)</sup>			
<b>Azoxystrobin</b>	C <sub>22</sub> H <sub>17</sub> N <sub>3</sub> O <sub>5</sub>	14.6	+		4.2	/1/	parent compound	15	
<b>ET270001</b>	404.1241	14.6							
									
BAF [L kg <sub>ww</sub> <sup>-1</sup> ] at t <sub>24</sub> <sup>ii)</sup> : 4; 4									
BAF <sub>k</sub> [L kg <sub>ww</sub> <sup>-1</sup> ] <sup>iii)</sup> : 6									
<b>AZ_M638 (H)</b>	C <sub>30</sub> H <sub>27</sub> O <sub>13</sub> N <sub>3</sub>	12.7	+	- CH <sub>2</sub>	-1.3	<b>d, p</b>	demethylation,	20	<b>390.1083</b>
<b>ET273401</b>	638.1617	12.7		+ C <sub>6</sub> H <sub>10</sub> O <sub>5</sub>		/3/, most likely structure	glucose conjugation,		358.0821
<b>(N)</b>				+ C <sub>3</sub> H <sub>2</sub> O <sub>3</sub>			malonyl conjugation		302.0916
<b>AZ_M640 (H)</b>	C <sub>30</sub> H <sub>29</sub> O <sub>13</sub> N <sub>3</sub>	13.0	+	- CH <sub>2</sub>	-1.8	<b>d, p</b>	demethylation,	20	<b>392.1239</b>
<b>ET273301</b>	640.1773	13.0		+ H <sub>2</sub>		/3/, most likely structure	hydrogenation,		342.0872
<b>(N)</b>				+ C <sub>6</sub> H <sub>10</sub> O <sub>5</sub>			glucose conjugation,		360.0979
				+ C <sub>3</sub> H <sub>2</sub> O <sub>3</sub>			malonyl conjugation		

Compound MassBank ID of displayed MS/MS spectrum	Formula [M] Exact mass of [M+H] <sup>+</sup> / [M-H] <sup>-</sup>	RT [min] <sup>iii)</sup>	Polarity	Elemental change <sup>iv)</sup>	Log D <sub>ow</sub> <sup>v)</sup>	Identification confidence <sup>vi)</sup>  /level according to Schymanski et al. (2014) <sup>6/ vii)</sup>	Description	CE [eV]	MS/MS confirmatory ions <sup>viii)</sup>
<b>AZ_M390a</b> <b>ET273701</b> (S)	C <sub>21</sub> H <sub>15</sub> N <sub>3</sub> O <sub>5</sub> 390.1084	11.9 11.7	+	- CH <sub>2</sub>	3.5	<b>D</b>  /2b/	demethylation	30	372.0979 344.1031 329.0795
<b>AZ_M390b</b> <b>ET273801</b> (S)	C <sub>21</sub> H <sub>15</sub> N <sub>3</sub> O <sub>5</sub> 390.1084	13.6 13.6	+	- CH <sub>2</sub>	0.4	<b>I</b> <sup>5-7</sup>  /1/	ester hydrolysis	30	372.0981 344.1032 302.0927
<b>AZ_M497 (H)</b> <b>ET271902</b> (S)	C <sub>23</sub> H <sub>20</sub> N <sub>4</sub> O <sub>7</sub> S 497.1125	11.5 11.4	+	- CH <sub>2</sub> + C <sub>2</sub> H <sub>5</sub> NO <sub>2</sub> S	-0.1	<b>d</b> (in negative ionization mode diagnostic taurine loss), <b>p</b> for conjugation of AZ_M390b  /2b/	demethylation, taurine conjugation	40	344.1031 329.0795 372.0979
<b>AZ_M392</b> <b>ET274601</b> (S)	C <sub>21</sub> H <sub>17</sub> N <sub>3</sub> O <sub>5</sub> 392.1241	13.5 13.5	+	- CH <sub>2</sub> + H <sub>2</sub>	0.1	<b>I</b> <sup>5</sup>  <b>p</b>  /3/, most likely structure	ester hydrolysis, hydrogenation	15	342.0871 392.1238 360.0977
<b>AZ_M630</b> <b>ET273251</b> (S)	C <sub>27</sub> H <sub>25</sub> N <sub>3</sub> O <sub>13</sub> S 630.1035	11.7 11.6	- <sup>ix)</sup>	- CH <sub>2</sub> + C <sub>6</sub> H <sub>10</sub> O <sub>5</sub> + SO <sub>3</sub>	-0.5	<b>d, p</b>  /3/, most likely structure	demethylation, glucose conjugation, sulfate conjugation	20	241.0024 96.9601 630.1038
<b>AZ_M420</b> <b>ET274902</b> (S)	C <sub>22</sub> H <sub>17</sub> N <sub>3</sub> O <sub>6</sub> 420.1190	11.2-14.5 11.1-14.4	+	+ O	3.6-3.7	<b>p</b> for hydroxylation at the ( <i>E</i> )-methyl β- methoxyacrylate group  /3/, 3 positional isomers	aliphatic hydroxylation	40	329.0796 360.0979 316.1075

Compound MassBank ID of displayed MS/MS spectrum	Formula [M] Exact mass of [M+H] <sup>+</sup> / [M-H] <sup>-</sup>	RT [min] <sup>iii)</sup>	Polarity	Elemental change <sup>iv)</sup>	Log D <sub>ow</sub> <sup>v)</sup>	Identification confidence <sup>vi)</sup>  /level according to Schymanski et al. (2014) <sup>6/ vii)</sup>	Description	CE [eV]	MS/MS confirmatory ions <sup>viii)</sup>
AZ_M214 ET274201 (S)	C <sub>11</sub> H <sub>7</sub> N <sub>3</sub> O <sub>2</sub> 214.0611	7.9 7.9	+	- C <sub>11</sub> H <sub>10</sub> O <sub>3</sub>	2.3	D I <sup>5</sup>	ether cleavage	40	214.0610 187.0501 120.0442
AZ_M362b ET274501 (S)	C <sub>20</sub> H <sub>15</sub> N <sub>3</sub> O <sub>4</sub> 362.1135	14.4 14.5	+	- C <sub>2</sub> H <sub>2</sub> O	0.8-2.8	d for C <sub>2</sub> H <sub>2</sub> O loss at the (E)-methyl β- methoxyacrylate group  /3/, ≥ 3 positional isomers	- C <sub>2</sub> H <sub>2</sub> O	20	362.1135 302.0922 330.0872
AZ_M485 (H) ET272401 (S)	C <sub>22</sub> H <sub>20</sub> N <sub>4</sub> O <sub>7</sub> S 485.1125	10.9 10.8	+	- C <sub>2</sub> H <sub>2</sub> + H <sub>2</sub> + C <sub>2</sub> H <sub>5</sub> NO <sub>2</sub> S	-0.9	d, p for conjugation of AZ_M390b  /3/ most likely structure	ester hydrolysis, demethylation, hydrogenation, taurine product	20	126.0220 342.0875 467.1022
AZ_M378 ET274102 (S)	C <sub>20</sub> H <sub>15</sub> N <sub>3</sub> O <sub>5</sub> 378.1084	12.4 12.4	+	- C <sub>2</sub> H <sub>2</sub>	-0.5	D /2b/	hydrogenation, didemethylation,	15	378.1082 342.0872 360.0972
AZ_M552 ET273904 (S)	C <sub>27</sub> H <sub>25</sub> N <sub>3</sub> O <sub>10</sub> 552.1613	12.4 12.4	+	- CH <sub>2</sub> + C <sub>6</sub> H <sub>10</sub> O <sub>5</sub>	1.8	d, p /3/, most likely structure	demethylation, glucose conjugation	15	358.0822 390.1085 552.1632
AZ_M541 (H) ET272201 (S)	C <sub>25</sub> H <sub>24</sub> N <sub>4</sub> O <sub>8</sub> S 541.1388	11.0 11.1	+	+ O + C <sub>3</sub> H <sub>7</sub> NO <sub>2</sub> S	0.5	d, p /3/, 3 positional isomers	aliphatic hydroxylation, cysteine product	20	491.1020 388.0923 328.0852

Compound MassBank ID of displayed MS/MS spectrum	Formula [M] Exact mass of [M+H] <sup>+</sup> / [M-H] <sup>-</sup>	RT [min] <sup>iii)</sup>	Polarity	Elemental change <sup>iv)</sup>	Log D <sub>ow</sub> <sup>v)</sup>	Identification confidence <sup>vi)</sup>  /level according to Schymanski et al. (2014) <sup>6/ vii)</sup>	Description	CE [eV]	MS/MS confirmatory ions <sup>viii)</sup>
<b>AZ_M436 (H<sup>+</sup>)</b>  <b>(S)</b> <b>ET272303</b>	C <sub>22</sub> H <sub>17</sub> N <sub>3</sub> O <sub>7</sub> 436.1139	12.0 12.0	+	+ O + O	≈1.9-3.9	<b>d, p</b> for only one hydroxylation at the ( <i>E</i> )- methyl β-methoxy- acrylate group	aliphatic hydroxylation, hydroxylation	60	<b>304.0721</b> 215.0452 361.0691
<b>AZ_M632 (H)</b>  <b>ET272952</b>  <b>(S)</b>	C <sub>27</sub> H <sub>27</sub> N <sub>3</sub> O <sub>13</sub> S 632.1192	12.0 11.8	- <sup>ix)</sup>	- CH <sub>2</sub> + H <sub>2</sub> + C <sub>6</sub> H <sub>10</sub> O <sub>5</sub> + SO <sub>3</sub>	-1.0	<b>d, p</b>  /3/, most likely structure	demethylation, hydrogenation, glucose conjugation, sulfate conjugation,	40	<b>241.0024</b> 96.9600 632.1190
<b>AZ_M554a (H)</b>  <b>ET272001</b>  <b>(S)</b>	C <sub>27</sub> H <sub>27</sub> N <sub>3</sub> O <sub>10</sub> 554.1769	11.9 11.8	+	- CH <sub>2</sub> + H <sub>2</sub> + C <sub>6</sub> H <sub>10</sub> O <sub>5</sub>	1.4	<b>p</b>  /3/, most likely structure	demethylation, hydrogenation, glucose conjugation	20	392.1241 342.0875 360.0979
<b>AZ_M684 (H)</b>  <b>ET273501</b>  <b>(N)</b>	C <sub>31</sub> H <sub>29</sub> O <sub>15</sub> N <sub>3</sub> 684.1671	11.7 11.7	+	+ O + O + C <sub>6</sub> H <sub>10</sub> O <sub>5</sub> + C <sub>3</sub> H <sub>2</sub> O <sub>3</sub>	≈ -0.9 to -3	<b>p</b>  /3/, many positional isomers	aliphatic hydroxylation, hydroxylation, glucose conjugation, malonyl conjugation	20	634.1296 652.1418 404.0873
<b>AZ_M362a</b>  <b>ET274403</b>  <b>(S)</b>	C <sub>20</sub> H <sub>15</sub> N <sub>3</sub> O <sub>4</sub> 362.1135	13.6 13.5	+	- C <sub>2</sub> H <sub>2</sub> O	0.8-2.8	<b>d</b> for C <sub>2</sub> H <sub>2</sub> O loss at the ( <i>E</i> )-methyl β-methoxy- acrylate group  /3/, ≥ 3 positional isomers	- C <sub>2</sub> H <sub>2</sub> O	20	<b>362.1136</b> 330.0873 302.0921
<b>AZ_M660 (H<sup>+</sup>)</b>  <b>ET273601</b>  <b>(S)</b>	C <sub>28</sub> H <sub>27</sub> O <sub>14</sub> N <sub>3</sub> S 660.1141	11.2 11.1	+	+O + C <sub>6</sub> H <sub>10</sub> O <sub>5</sub> + SO <sub>3</sub>	-0.1 to -0.5	<b>d, p</b>  /3/, 3 positional isomers	aliphatic hydroxylation, glucose conjugation, sulfate conjugation,	20	<b>420.1190</b> 205.1073 550.1457

Compound MassBank ID of displayed MS/MS spectrum	Formula [M] Exact mass of [M+H] <sup>+</sup> / [M-H] <sup>-</sup>	RT [min] <sup>iii)</sup>	Polarity	Elemental change <sup>iv)</sup>	Log D <sub>ow</sub> <sup>v)</sup>	Identification confidence <sup>vi)</sup>  /level according to Schymanski et al. (2014) <sup>6/ vii)</sup>	Description	CE [eV]	MS/MS confirmatory ions <sup>viii)</sup>
AZ_M513 (H) ET272701 (S)	C <sub>23</sub> H <sub>20</sub> N <sub>4</sub> O <sub>8</sub> S 513.1074	11.4 11.3	+	- CH <sub>2</sub> + O + C <sub>2</sub> H <sub>5</sub> NO <sub>2</sub> S	-0-7 to 0.1	<b>d, p</b> for taurine loss and conjugation of AZ_M390b  /3/ 2 positional isomers	demethylation, aliphatic hydroxylation, taurine conjugation	20	<b>356.0666</b> 513.1076 481.0806
AZ_M554b (H) ET272101 (S)	C <sub>27</sub> H <sub>27</sub> N <sub>3</sub> O <sub>10</sub> 554.1769	12.8 12.8	+	- CH <sub>2</sub> + H <sub>2</sub> + C <sub>6</sub> H <sub>10</sub> O <sub>5</sub>	1.4	<b>p</b>  /3/, most likely structure	demethylation, hydrogenation, glucose conjugation	20	392.1239 342.0875 360.0979
AZ_M582b (H) ET272604 (S)	C <sub>28</sub> H <sub>27</sub> N <sub>3</sub> O <sub>11</sub> 582.1718	13.2 13.2	+	+ O + C <sub>6</sub> H <sub>10</sub> O <sub>5</sub>	1.9-2.2	<b>d, p</b> for hydroxylation and glucose conjugation at the ( <i>E</i> )-methyl β- methoxyacrylate group  /3/, 3 positional isomers	aliphatic hydroxylation, glucose conjugation	15	<b>145.0492</b> 334.1185 316.1089
AZ_M582a (H) ET272501 (S)	C <sub>28</sub> H <sub>27</sub> N <sub>3</sub> O <sub>11</sub> 582.1718	11.2 11.1	+	+ O + C <sub>6</sub> H <sub>10</sub> O <sub>5</sub>	1.9-2.2	<b>p</b> for hydroxylation and glucose conjugation at the ( <i>E</i> )-methyl β-meth- oxyacrylate group  /3/, 3 positional isomers	aliphatic hydroxylation, glucose conjugation	15	550.1453 388.0932 420.1190
AZ_M498 ET273152 (S)	C <sub>22</sub> H <sub>17</sub> N <sub>3</sub> O <sub>9</sub> S 498.0613	11.4 11.3	- <sup>ix)</sup>	+ O + SO <sub>3</sub>	1.3-1.7	<b>p</b> for hydroxylation and sulfate conjugation at the ( <i>E</i> )-methyl β- methoxyacrylate group  /3/, 3 positional isomers	aliphatic hydroxylation, sulfate conjugation	15	498.0614 418.1045 358.0818
AZ_M493 ET274303 (S)	C <sub>24</sub> H <sub>20</sub> N <sub>4</sub> O <sub>6</sub> S 493.1176	12.9-14.0	+	- CH <sub>4</sub> O + C <sub>3</sub> H <sub>7</sub> NO <sub>2</sub> S	1.2-1.3	<b>d, p</b>  /3/, most likely structures	- CH <sub>4</sub> O, cysteine product	20	<b>132.0115</b> 330.0869 461.0911

Compound MassBank ID of displayed MS/MS spectrum	Formula [M] Exact mass of [M+H] <sup>+</sup> / [M-H] <sup>-</sup>	RT [min] <sup>iii)</sup>	Polarity	Elemental change <sup>iv)</sup>	Log D <sub>ow</sub> <sup>v)</sup>	Identification confidence <sup>vi)</sup>  /level according to Schymanski et al. (2014) <sup>6/ vii)</sup>	Description	CE [eV]	MS/MS confirmatory ions <sup>viii)</sup>
<b>AZ_M618</b> <b>ET273052</b> <b>(S)</b>	C <sub>26</sub> H <sub>25</sub> N <sub>3</sub> O <sub>13</sub> S 618.1035	11.2 11.1	- <sup>ix)</sup>	- CH <sub>2</sub> + C <sub>6</sub> H <sub>10</sub> O <sub>5</sub> + SO <sub>3</sub> - CH <sub>2</sub> + H <sub>2</sub>	-4.6	<b>d, p</b>  /3/, most likely structure	demethylation, glucose conjugation, sulfate conjugation, ester hydrolysis, hydrogenation	20	<b>241.0025</b>  618.1044 96.9601
<b>AZ_M525</b> <b>ET274005</b> <b>(S)</b>	C <sub>25</sub> H <sub>24</sub> N <sub>4</sub> O <sub>7</sub> S 525.1438	12.5-13.3 12.5-13.4	+	+ C <sub>3</sub> H <sub>7</sub> NO <sub>2</sub> S	1.1	<b>p</b>  /3/, most likely structure	cysteine product	20	372.0980 330.0870 461.0893
<b>AZ_M514</b> <b>ET272851</b> <b>(S)</b>	C <sub>22</sub> H <sub>17</sub> N <sub>3</sub> O <sub>10</sub> S 514.0562	11.2 11.1	- <sup>ix)</sup>	+ O + O + SO <sub>3</sub>	-0.8-2.0	<b>d</b> for only one hydroxylation at the ( <i>E</i> )- methyl β-methoxy- acrylate group  <b>p</b> for hydroxylation and sulfate conjugation at the ( <i>E</i> )-methyl β- methoxyacrylate group  /3/ many positional isomers	aliphatic hydroxylation, hydroxylation, sulfate conjugation	20	<b>359.0535</b> 434.1000 514.0580

## Explanations to Table S17:

<sup>i)</sup> See Equation 4 in the corresponding publication for the calculation of BAFs at steady state.

<sup>ii)</sup> See Equation 5 in the corresponding publication for the calculation of kinetic BAF<sub>k</sub>s.

<sup>iii)</sup> In case of a retention time range, several possibly positional isomers were integrated as one peak, due to bad peak separation.

<sup>iv)</sup> The elemental change refers to the change in the molecular formula of the biotransformation product in comparison with the parent compound.

<sup>v)</sup> Log D<sub>ow</sub> values were predicted by MarvinSketch version 14.10.20.0 at pH 7.9 and 25 °C. Log D<sub>ow</sub> values correspond to corrected log K<sub>ow</sub> values to account for pH-dependent dissociation. At pH 7.9 azoxystrobin is neutral thus log D<sub>ow</sub> is equal to log K<sub>ow</sub>. If different positional isomers are possible for one BTP, a range of log D<sub>ow</sub> values is given.

<sup>vi)</sup> D: diagnostic fragment/evidence for one structure; d: diagnostic fragment/evidence for positional isomers; l: structure reported in literature; m: MS/MS data from literature; p: biotransformation pathway information; d, p: diagnostic fragment for positional isomers (d) in combination with pathway information (p) give evidence for one possible structure.

<sup>vii)</sup> Levels are defined as follows: 5 (*exact mass*), 4 (*unequivocal molecular formula*), 3 (*tentative candidates: e.g., positional isomers*), 2 (*probable structure: library spectrum match (a) or diagnostic evidence for one structure (b)*) and 1 (*confirmed structure*).

<sup>viii)</sup> Diagnostic fragments (d, D) are listed first and are represented in bold in the table, other characteristic fragments are then presented according to their relative abundance. Only fragments where a chemical formula and structure could be attributed are considered.

<sup>ix)</sup> The sulfate-containing BTPs are more sensitive in negative ionization mode. However, they were quantified in positive ionization mode because azoxystrobin was detected and quantified in positive ionization mode.

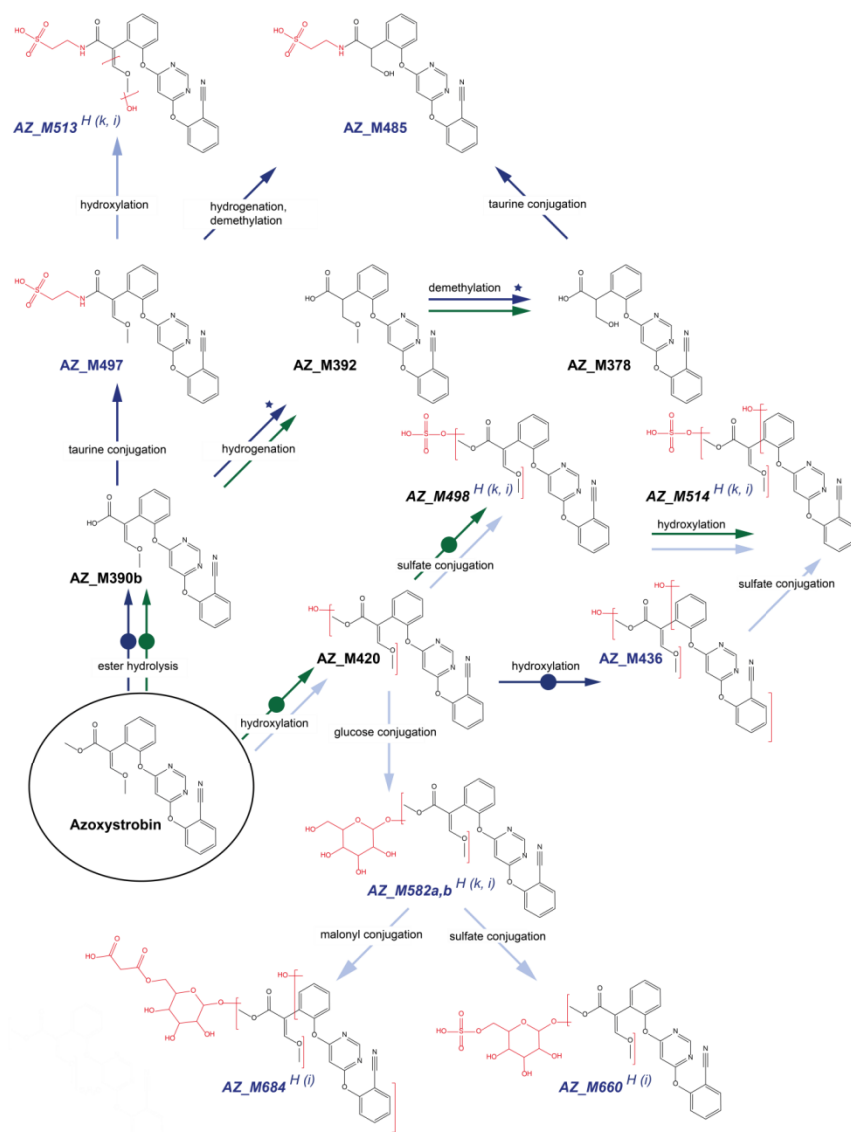
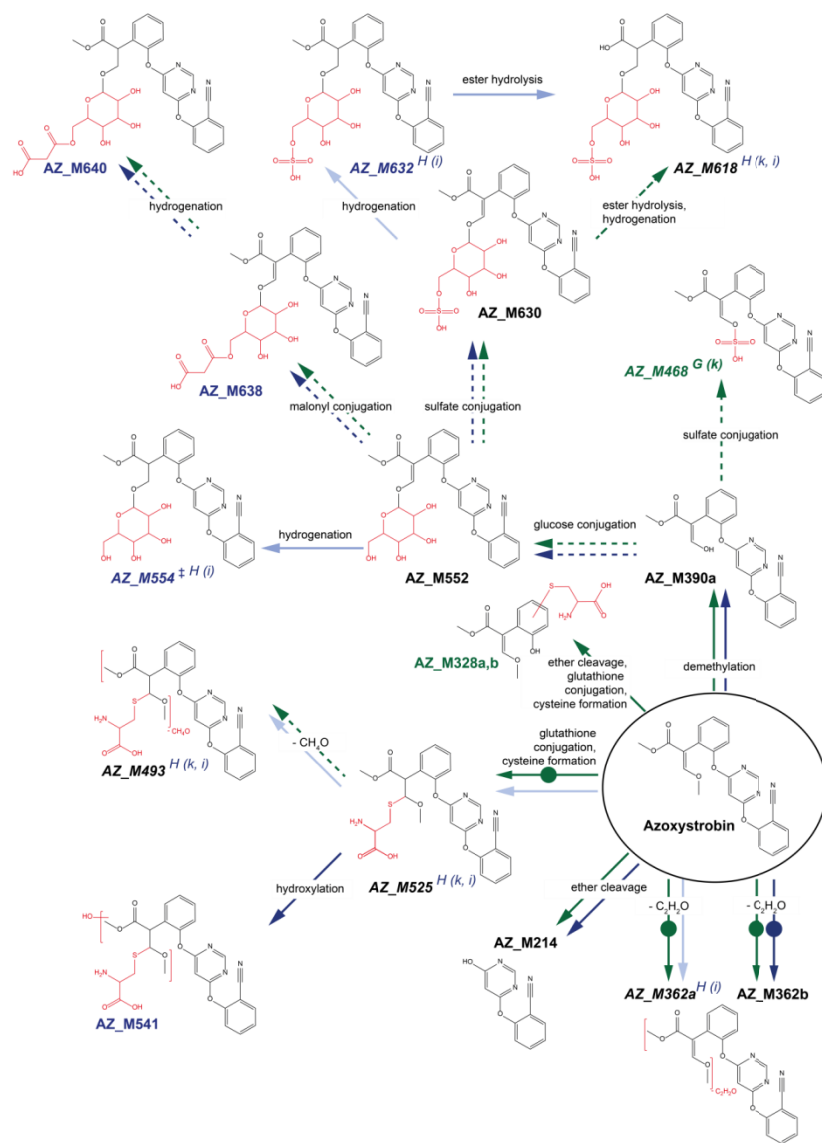


**Figure S6: Proposed biotransformation pathway of azoxystrobin in *G. pulex* and *H. azteca* based on the validated biotransformation pathway of *G. pulex*.<sup>4</sup> Structural modifications of the BTPs are highlighted in red. BTPs written in black were detected in both species, whereas BTPs written in green are specific for *G. pulex* and BTPs written in blue are specific for *H. azteca*. Superscript text after italic written BTPs marks BTPs that were either not detected in the kinetic experiments (k) or not detected in the inhibition experiments (i, IC<sub>50, PRZ, AZ</sub>) of *G. pulex* (G) or *H. azteca* (H) but in the BTP screening experiment.**

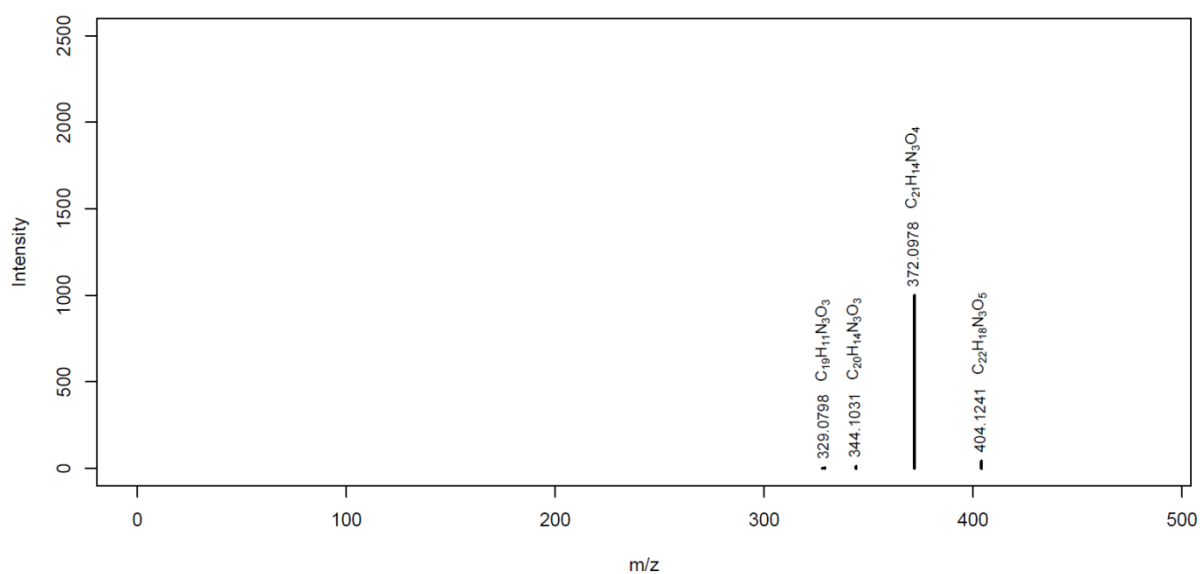
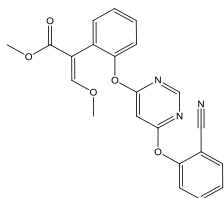
The color and shape of the arrows distinguishes between biotransformation reaction types and test species (blue: *H. azteca*, green: *G. pulex*): continuous: reaction influenced by prochloraz; dashed: reaction influenced by prochloraz only due to previous reactions being influenced by prochloraz; continuous with circle: reaction not influenced by prochloraz; continuous light blue: no information on influence of prochloraz for *H. azteca*. The small blue stars located at the arrowhead of the prochloraz influenced biotransformation reaction towards the BTPs AZ\_M392 and AZ\_M378 for *H. azteca* mark the unexpected increase in internal concentrations of AZ\_M392 and AZ\_M378 with increasing prochloraz concentration.

<sup>‡</sup>) AZ\_M554 is actually characterized by two low intensity peaks but it is unclear whether AZ\_M554 is additionally formed out of AZ\_M390b.

The different MassBank IDs for one compound refer to different collision energies applied during MS/MS fragmentation. The MassBank ID displayed in bold indicates the depicted MS/MS spectrum. Spectra are also available electronically in the MassBank database.<sup>10</sup>

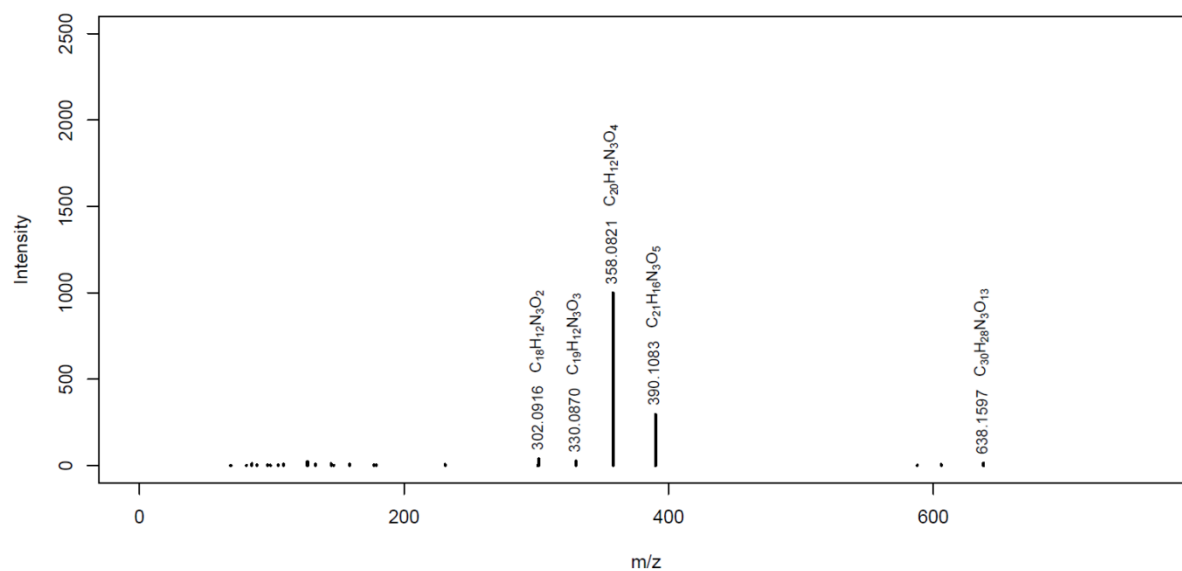
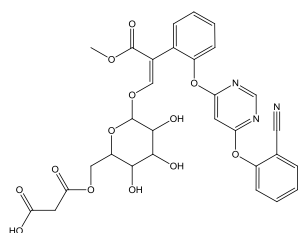
### Azoxystrobin (AZ)

MassBank ID: **ET270001**



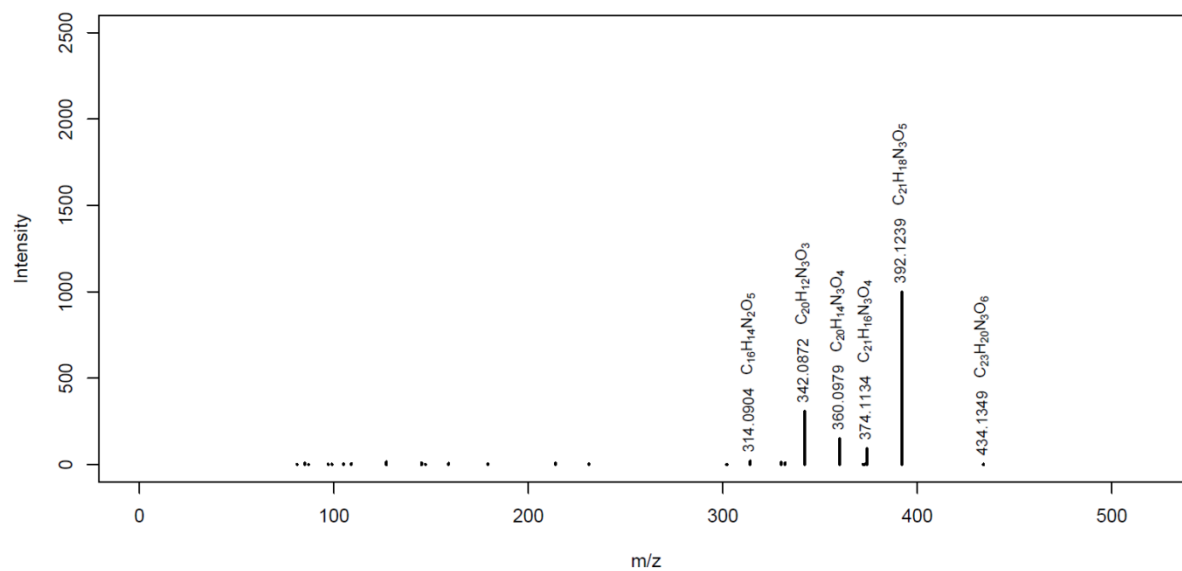
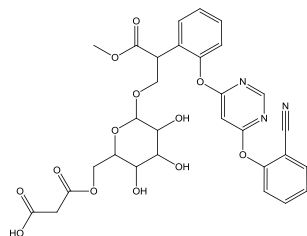
### AZ\_M638

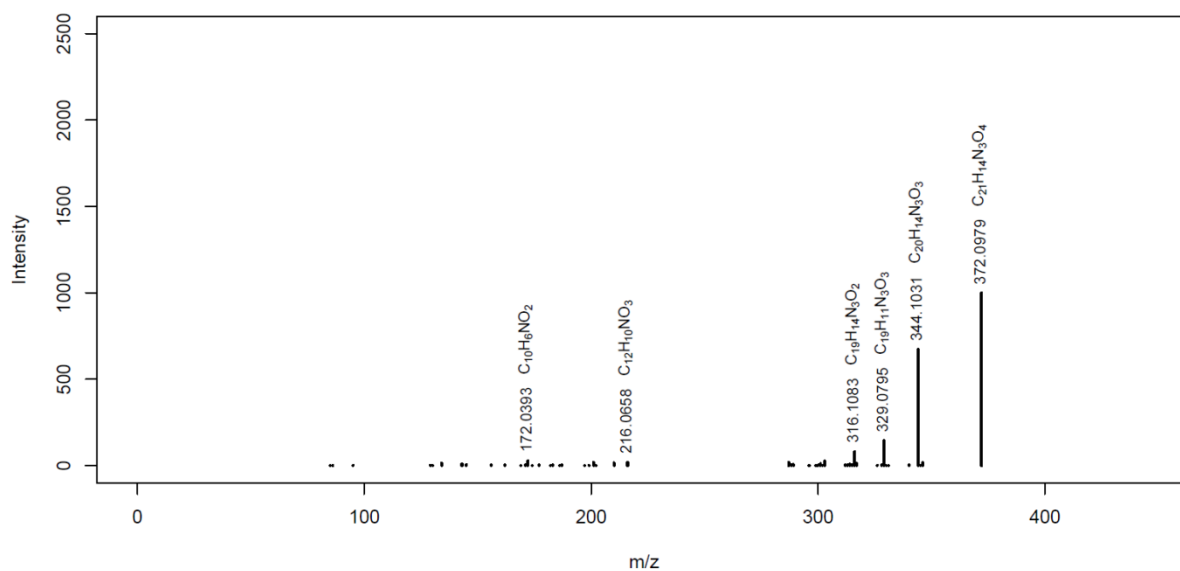
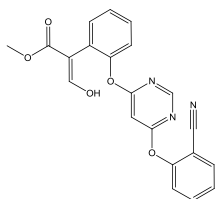
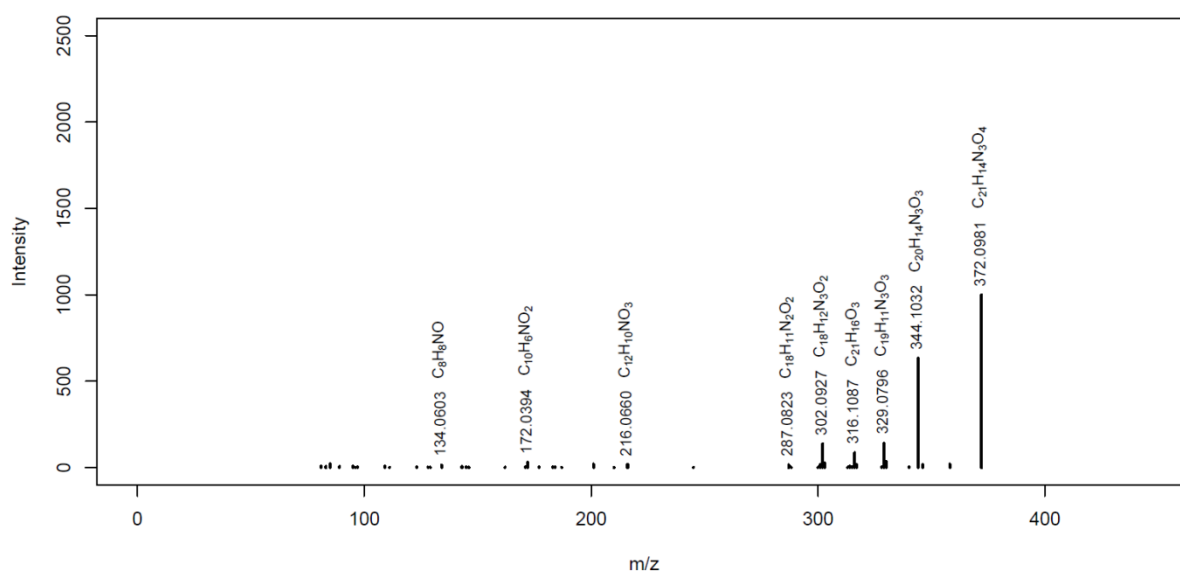
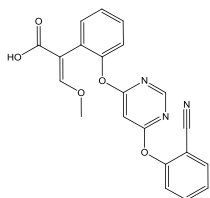
MassBank ID: **ET273401**, ET273402, ET273403, ET273404

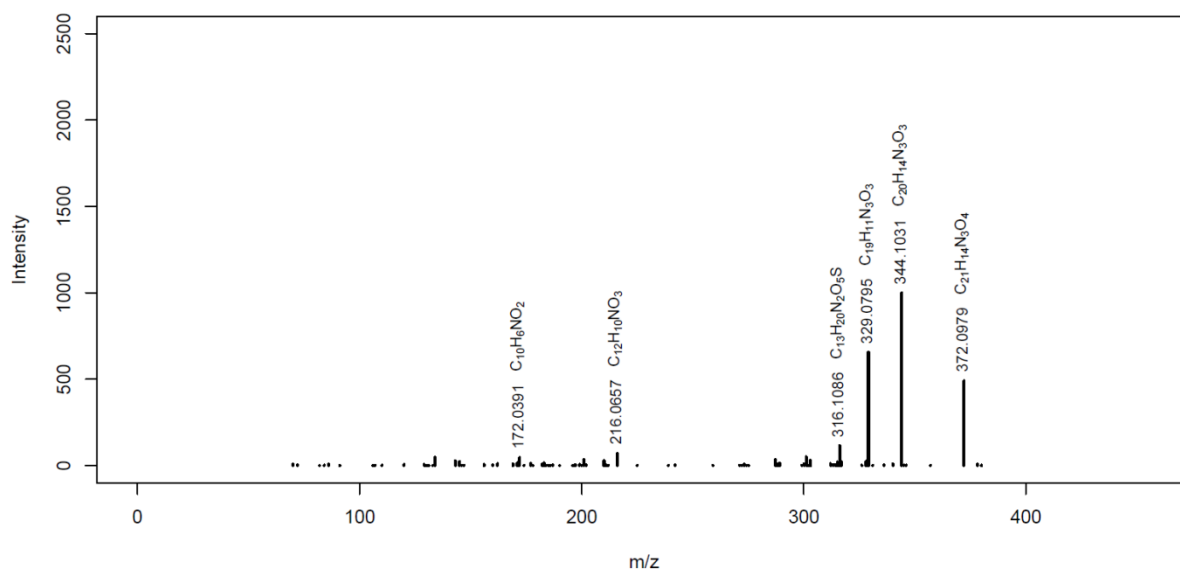
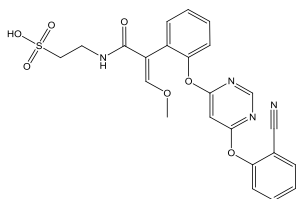
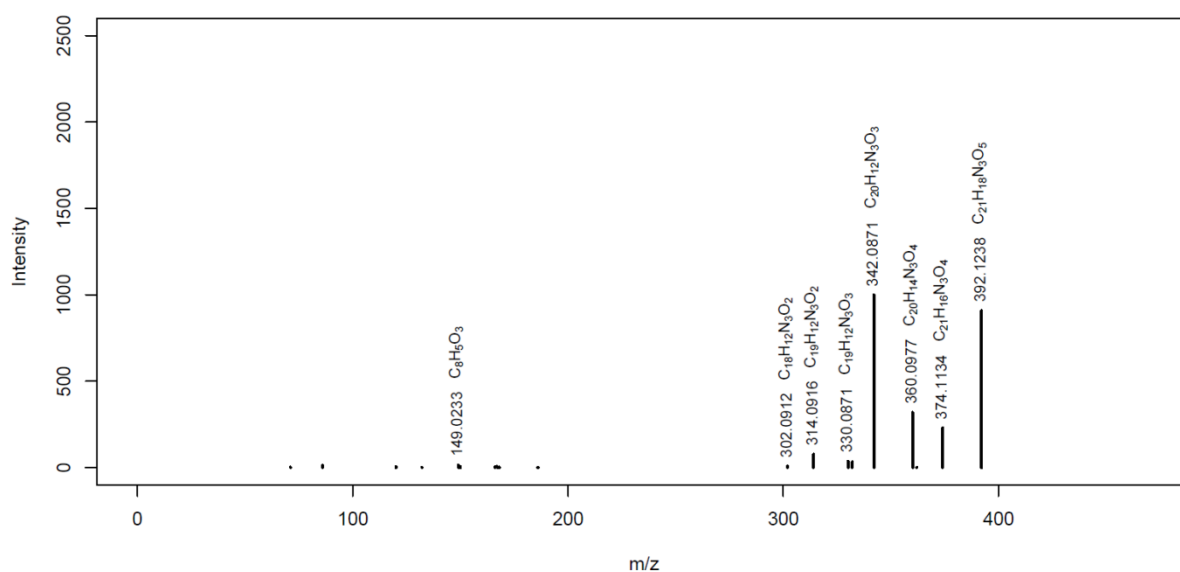
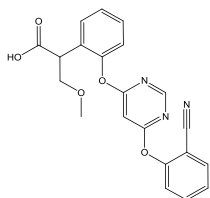


### AZ\_M640

MassBank ID: **ET273501**, ET273502, ET273503, ET273504

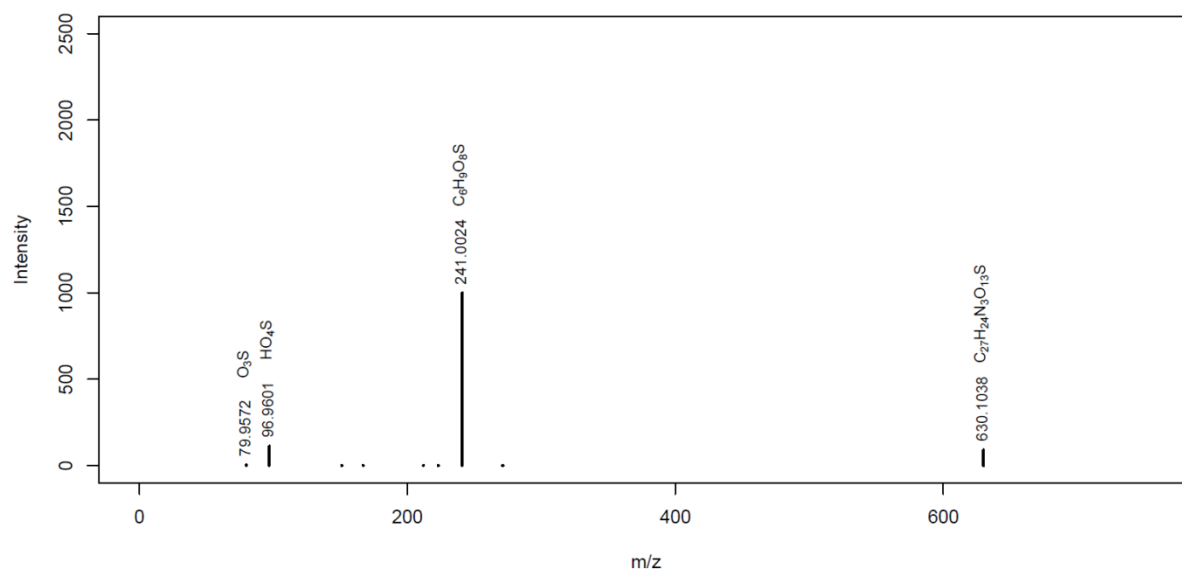
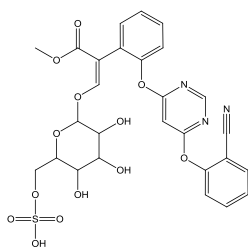


**AZ\_M390a**MassBank ID: **ET273701****AZ\_M390b**MassBank ID: **ET273801**

**AZ\_M497**MassBank ID: ET271901, **ET271902**, ET271903, ET271904**AZ\_M392**MassBank ID: **ET274601**

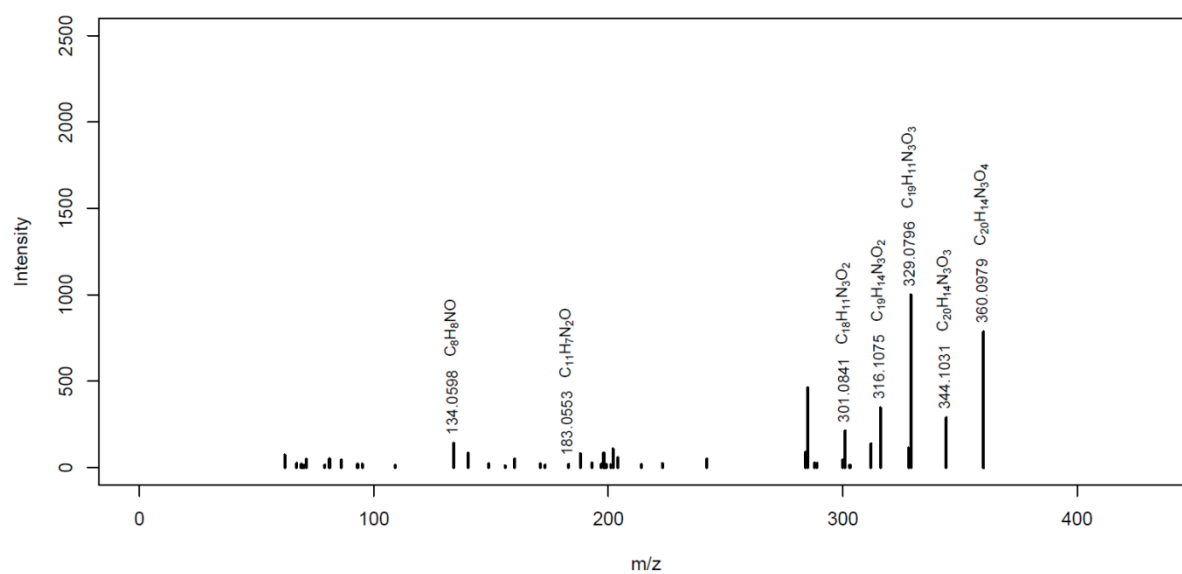
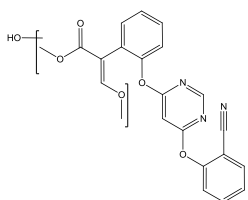
### AZ\_M630

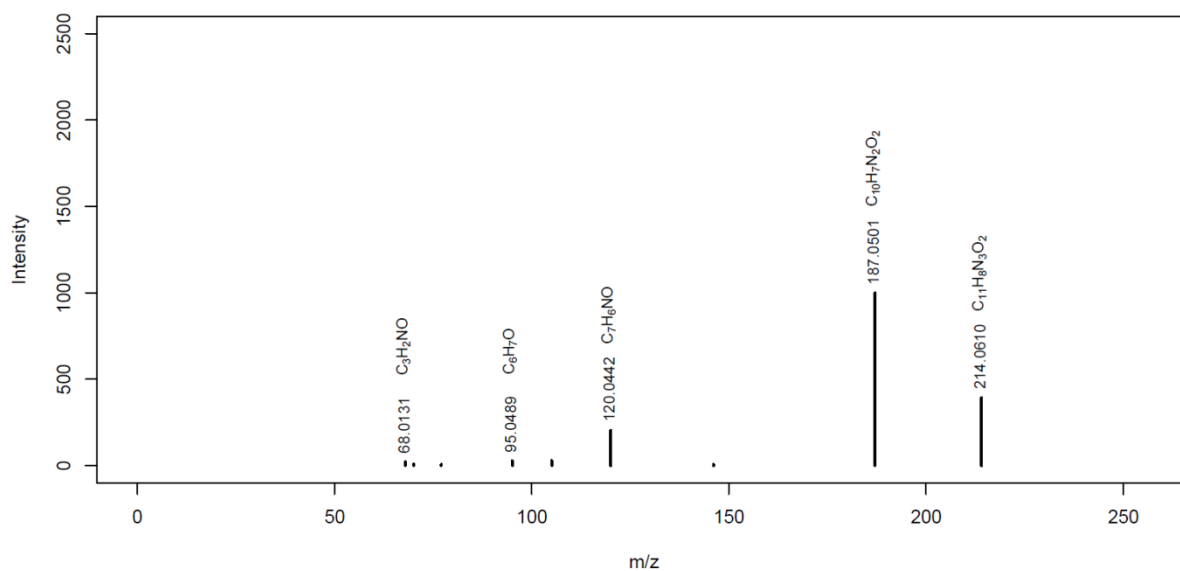
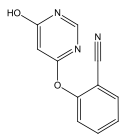
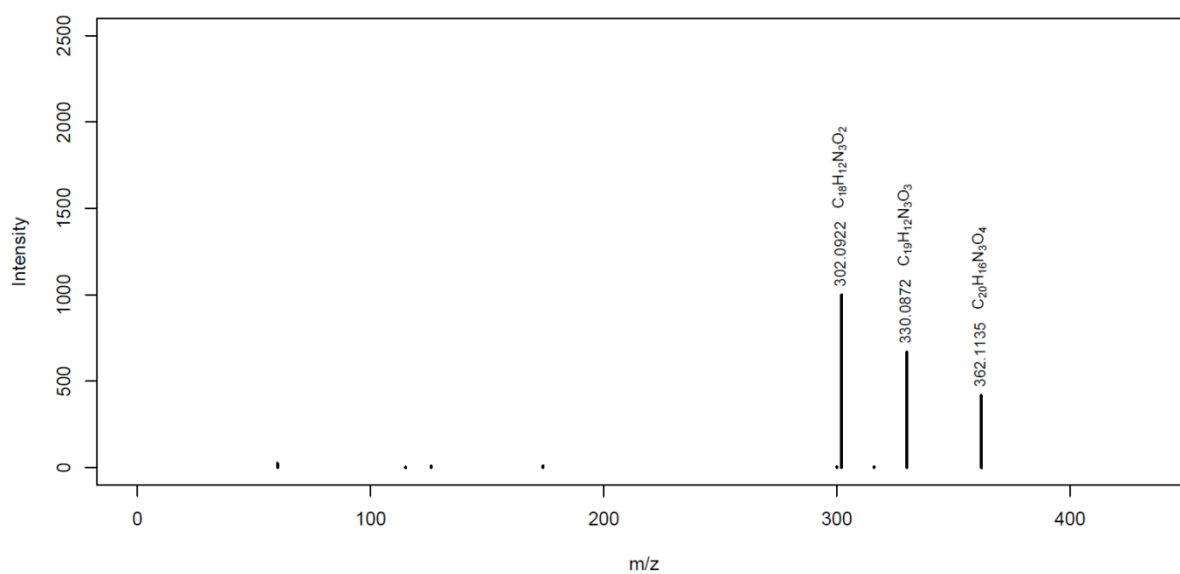
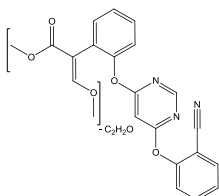
MassBank ID: ET273251



### AZ\_M420

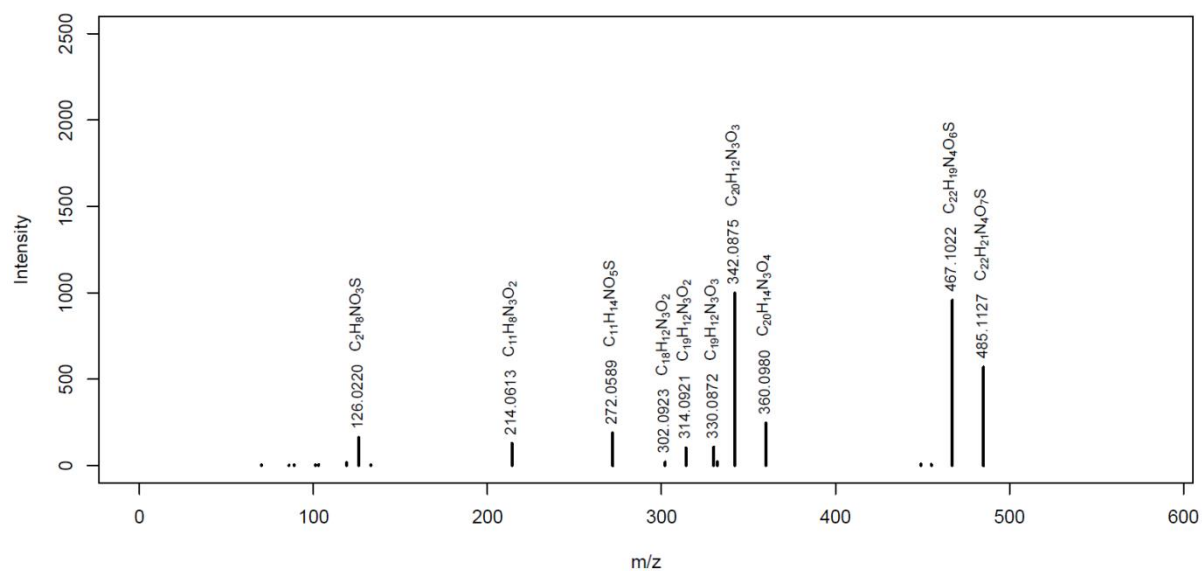
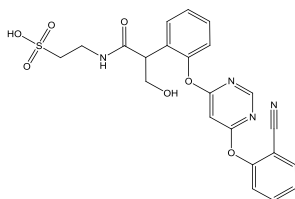
MassBank ID: ET274902



**AZ\_M214**MassBank ID: **ET274201****AZ\_M362b**MassBank ID: **ET274501**

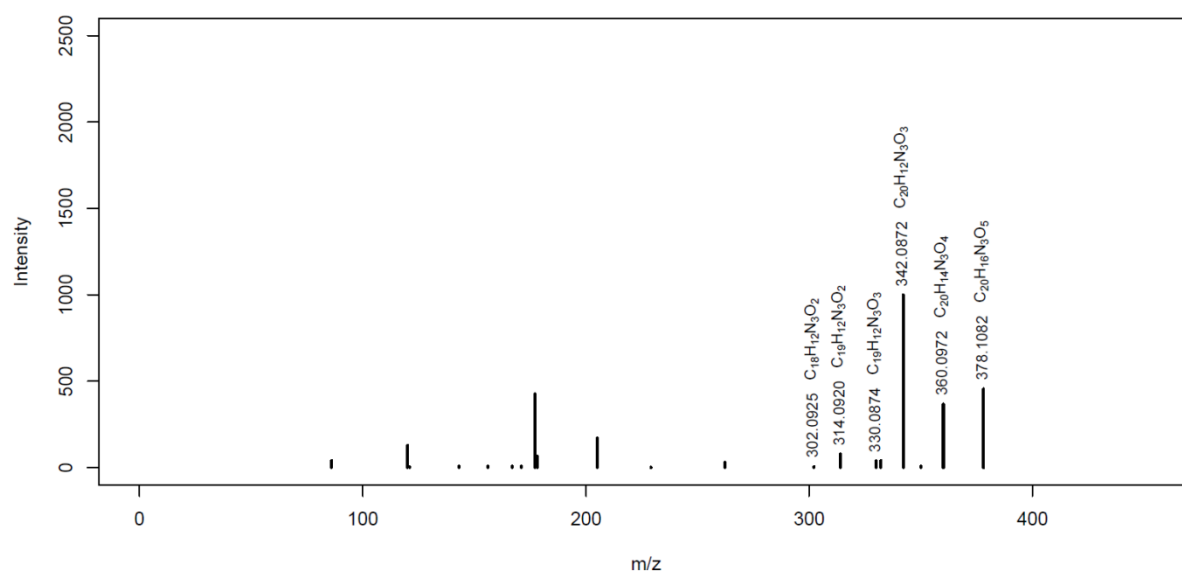
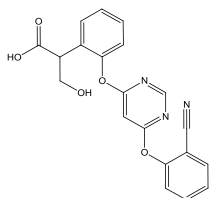
### AZ\_M485

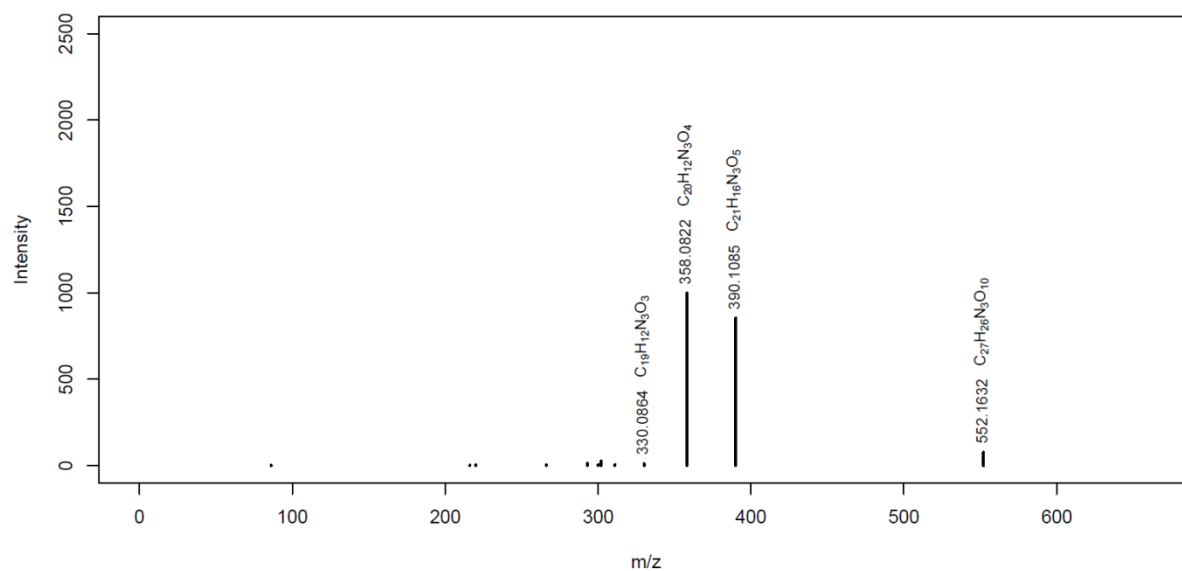
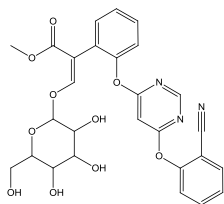
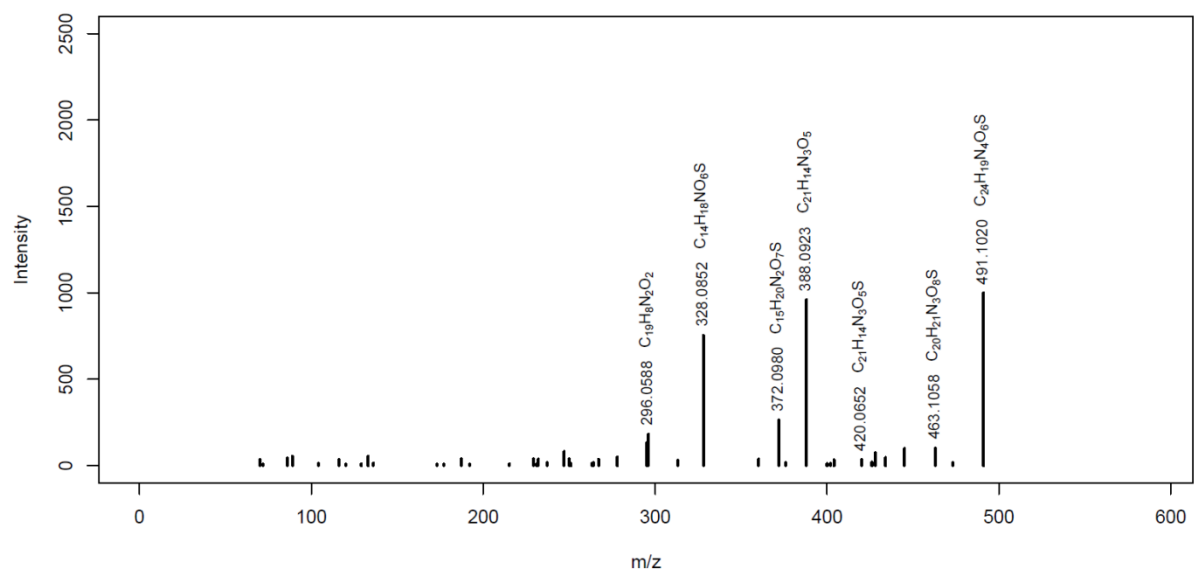
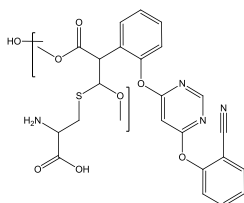
MassBank ID: ET272401, ET272402, ET272403, ET272404



### AZ\_M378

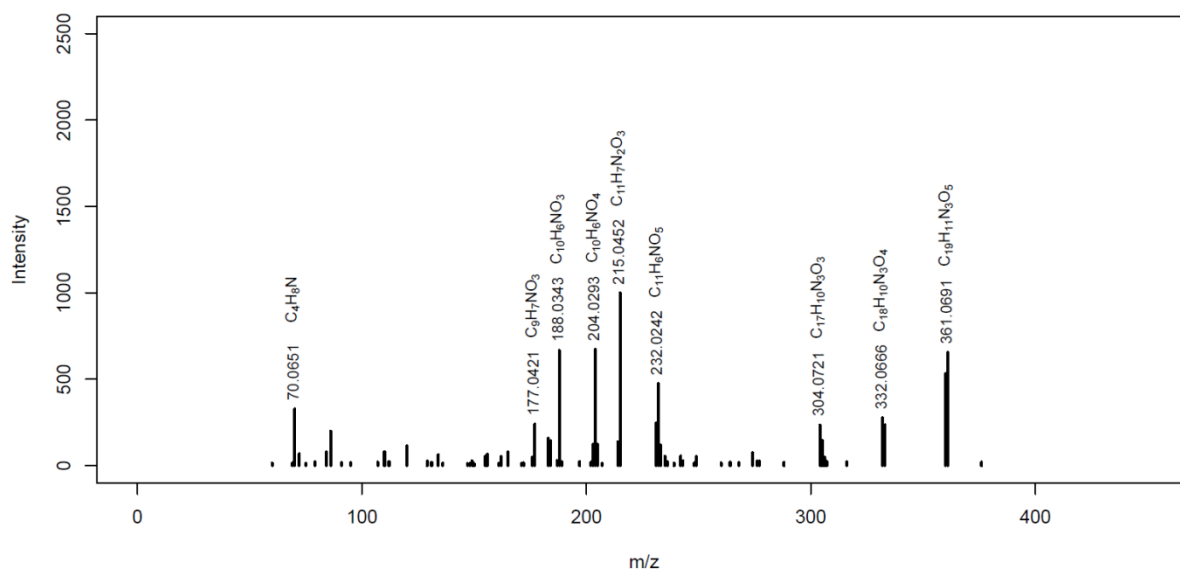
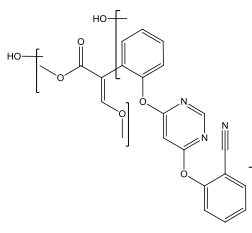
MassBank ID: ET274102



**AZ\_M552**MassBank ID: **ET273904****AZ\_M541**MassBank ID: **ET272201**, ET272202, ET272203, ET272204

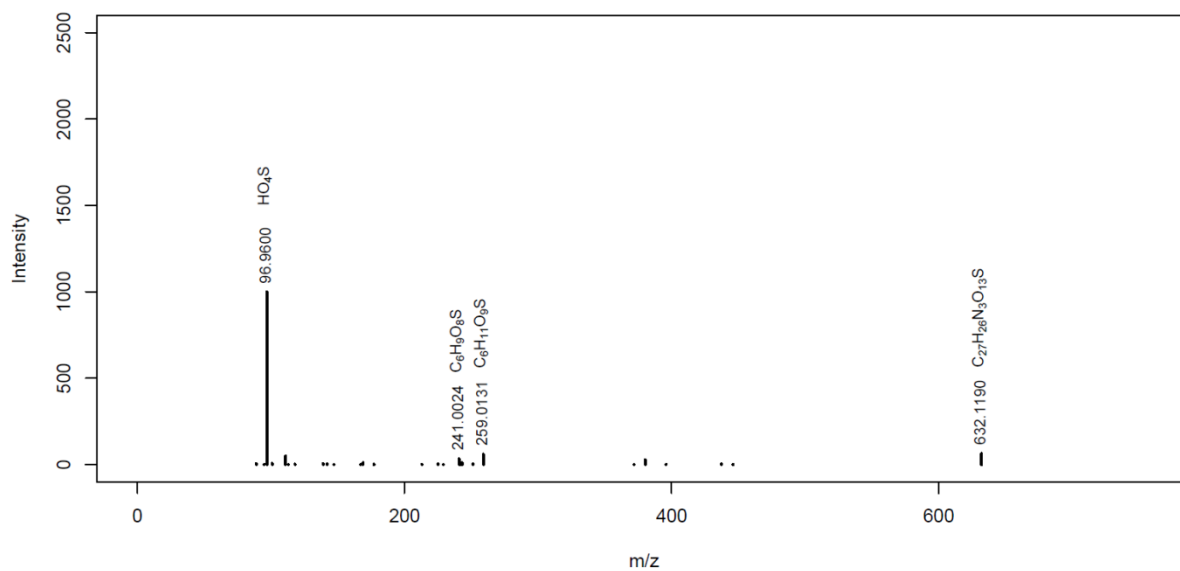
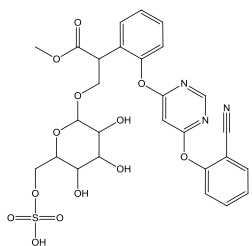
### AZ\_M436

MassBank ID: ET272301, ET272302, **ET272303**, ET272304



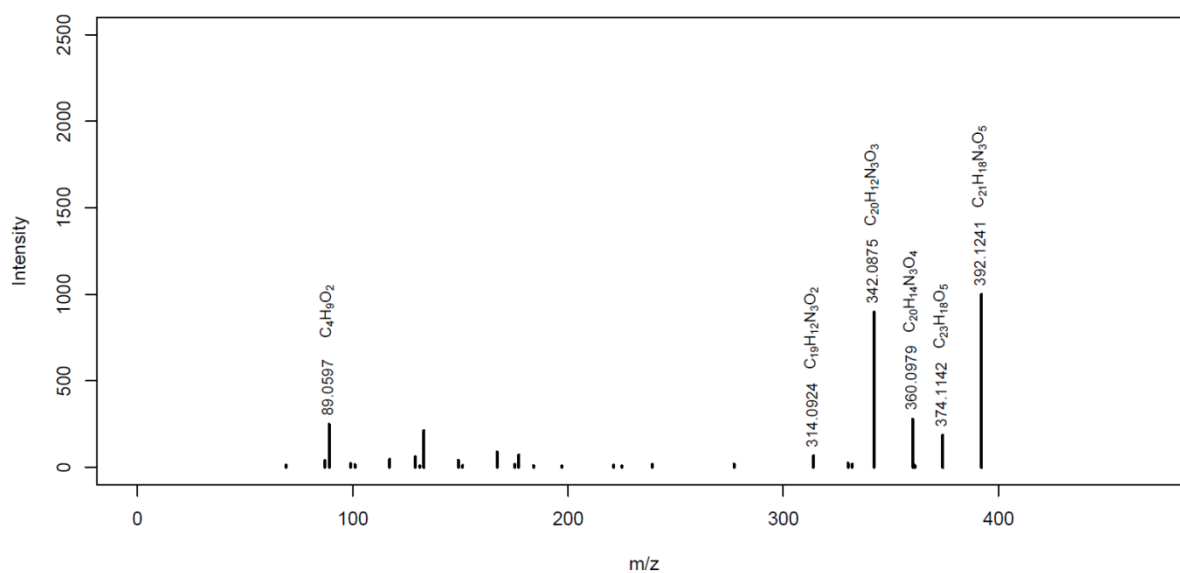
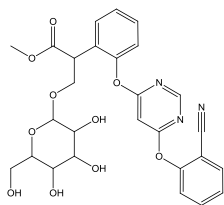
### AZ\_M632

MassBank ID: ET272951, **ET272952**, ET272953, ET272954



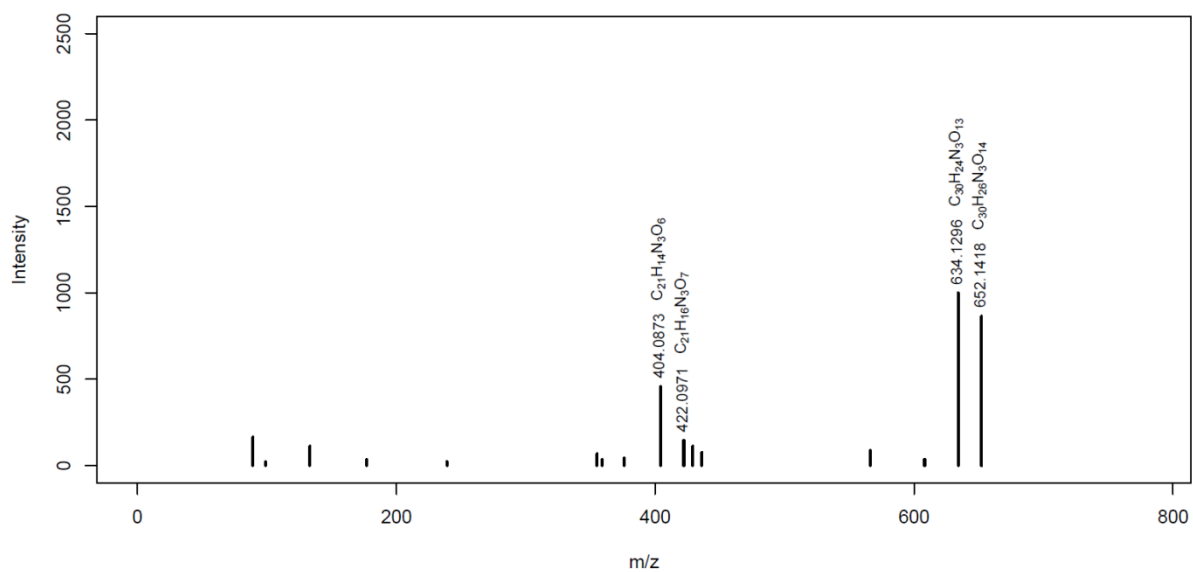
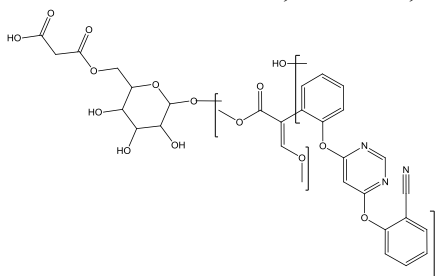
### AZ\_M554a

MassBank ID: **ET272001**, ET272002, ET272003, ET272004



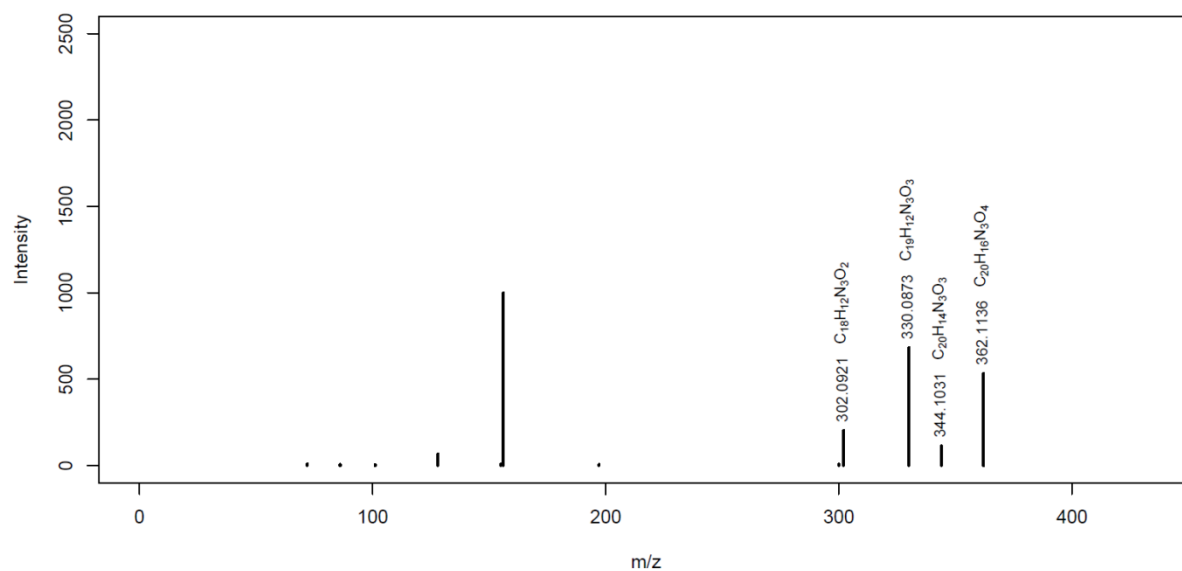
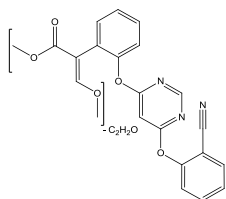
### AZ\_M684

MassBank ID: **ET273501**, ET273502, ET273503, ET273504



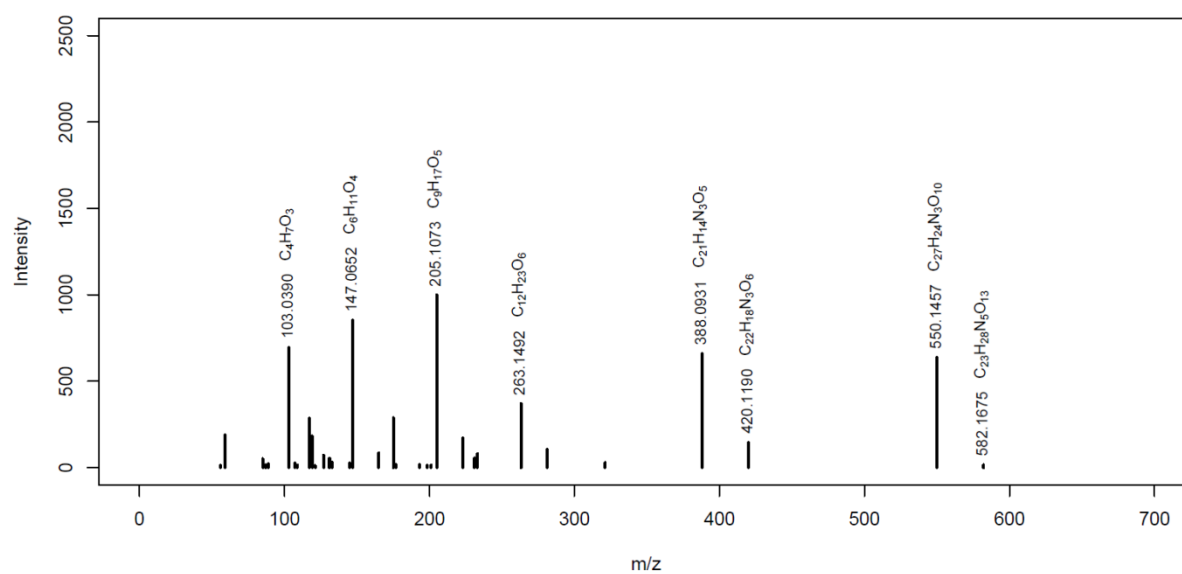
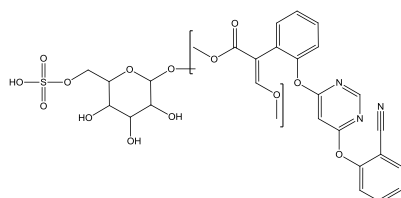
### AZ\_M362a

MassBank ID: ET274403



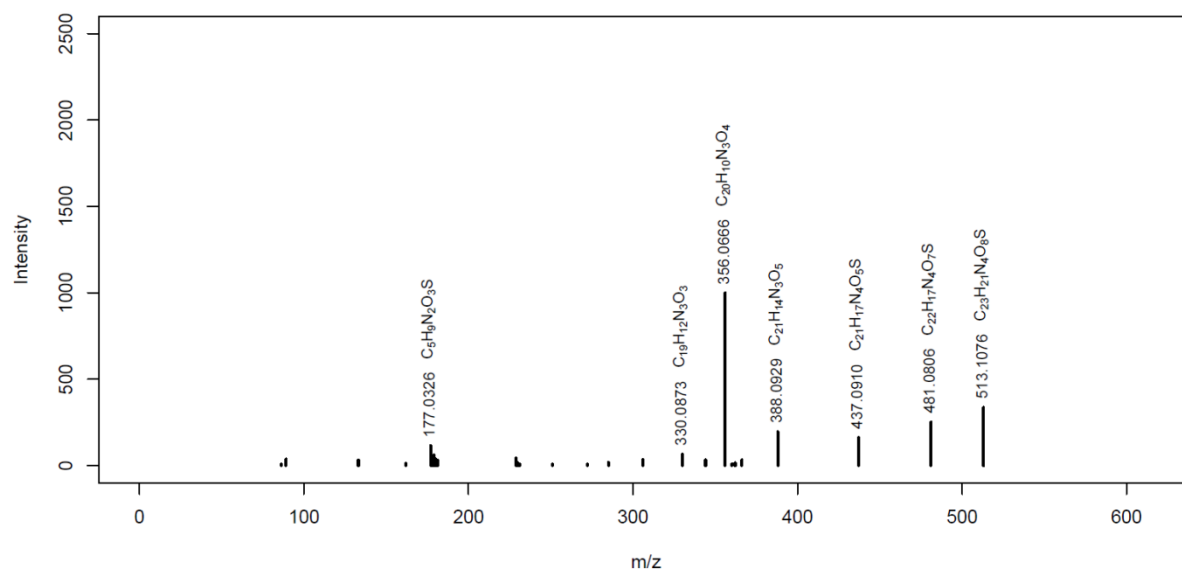
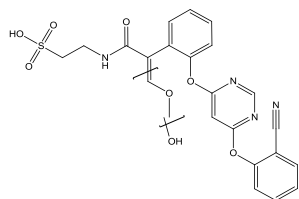
### AZ\_M660

MassBank ID: ET273601, ET273602, ET273603, ET273604



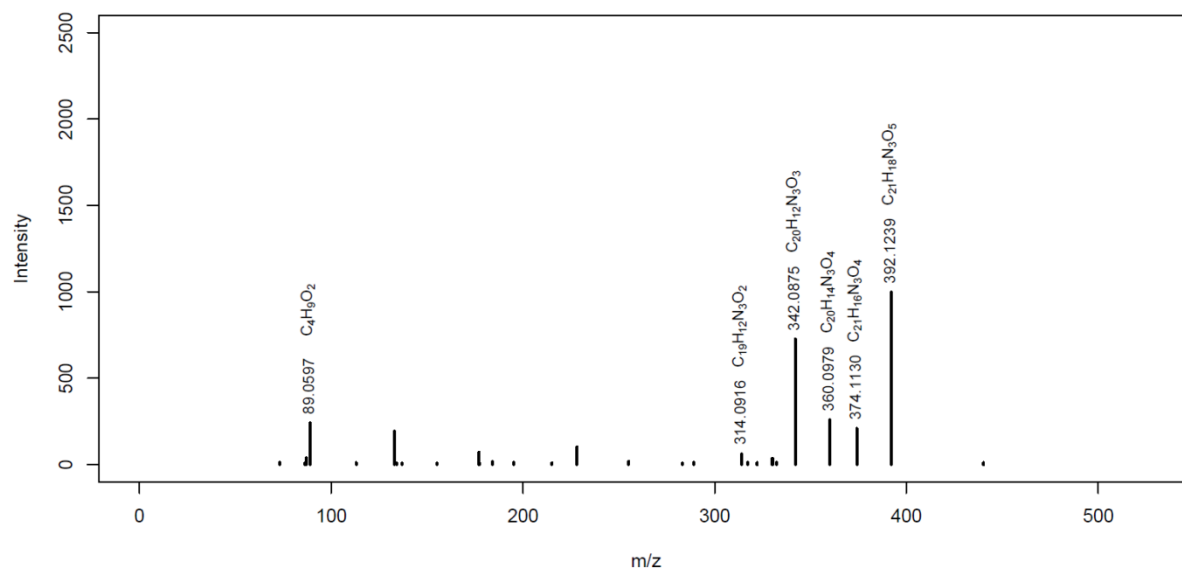
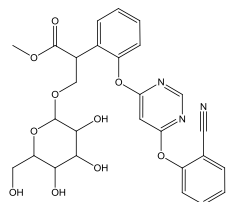
### AZ\_M513

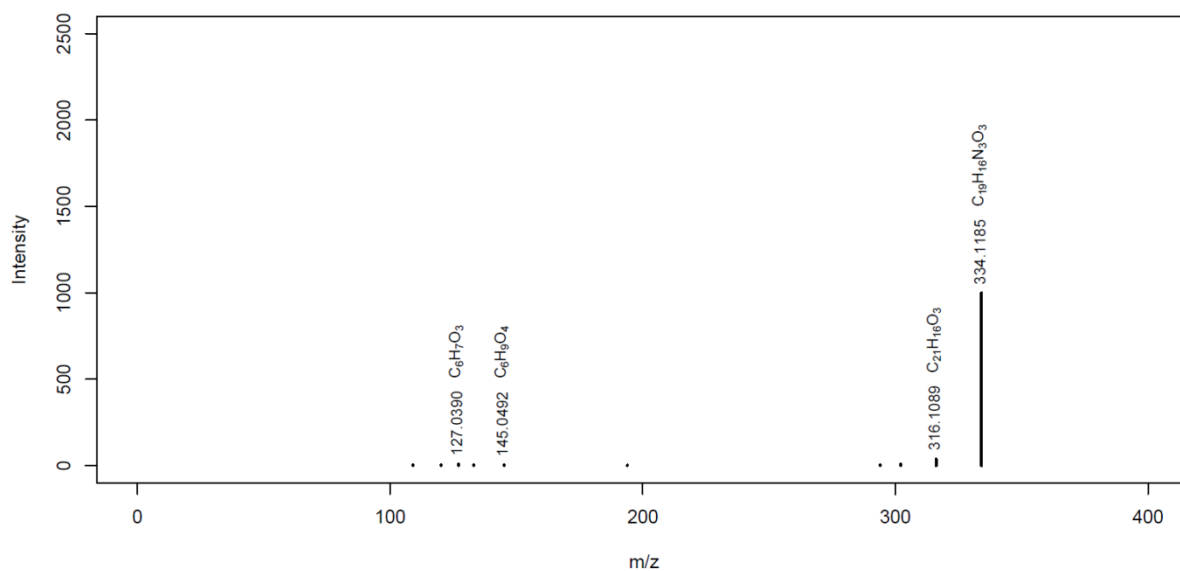
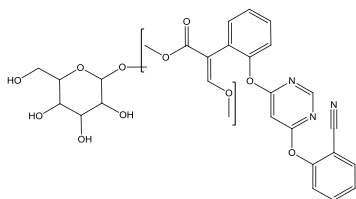
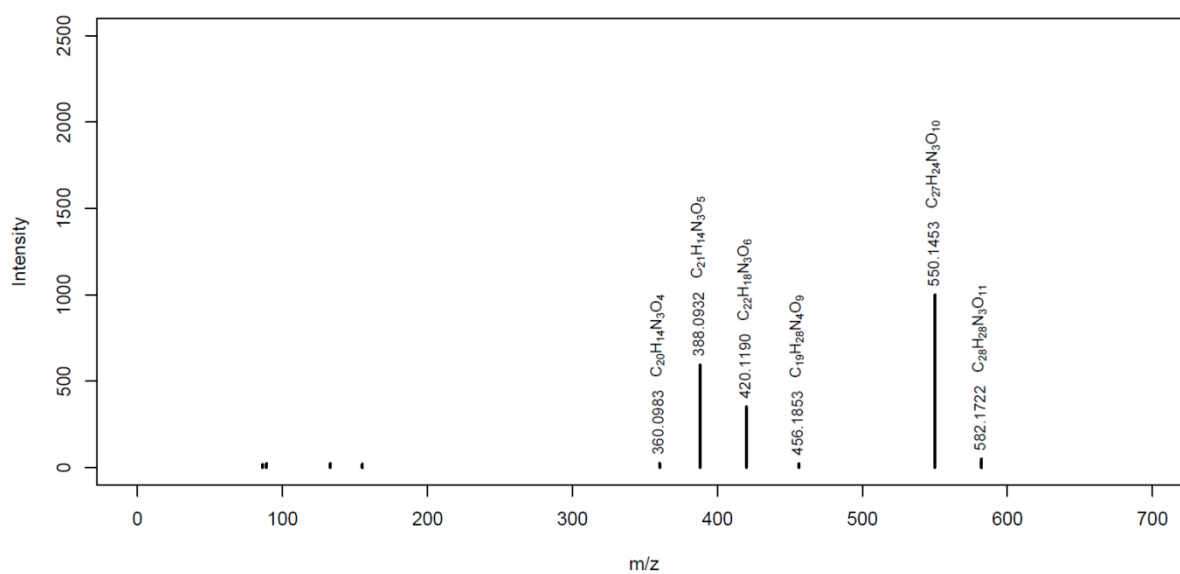
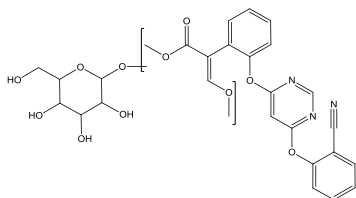
MassBank ID: **ET272701**, ET272702, ET272703, ET272704



### AZ\_M554b

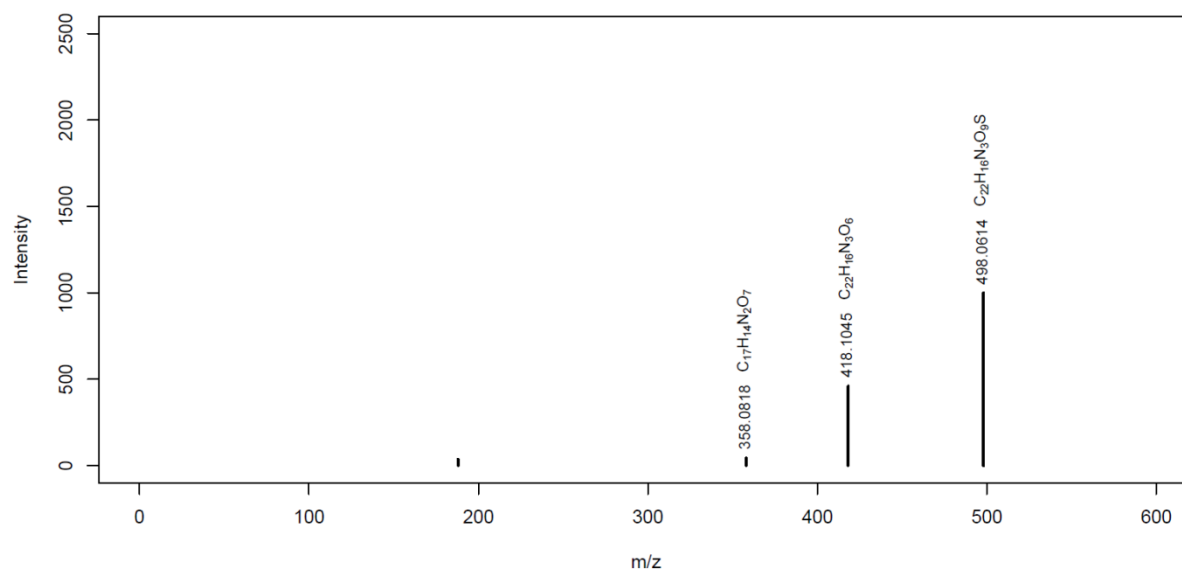
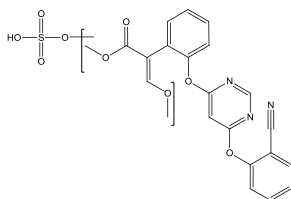
MassBank ID: **ET272101**, ET272102, ET272103, ET272104



**AZ\_M582b**MassBank ID: **ET272604****AZ\_M582a**MassBank ID: **ET272501**

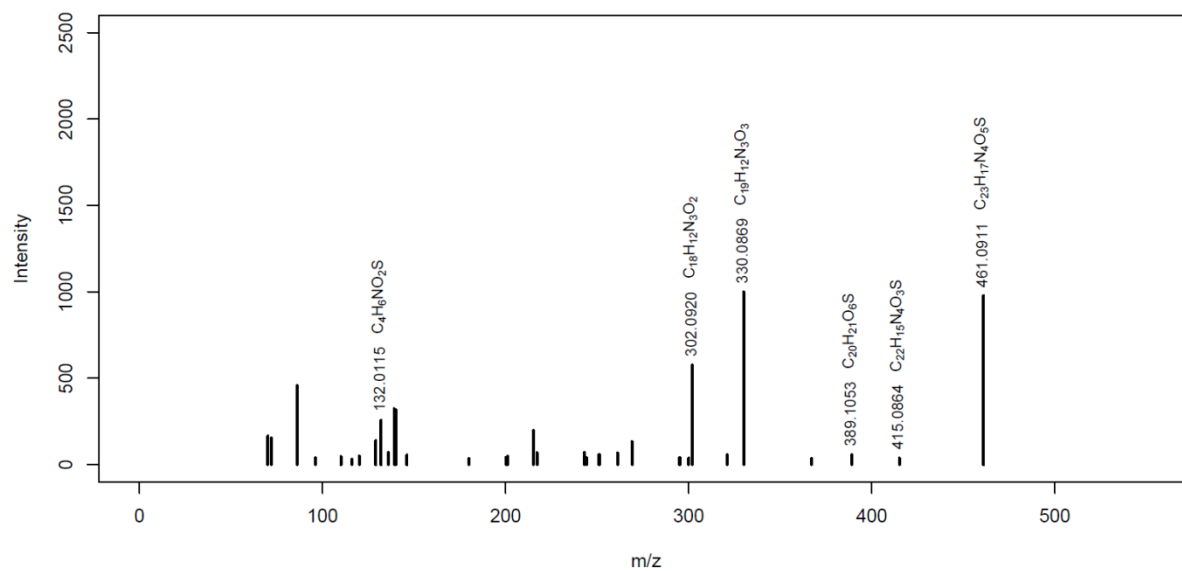
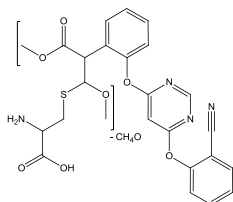
### AZ\_M498

MassBank ID: ET273152



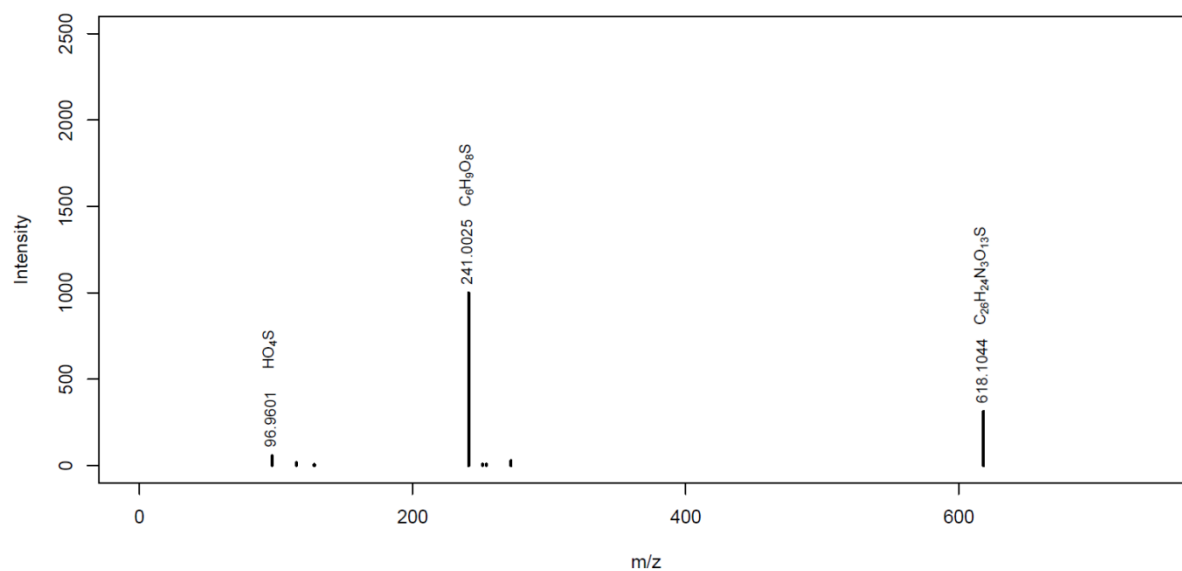
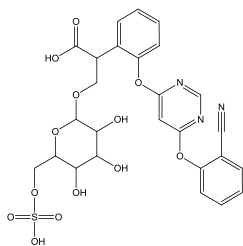
### AZ\_M493

MassBank ID: ET274303



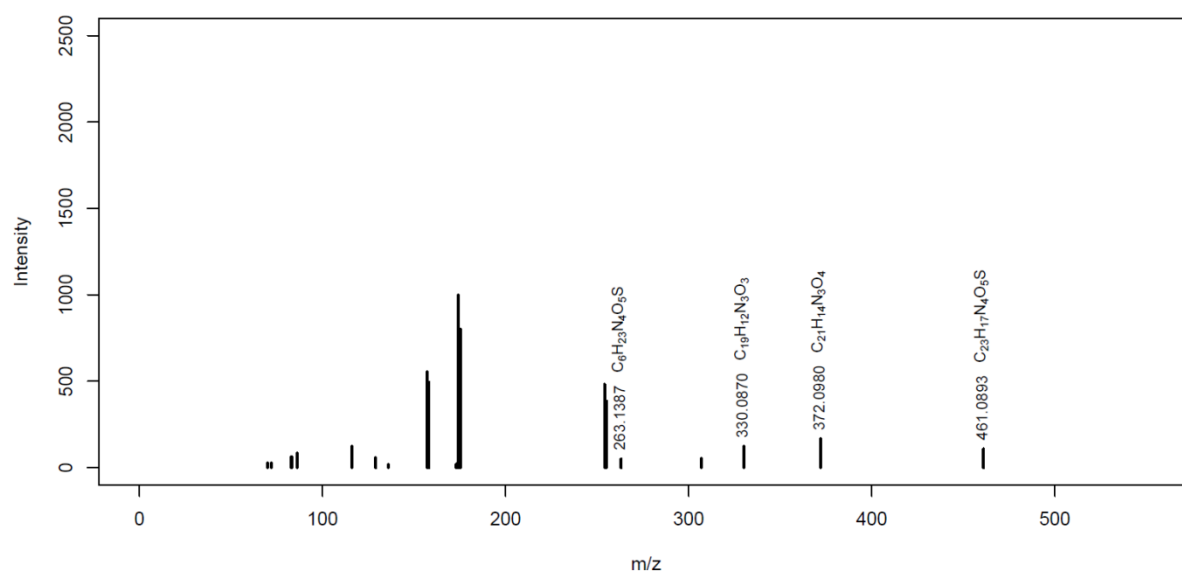
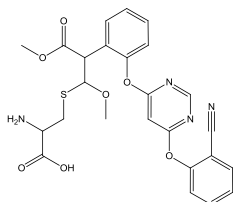
### AZ\_M618

MassBank ID: ET273051, **ET273052**, ET273053, ET273054



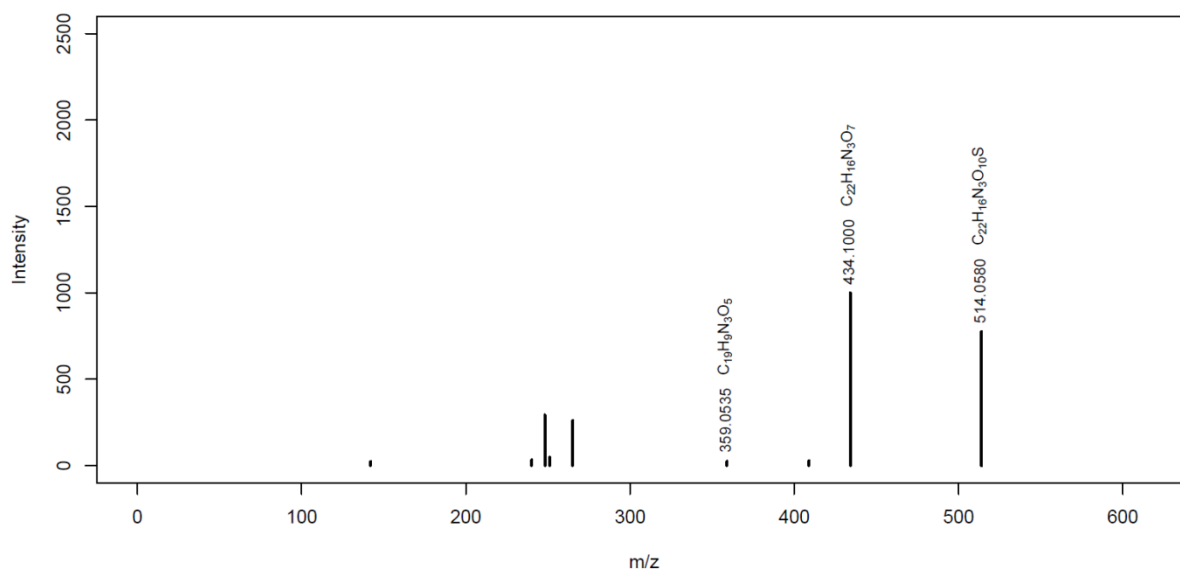
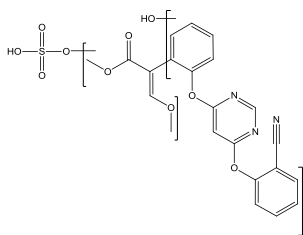
### AZ\_M525

MassBank ID: **ET274005**

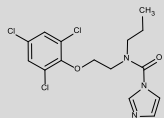


# AZ\_M514

MassBank ID: **ET272851**, ET272852, ET272853, ET272854



**Table S18: Overview of prochloraz and identified biotransformation products formed in the aquatic invertebrate *H. azteca*. Biotransformation products are listed according to their relative peak intensity. Information about mass error and retention time (RT) are given for both replicate samples. CE stands for collision energy applied for fragmentation in the MS/MS experiment. Below each biotransformation product the abbreviation (S) stands for “identified by suspect screening (S)”, whereas (N) stands for “identified by nontarget” screening. The abbreviation (H) stands for BTPs that were only identified in *H. azteca* and not in *G. pulex*. (H<sub>‡</sub>) stands for BTPs that were identified afterward in *G. pulex*, but with intensities below the set threshold of 1E6. The asterisk marks biotransformation products where the activeazole moiety was altered. The mass error of all identified BTPs was < 3ppm.**

Compound	Formula [M]	RT [min] <sup>iii)</sup>	Polarity	Elemental change <sup>iv)</sup>	Log D <sub>ow</sub> <sup>v)</sup>	Identification confidence <sup>vi)</sup>	Description	CE [eV]	MS/MS confirmatory ions <sup>viii)</sup>
MassBank ID of displayed MS/MS spectrum	Exact mass of [M+H] <sup>+</sup> / [M-H] <sup>-</sup>					/level according to Schymanski et al. (2014) <sup>11/</sup> <sup>vii)</sup>			
<b>Prochloraz (PRZ)</b>	C <sub>15</sub> H <sub>16</sub> Cl <sub>3</sub> N <sub>3</sub> O <sub>2</sub>	16.3	+		3.6	/1/	parent compound	30	308.0006
<b>ET200001</b>	376.0381	16.3							70.0288
									265.9536
BAF [L kg <sub>ww</sub> <sup>-1</sup> ] at t <sub>24</sub> <sup>ii)</sup> : 110									
BAF <sub>k</sub> [L kg <sub>ww</sub> <sup>-1</sup> ] <sup>ii)</sup> : 117									
<b>PRZ_M353 *</b>	C <sub>13</sub> H <sub>15</sub> Cl <sub>3</sub> N <sub>2</sub> O <sub>3</sub>	17.0	+	- C <sub>2</sub> HN	3.4	<b>D</b>	partial loss of hydroxylated imidazole ring,	30	<b>308.0007</b>
<b>ET202601</b>	353.0221	17.0		+ O		<b>p</b>	aldehyde formation		70.0288
<b>(S)</b>						<b>l</b> <sup>12-14</sup>			265.9536
						<b>m</b> <sup>12</sup>			
						/2b/			
<b>PRZ_M325 *</b>	C <sub>12</sub> H <sub>15</sub> Cl <sub>3</sub> N <sub>2</sub> O <sub>2</sub>	17.1	+	- C <sub>3</sub> HN	3.4	<b>D</b>	partial loss of imidazole ring	35	<b>282.0213</b>
<b>ET202701</b>	325.0272	17.2				<b>l</b> <sup>13-15</sup>			<b>325.0273</b>
<b>(S)</b>						<b>p</b>			129.1022
						/1/			

Compound MassBank ID of displayed MS/MS spectrum	Formula [M] Exact mass of [M+H] <sup>+</sup> / [M-H] <sup>-</sup>	RT [min] <sup>iii)</sup>	Polarity	Elemental change <sup>iv)</sup>	Log D <sub>ow</sub> <sup>v)</sup>	Identification confidence <sup>vi)</sup>  /level according to Schymanski et al. (2014) <sup>i1)</sup> / vii)	Description	CE [eV]	MS/MS confirmatory ions <sup>viii)</sup>
<b>PRZ_M558 * (H)</b>	C <sub>20</sub> H <sub>26</sub> Cl <sub>3</sub> N <sub>3</sub> O <sub>7</sub> S	16.7	+	- C <sub>3</sub> H <sub>2</sub> N <sub>2</sub>	-2.9	<b>D</b>	loss of imidazole ring,	20	<b>308.0009</b>
<b>ET204901</b>	558.0630	16.7		+ C <sub>10</sub> H <sub>15</sub> N <sub>3</sub> O <sub>6</sub> S		<b>p</b>	glutathione conjugation,		<b>429.0207</b>
(S)				- C <sub>2</sub> H <sub>5</sub> NO <sub>2</sub>		/2b/ most likely structure	loss of glycine		558.0634
<b>PRZ_M282 *</b>	C <sub>11</sub> H <sub>14</sub> Cl <sub>3</sub> NO	13.7	+	- C <sub>4</sub> H <sub>2</sub> N <sub>2</sub> O	2.4	<b>D</b>	loss of imidazole ring and CO	30	<b>282.0212</b>
<b>ET203201</b>	282.0214	13.7				<b>p</b>			86.0964
(S)						/1/			72.0807
<b>PRZ_M323b *</b>	C <sub>12</sub> H <sub>12</sub> Cl <sub>3</sub> NO <sub>3</sub>	16.0	+	- C <sub>3</sub> H <sub>4</sub> N <sub>2</sub>	2.6-3.2	<b>d</b> for keto group at propyl side chain (low intense diagnostic fragment in <i>G. pulex</i> , in <i>H. azteca</i> missing, most likely same position of aliphatic hydroxylation in <i>H. azteca</i> compared to <i>G. pulex</i> )	imidazole ring loss,	30	84.0808
<b>ET202301</b>	323.9956	16.0		+ O			aliphatic hydroxylation and further oxidation to a ketone		128.0706
(S)						/3/, 3 positional isomers			280.0057
<b>PRZ_M239 *</b>	C <sub>8</sub> H <sub>8</sub> Cl <sub>3</sub> NO	12.8	+	- C <sub>7</sub> H <sub>8</sub> N <sub>2</sub> O	1.4	<b>D</b>	remaining chlorophenyl moiety and C <sub>2</sub> H <sub>5</sub> NO	30	<b>239.9743</b>
<b>ET202501</b>	239.9744	12.8				/2b/			222.9481
(S)									196.9315
<b>PRZ_M392b *</b>	C <sub>15</sub> H <sub>16</sub> Cl <sub>3</sub> N <sub>3</sub> O <sub>3</sub>	15.4	+	+ O	2.3	<b>d, p</b> for hydroxylation at C-5 in imidazole ring (possible epoxide formation at C4-C5 as intermediate)	imidazole ring hydroxylation	30	<b>308.0006</b>
<b>ET202201</b>	392.0330	15.4							70.0287
(S)						/3/, most likely structure			265.9535
<b>PRZ_M435 *</b>	C <sub>17</sub> H <sub>21</sub> Cl <sub>3</sub> N <sub>4</sub> O <sub>3</sub>	15.5	+	+ C <sub>2</sub> H <sub>2</sub> O	-	<b>d</b> for acetylation at CO- imidazole ring moiety	acetylation at CO-imidazole ring moiety; NH <sub>4</sub> <sup>+</sup> adduct	20	<b>282.0212</b>
<b>(NH<sub>4</sub><sup>+</sup> adduct)</b>	435.0752	15.5							435.0750
<b>ET203301</b>						/3/, acetylation most likely at keto group			154.0610
(S)									

Compound	Formula [M]	RT [min] <sup>iii)</sup>	Polarity	Elemental change <sup>iv)</sup>	Log D <sub>ow</sub> <sup>v)</sup>	Identification confidence <sup>vi)</sup>	Description	CE [eV]	MS/MS confirmatory ions <sup>viii)</sup>
MassBank ID of displayed MS/MS spectrum	Exact mass of [M+H] <sup>+</sup> / [M-H] <sup>-</sup>					/level according to Schymanski et al. (2014) <sup>11/</sup> <sup>vii)</sup>			
<b>PRZ_M640 (H<sub>2</sub><sup>+</sup>)</b>	C <sub>24</sub> H <sub>28</sub> Cl <sub>3</sub> N <sub>3</sub> O <sub>11</sub>	11.7-14.4	+	+ O	-1.9 to -2.8	<b>d, p</b>	Hydroxylation at propyl side chain,	20	<b>323.9958</b>
<b>ET204101</b>	640.0862	(4 partly separated peaks)		+ C <sub>6</sub> H <sub>10</sub> O <sub>5</sub>		/3/, most likely structure	glucose conjugation,		69.0449
<b>(N)</b>				+ C <sub>3</sub> H <sub>2</sub> O <sub>3</sub>			malonyl conjugation		128.9958
<b>PRZ_M323a *</b>	C <sub>12</sub> H <sub>12</sub> Cl <sub>3</sub> NO <sub>3</sub>	15.7	+	- C <sub>3</sub> H <sub>4</sub> N <sub>2</sub>	2.6-3.2	<b>d</b> for keto group at propyl side chain (low intense diagnostic fragment in <i>G. pulex</i> , in <i>H. azteca</i> missing, most likely same position of aliphatic hydroxylation in <i>H. azteca</i> compared to <i>G. pulex</i> )	imidazole ring loss,	30	84.0808
<b>ET202401</b>	323.9956	15.7		+ O			aliphatic hydroxylation and further oxidation to a ketone		128.0706
<b>(S)</b>						/3/, 3 positional isomers			280.0057
<b>PRZ_M382 *</b>	C <sub>14</sub> H <sub>18</sub> Cl <sub>3</sub> N <sub>3</sub> O <sub>3</sub>	16.6	+	- CH <sub>2</sub>	3.02	<b>d, p</b> for C-4 loss at hydroxylated (at C-5) imidazole ring	partial loss of hydroxylated imidazole ring	20	<b>308.0007</b>
<b>ET203401</b>	382.0487	16.6		+ O					<b>365.0225</b>
<b>(S)</b>						/3/, most likely structure			<b>337.0271</b>
<b>PRZ_M326 * (H)</b>	C <sub>11</sub> H <sub>10</sub> Cl <sub>3</sub> NO <sub>4</sub>	14.5	+	- C <sub>4</sub> H <sub>2</sub> N <sub>2</sub> O	-	<b>d</b> for at least two hydroxylations at the aliphatic part of the molecule	loss of imidazole ring and CO, hydroxylations and further oxidations to ketones	20	<b>130.0501</b>
<b>ET204201</b>	325.9748	14.5		+ OH					265.9540
<b>(S)</b>				+ O		/3/, several positional isomers			325.9751
				+ O					
<b>PRZ_M298 *</b>	C <sub>11</sub> H <sub>14</sub> Cl <sub>3</sub> NO <sub>2</sub>	13.3	+	- C <sub>4</sub> H <sub>2</sub> N <sub>2</sub> O	1.4-2.9	/3/, 6 positional isomers	loss of imidazole ring and CO, hydroxylation	50	70.0651
<b>ET202801</b>	298.0163	13.3		+ O					280.0061
<b>(S)</b>									222.9483
<b>PRZ_M392a</b>	C <sub>15</sub> H <sub>16</sub> Cl <sub>3</sub> N <sub>3</sub> O <sub>3</sub>	14.2	+	+ O	2.1-2.5	<b>d</b> for hydroxylation at propyl side chain	aliphatic hydroxylation	30	<b>251.9742</b>
<b>ET202101</b>	392.0330	14.2							69.0447
<b>(S)</b>						/3/, 3 positional isomers			128.0706

Compound	Formula [M]	RT [min] <sup>iii)</sup>	Polarity	Elemental change <sup>iv)</sup>	Log D <sub>ow</sub> <sup>v)</sup>	Identification confidence <sup>vi)</sup>	Description	CE [eV]	MS/MS confirmatory ions <sup>viii)</sup>
MassBank ID of displayed MS/MS spectrum	Exact mass of [M+H] <sup>+</sup> / [M-H] <sup>-</sup>					/level according to Schymanski et al. (2014) <sup>i)</sup> / <sup>vii)</sup>			
<b>PRZ_M589 (H)</b>	C <sub>24</sub> H <sub>25</sub> O <sub>8</sub> N <sub>3</sub> Cl <sub>3</sub>	14.8	+			/4/	unclear, most likely related to PRZ_M435*	20	282.0218
<b>ET204001</b>	589.0780	14.7							308.0646
<b>(N)</b>									264.0748
<b>PRZ_M374 (H)</b>	C <sub>15</sub> H <sub>14</sub> Cl <sub>3</sub> N <sub>3</sub> O <sub>2</sub>	17.0	+	- H <sub>2</sub>	3.5-3.7	/3/, 3 positional isomers	dehydrogenation	20	305.9851
<b>ET205001</b>	374.0224	17.0							277.9902
<b>(S)</b>									222.9478
<b>PRZ_M397 *(H<sub>2</sub><sup>+</sup>)</b>	C <sub>15</sub> H <sub>19</sub> Cl <sub>3</sub> N <sub>2</sub> O <sub>4</sub>	17.5	+	+ O	1.9	d, p	N loss of dihydroxylated imidazole ring	20	<b>308.0010</b>
<b>ET204301</b>	397.0483	17.6		+ O					<b>397.0488</b>
<b>(S)</b>				- NH <sub>4</sub>					265.9539
<b>PRZ_M615 * (H)</b>	C <sub>22</sub> H <sub>29</sub> Cl <sub>3</sub> N <sub>4</sub> O <sub>8</sub> S	16.5	+	- C <sub>3</sub> H <sub>2</sub> N <sub>2</sub>	-4	<b>d, p</b>	loss of imidazole ring,	15	<b>486.0418</b>
<b>ET203701</b>	615.0844	16.4		+ C <sub>10</sub> H <sub>15</sub> N <sub>3</sub> O <sub>6</sub> S		/3/, most likely structure	glutathione conjugation		<b>383.0152</b>
<b>(S)</b>									615.0841
<b>PRZ_M386 *(H<sub>2</sub><sup>+</sup>)</b>	C <sub>12</sub> H <sub>13</sub> Cl <sub>3</sub> N <sub>2</sub> O <sub>4</sub> S	14.2	+	- C <sub>3</sub> H <sub>2</sub> N <sub>2</sub>	0.3	<b>D</b>	loss of imidazole ring,	15	<b>122.0270</b>
<b>ET201902</b>	386.9734	14.2		- C <sub>3</sub> H <sub>6</sub>		/2b/	loss of propyl side chain,		<b>239.9739</b>
<b>(S)</b>				+ C <sub>3</sub> H <sub>5</sub> NO <sub>2</sub> S			cysteine product		386.9738
<b>PRZ_M573.1 * (H)</b>	C <sub>24</sub> H <sub>25</sub> Cl <sub>3</sub> N <sub>3</sub> O <sub>7</sub>	16.1	+	- C <sub>3</sub> HN	-1.9	<b>d, p</b>	partial loss of imidazole ring,	20	<b>325.0276</b>
<b>ET204801</b>	573.0830	16.2		+ C <sub>6</sub> H <sub>10</sub> O <sub>5</sub>		/3/, most likely structure	glucose conjugation,		308.0010
<b>(N)</b>				+ C <sub>3</sub> H <sub>2</sub> O <sub>3</sub>			malonyl conjugation		367.0383
<b>PRZ_M632c (H)</b>	C <sub>21</sub> H <sub>26</sub> Cl <sub>3</sub> N <sub>3</sub> O <sub>11</sub> S	12.7	- <sup>(ix)</sup>	+ O		/4/	unclear, sulfate and glucose attached at different sites	40	194.9176
<b>ET203152</b>	632.0281	12.7		+ C <sub>6</sub> H <sub>10</sub> O <sub>8</sub> S					96.9601
<b>(S)</b>									436.1038
<b>PRZ_M573 *</b>	C <sub>19</sub> H <sub>23</sub> Cl <sub>3</sub> N <sub>4</sub> O <sub>8</sub> S	14.0	+	- C <sub>3</sub> H <sub>2</sub> N <sub>2</sub>	-1.9	/3/, most likely structure	loss of imidazole ring,	10	573.0375
<b>ET203502</b>	573.0375	14.0		- C <sub>3</sub> H <sub>6</sub>			loss of propyl side chain,		443.9947
<b>(S)</b>				+ C <sub>10</sub> H <sub>15</sub> N <sub>3</sub> O <sub>6</sub> S			glutathione conjugation		340.9676

Compound MassBank ID of displayed MS/MS spectrum	Formula [M] Exact mass of [M+H] <sup>+</sup> / [M-H] <sup>-</sup>	RT [min] <sup>iii)</sup>	Polarity	Elemental change <sup>iv)</sup>	Log D <sub>ow</sub> <sup>v)</sup>	Identification confidence <sup>vi)</sup>  /level according to Schymanski et al. (2014) <sup>11)/ vii)</sup>	Description	CE [eV]	MS/MS confirmatory ions <sup>viii)</sup>
PRZ_M310 *	C <sub>12</sub> H <sub>14</sub> O <sub>2</sub> NCl <sub>3</sub>	16.9/17.5	+	- C <sub>3</sub> H <sub>2</sub> N <sub>2</sub>	3.7	/3/, most likely structure	loss of imidazole ring	20	136.0757
ET205202	310.0163	16.9/17.5							149.0234
(S)									114.0913
PRZ_M632a	C <sub>21</sub> H <sub>26</sub> Cl <sub>3</sub> N <sub>3</sub> O <sub>11</sub> S	10.8	- (ix)	+ O	-1.3	D for conjugation at the chlorophenyl moiety	aromatic hydroxylation,	40	209.9047
ET202952	632.0281	10.7		+ C <sub>6</sub> H <sub>10</sub> O <sub>5</sub>		/2b/	glucose conjugation,		96.9601
(S)				+ SO <sub>3</sub>			sulfate conjugation		241.0024
PRZ_M554a (H <sub>2</sub> <sup>+</sup> )	C <sub>21</sub> H <sub>26</sub> Cl <sub>3</sub> N <sub>3</sub> O <sub>8</sub>	13.6	+	+ O	0.7-1.3	d for hydroxylation at propyl side chain	hydroxylation at propyl side chain,	40	251.9749
ET203801	554.0858	13.6		+ C <sub>6</sub> H <sub>10</sub> O <sub>5</sub>		/3/ 3 positional isomers	glucose conjugation		69.0499
(S)									323.9959
PRZ_M469	C <sub>15</sub> H <sub>16</sub> Cl <sub>3</sub> N <sub>3</sub> O <sub>6</sub> S	11.2	- (ix)	+ O	0.5	D for sulfate conjugation at the chlorophenyl moiety	aromatic hydroxylation,	15	209.9043
ET202051	469.9753	11.2		+ SO <sub>3</sub>		/2b/	sulfate conjugation		96.9604
(S)									390.0185
PRZ_M477	C <sub>18</sub> H <sub>22</sub> Cl <sub>2</sub> N <sub>4</sub> O <sub>5</sub> S	11.2	+	+ C <sub>3</sub> H <sub>6</sub> NO <sub>2</sub> S		d for no conjugation at the CO-imidazole ring moiety	cysteine product,	10	381.0441
ET203601	477.0761	11.1		+ O		/3/, structural possibilities unclear	hydroxylation,		409.0380
(S)				- Cl			dehalogenation		477.0784
PRZ_M632b	C <sub>21</sub> H <sub>26</sub> Cl <sub>3</sub> N <sub>3</sub> O <sub>11</sub> S	11.4	- (viii)	+ O	-1.3	D for conjugation at the chlorophenyl moiety	aromatic hydroxylation,	40	209.9049
ET203051	632.0281	11.3		+ C <sub>6</sub> H <sub>10</sub> O <sub>5</sub>		/2b/	glucose conjugation,		241.0024
(S)				+ SO <sub>3</sub>			sulfate conjugation		96.9602
PRZ_M554b (H <sub>2</sub> <sup>+</sup> )	C <sub>21</sub> H <sub>26</sub> Cl <sub>3</sub> N <sub>3</sub> O <sub>8</sub>	14.1	+	+ O	0.7-1.3	/3/ 3 positional isomers	most likely hydroxylation at propyl side chain similar to PRZ_M554a,	40	69.0450
ET203901	554.0858	14.1		+ C <sub>6</sub> H <sub>10</sub> O <sub>5</sub>			glucose conjugation		84.0810
(S)									280.0053

Compound	Formula [M]	RT [min] <sup>iii)</sup>	Polarity	Elemental change <sup>iv)</sup>	Log D <sub>ow</sub> <sup>v)</sup>	Identification confidence <sup>vi)</sup>	Description	CE [eV]	MS/MS confirmatory ions <sup>viii)</sup>
MassBank ID of displayed MS/MS spectrum	Exact mass of [M+H] <sup>+</sup> / [M-H] <sup>-</sup>					/level according to Schymanski et al. (2014) <sup>i)</sup> / <sup>vii)</sup>			
<b>PRZ_M515 (H<sub>2</sub><sup>+</sup>)</b>	515.0418	15.1	+	- C <sub>3</sub> H <sub>2</sub> N <sub>2</sub>		/3/	loss of imidazole ring,	20	282.0218
<b>ET204402</b>		15.1		+ C <sub>3</sub> H <sub>6</sub> NO <sub>2</sub> S			cysteine product		86.0967
<b>(N)</b>				+ C <sub>4</sub> H <sub>5</sub> NO <sub>3</sub>			aspartic acid conjugation		

<sup>i)</sup> See Equation 4 in the corresponding publication for the calculation of BAFs at steady state.

<sup>ii)</sup> See Equation 5 in the corresponding publication for the calculation of kinetic BAF<sub>k</sub>s.

<sup>iii)</sup> In case of a retention time range, several possibly positional isomers were integrated as one peak, due to bad peak separation.

<sup>iv)</sup> The elemental change refers to the change in the molecular formula of the biotransformation product in comparison with the parent compound.

<sup>v)</sup> Log D<sub>ow</sub> values were predicted by MarvinSketch version 14.10.20.0 at pH 7.9 and 25 °C. Log D<sub>ow</sub> values correspond to corrected log K<sub>ow</sub> values to account for pH-dependent dissociation. At pH 7.9 azoxystrobin is neutral thus log D<sub>ow</sub> is equal to log K<sub>ow</sub>. If different positional isomers are possible for one BTP, a range of log D<sub>ow</sub> values is given.

<sup>vi)</sup> D: diagnostic fragment/evidence for one structure; d: diagnostic fragment/evidence for positional isomers; l: structure reported in literature; m: MS/MS data from literature; p: biotransformation pathway information; d, p: diagnostic fragment for positional isomers (d) in combination with pathway information (p) give evidence for one possible structure.

<sup>vii)</sup> Levels are defined as follows: 5 (*exact mass*), 4 (*unequivocal molecular formula*), 3 (*tentative candidates: e.g., positional isomers*), 2 (*probable structure: library spectrum match (a) or diagnostic evidence for one structure (b)*) and 1 (*confirmed structure*).

<sup>viii)</sup> Diagnostic fragments (d, D) are listed first and are represented in bold in the table, other characteristic fragments are then presented according to their relative abundance. Only fragments where a chemical formula and structure could be attributed are considered.

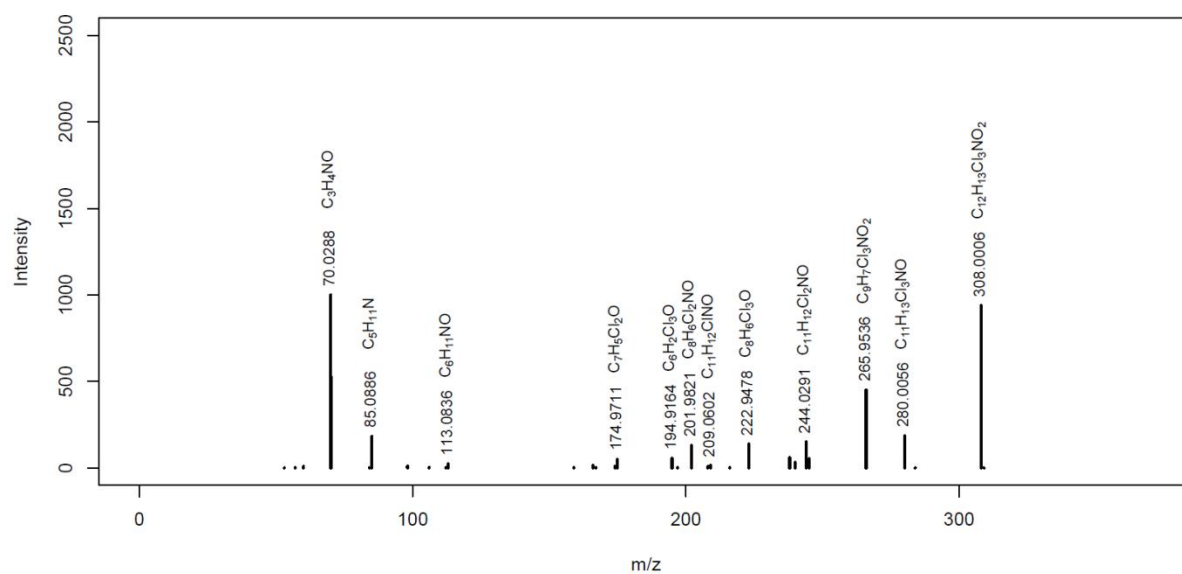
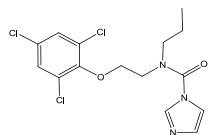
<sup>ix)</sup> The sulfate-containing BTPs are more sensitive in negative ionization mode. However, they were quantified in positive ionization mode because azoxystrobin was detected and quantified in positive ionization mode.



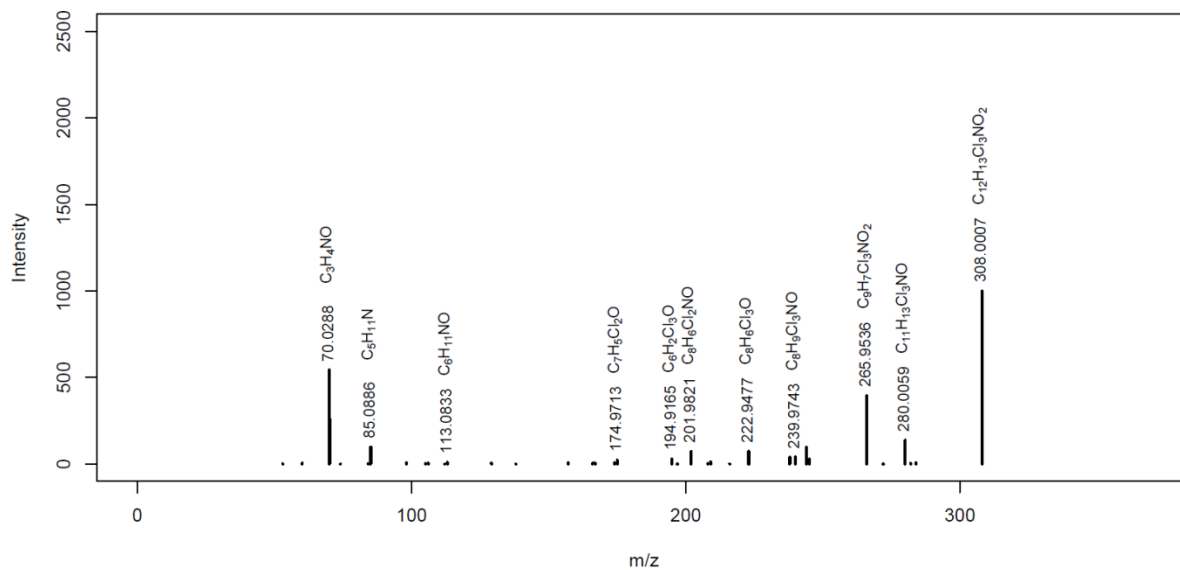
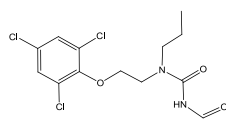
The different MassBank IDs for one compound refer to different collision energies applied during MS/MS fragmentation. The MassBank ID displayed in bold indicates the depicted MS/MS spectrum. Spectra are also available electronically in the MassBank database<sup>8</sup>.

### Prochloraz (PRZ)

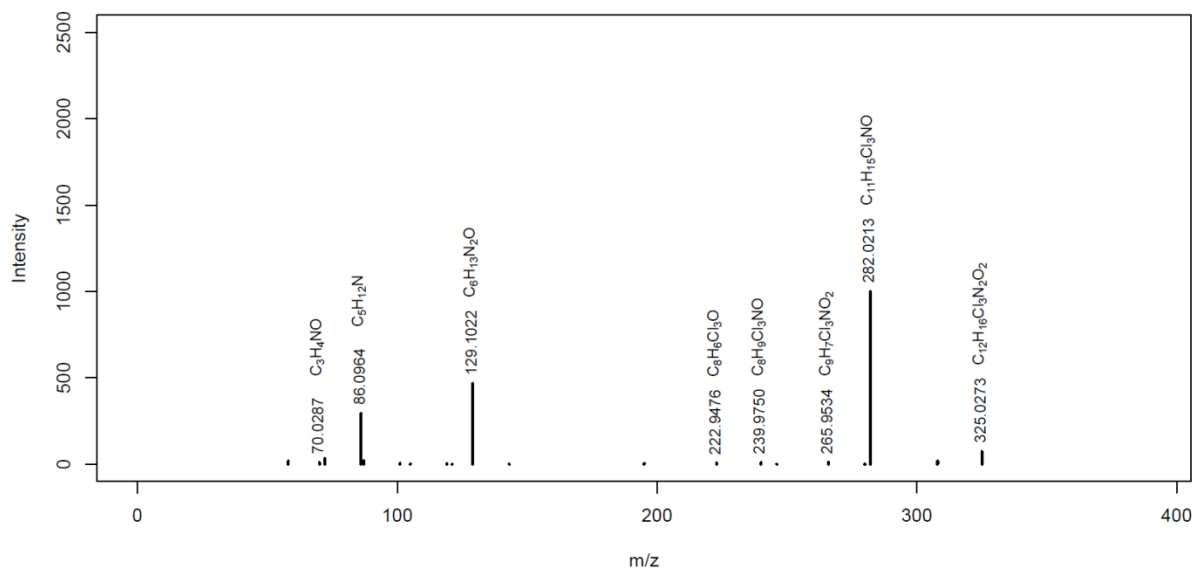
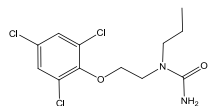
MassBank ID: **ET200001**

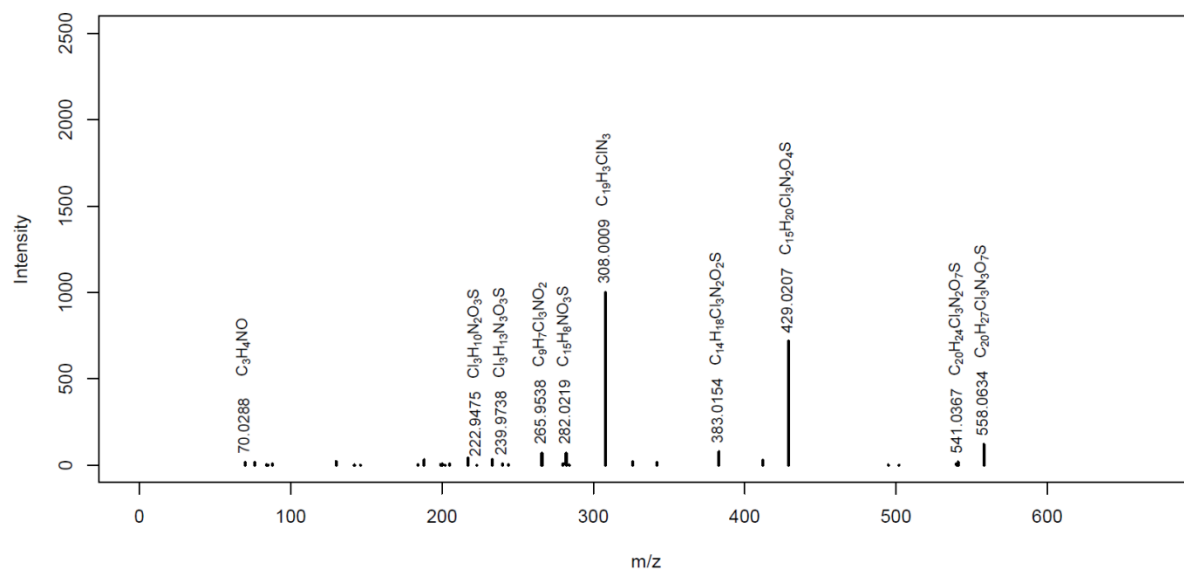
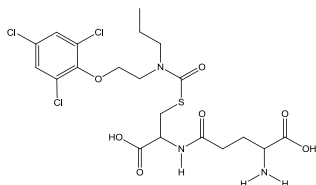
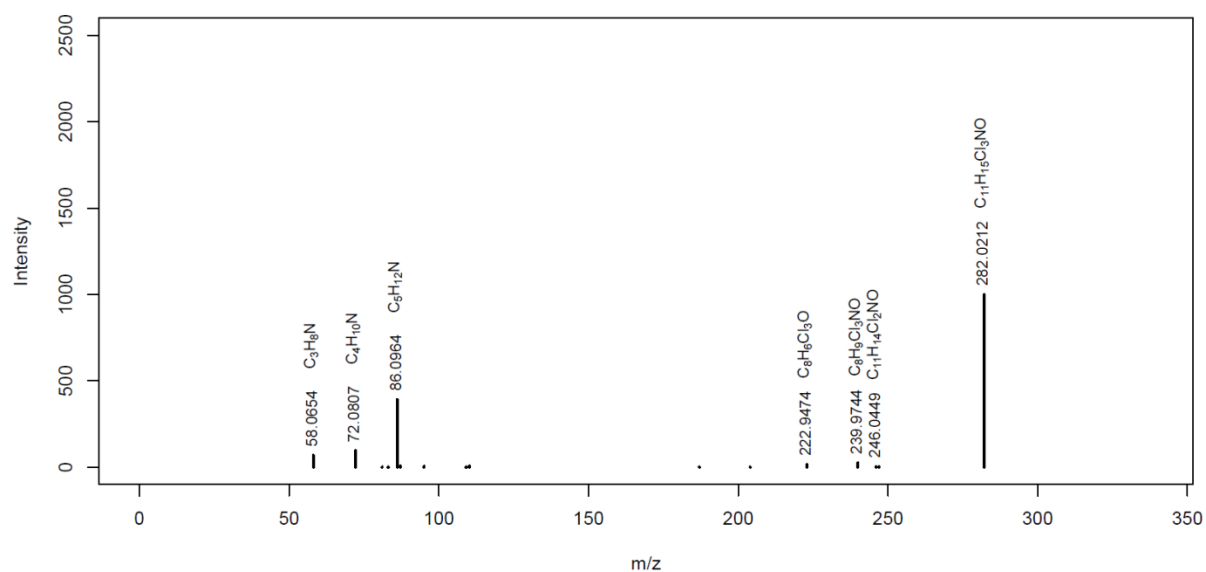
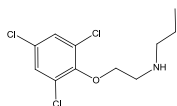


**PRZ\_M353 \***  
MassBank ID: **ET202601**

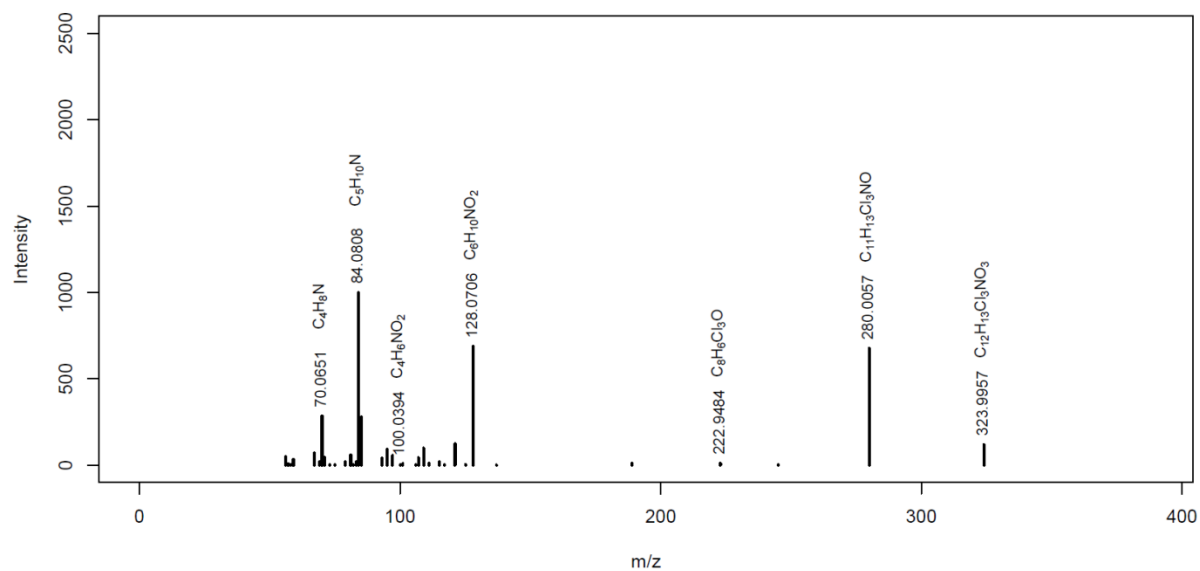
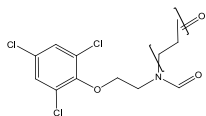


**PRZ\_M325 \***  
MassBank ID: **ET202701**

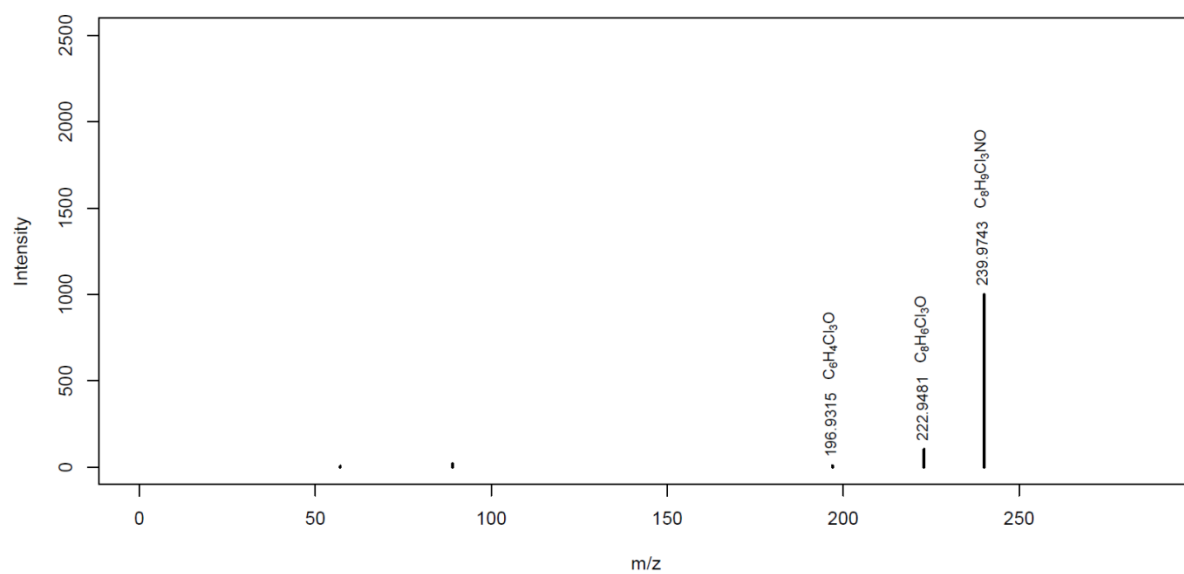
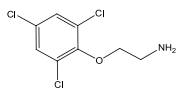


**PRZ\_M558 \***MassBank ID: **ET204901****PRZ\_M282 \***MassBank ID: **ET203201**

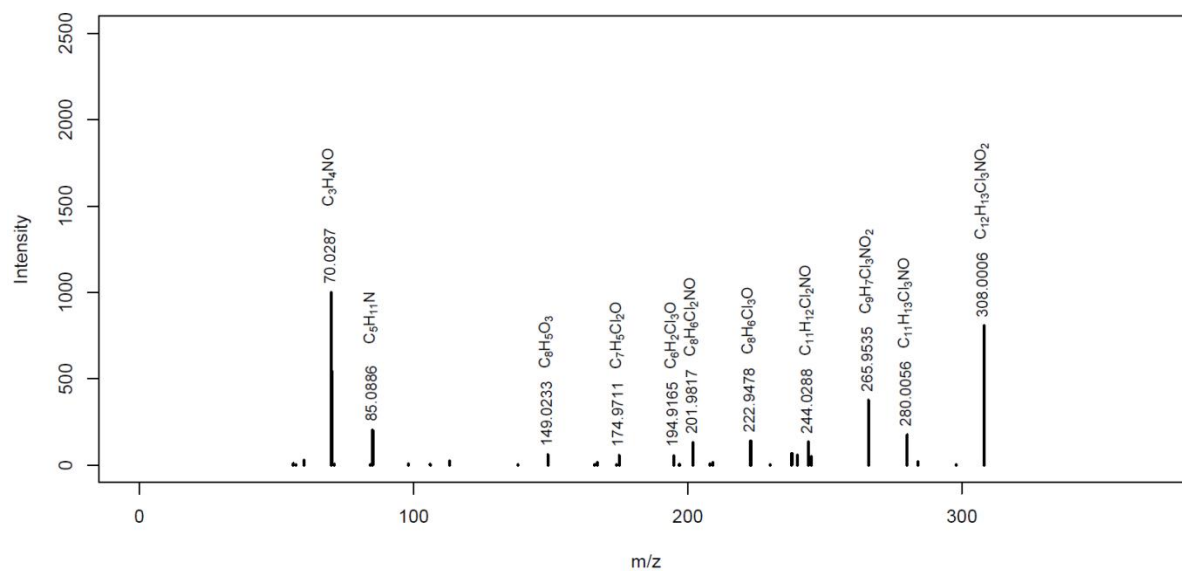
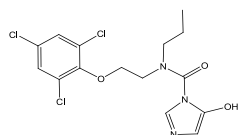
**PRZ\_M323b \***  
MassBank ID: **ET202301**



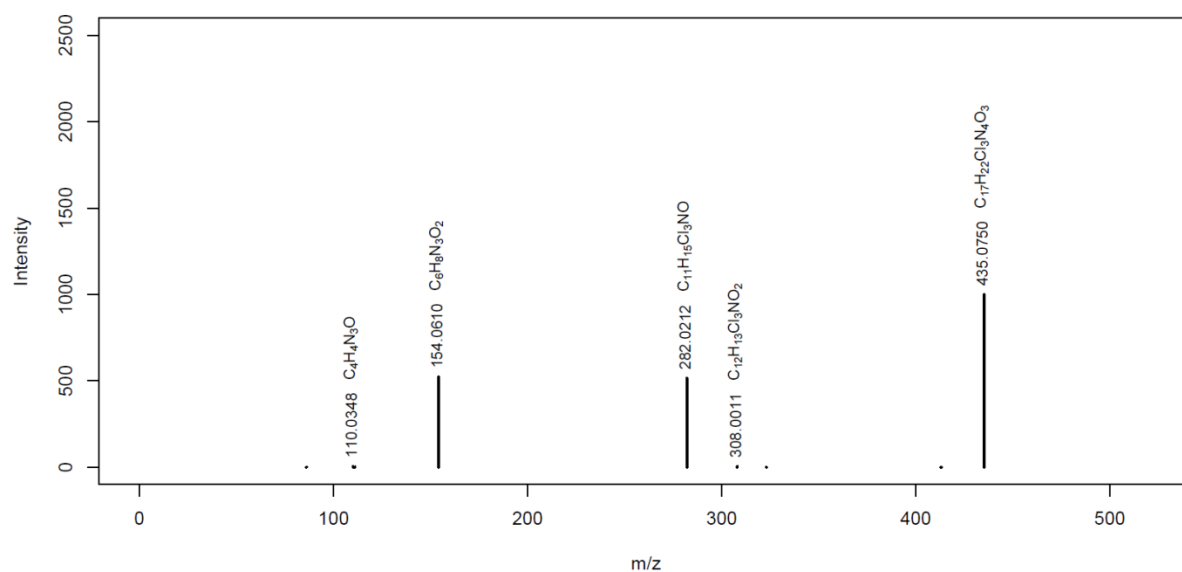
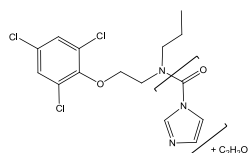
**PRZ\_M239 \***  
MassBank ID: **ET202501**



**PRZ\_M392b \***  
MassBank ID: **ET202201**

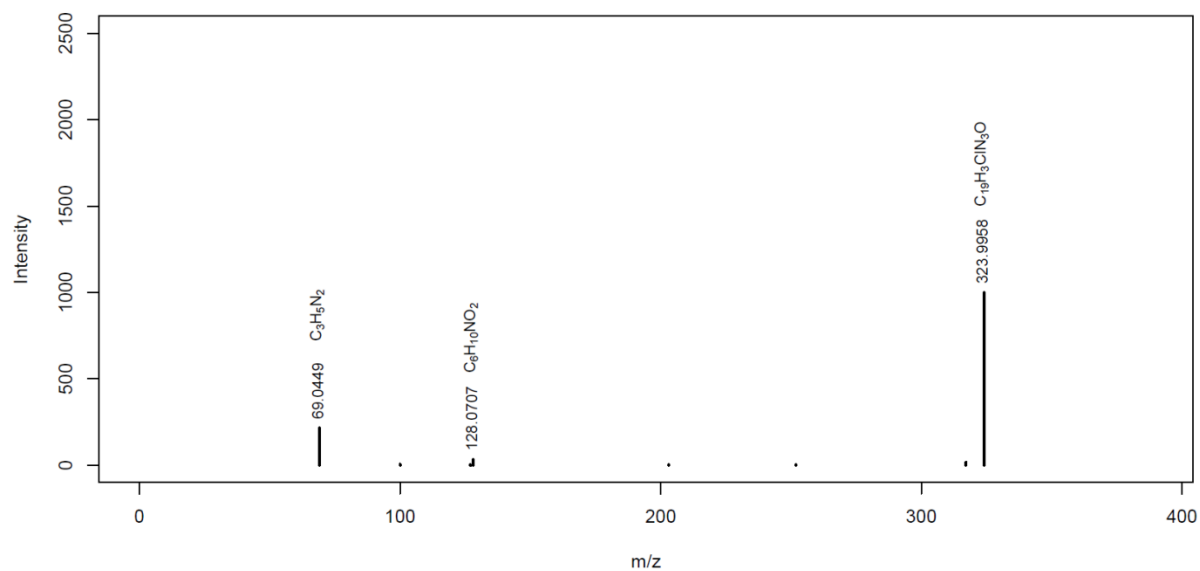
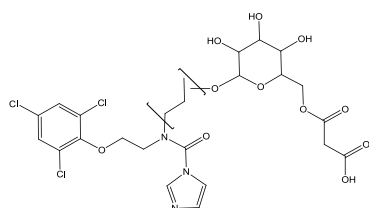


**PRZ\_M435 \***  
MassBank ID: **ET203301**



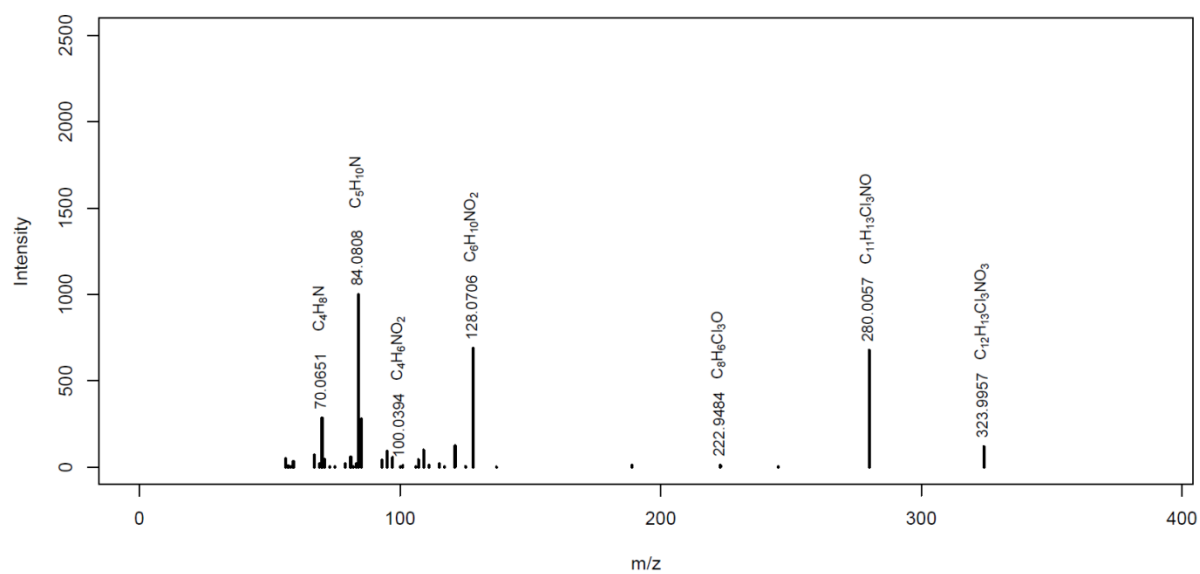
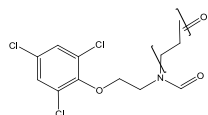
**PRZ\_M640**

MassBank ID: **ET204101**

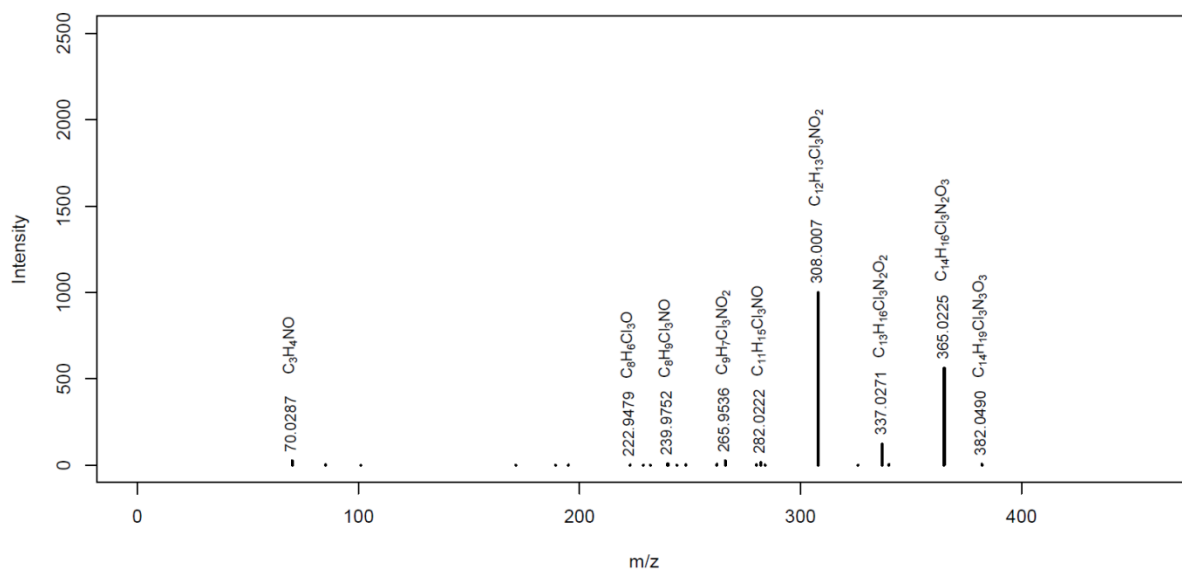
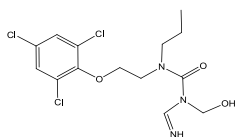


**PRZ\_M323a \***

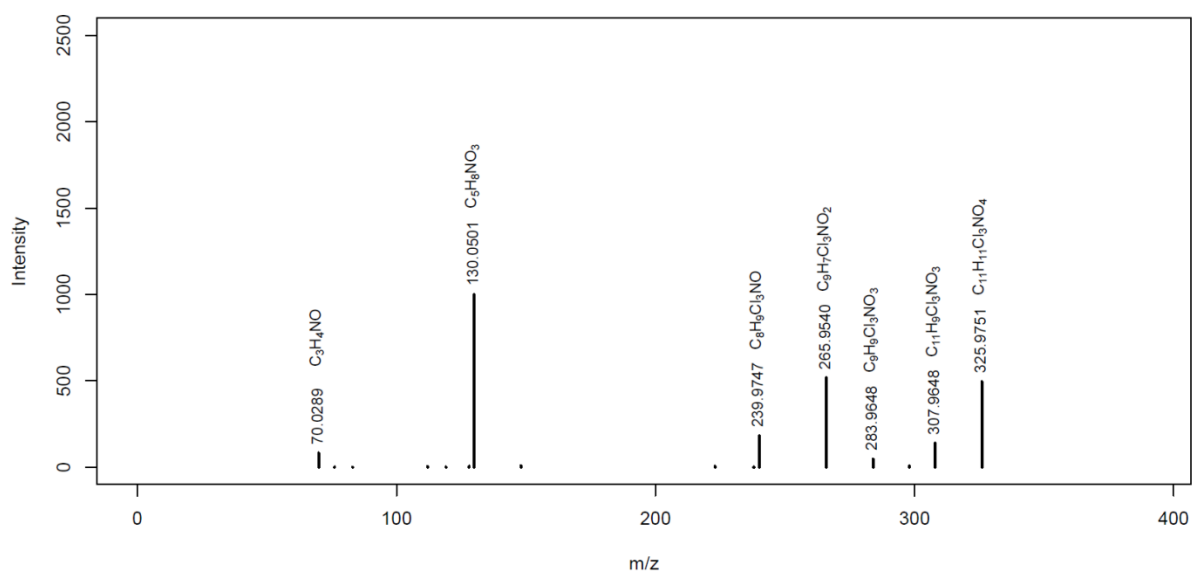
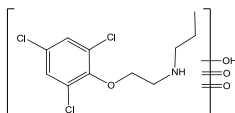
MassBank ID: **ET202401**



**PRZ\_M382 \***  
MassBank ID: **ET203401**

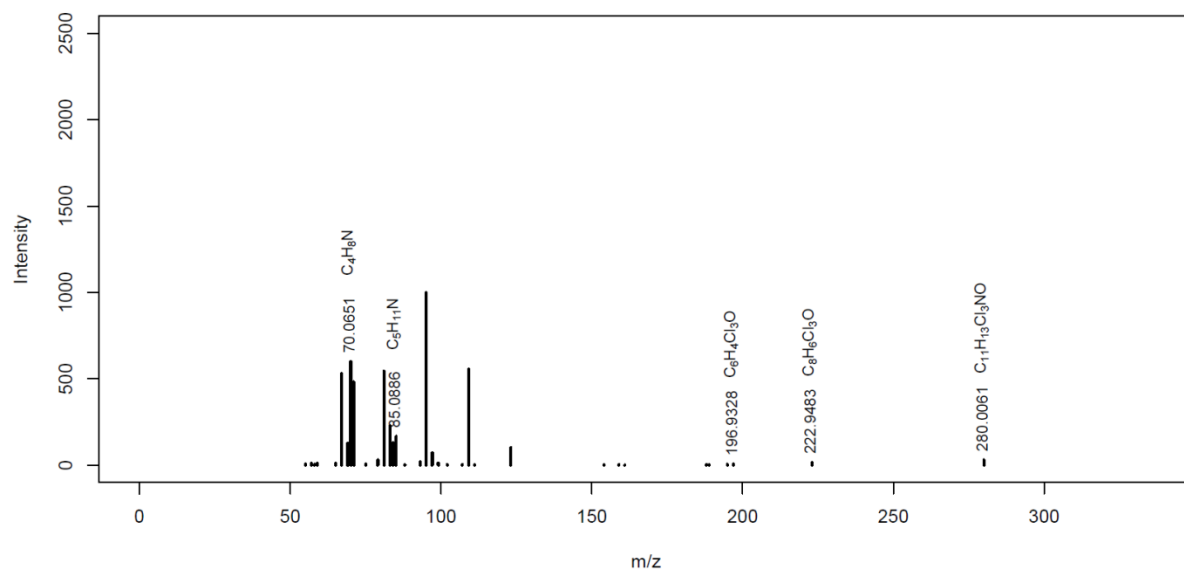
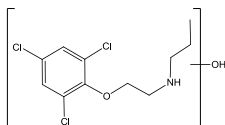


**PRZ\_M326 \***  
MassBank ID: **ET204201**



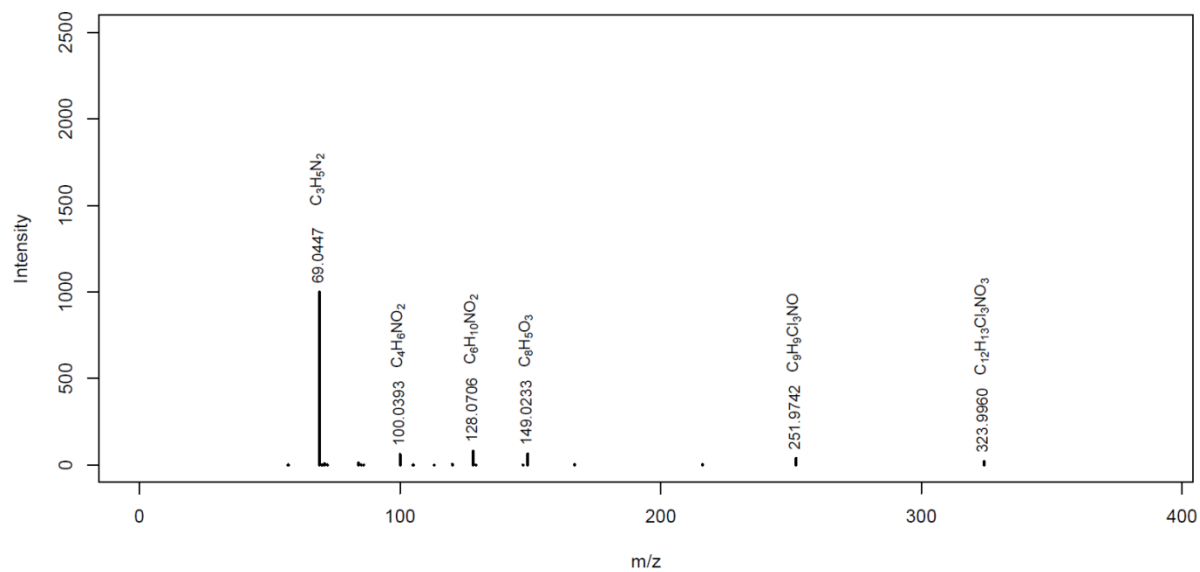
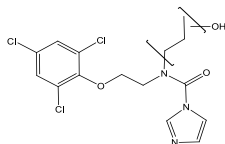
**PRZ\_M298 \***

MassBank ID: **ET202801**



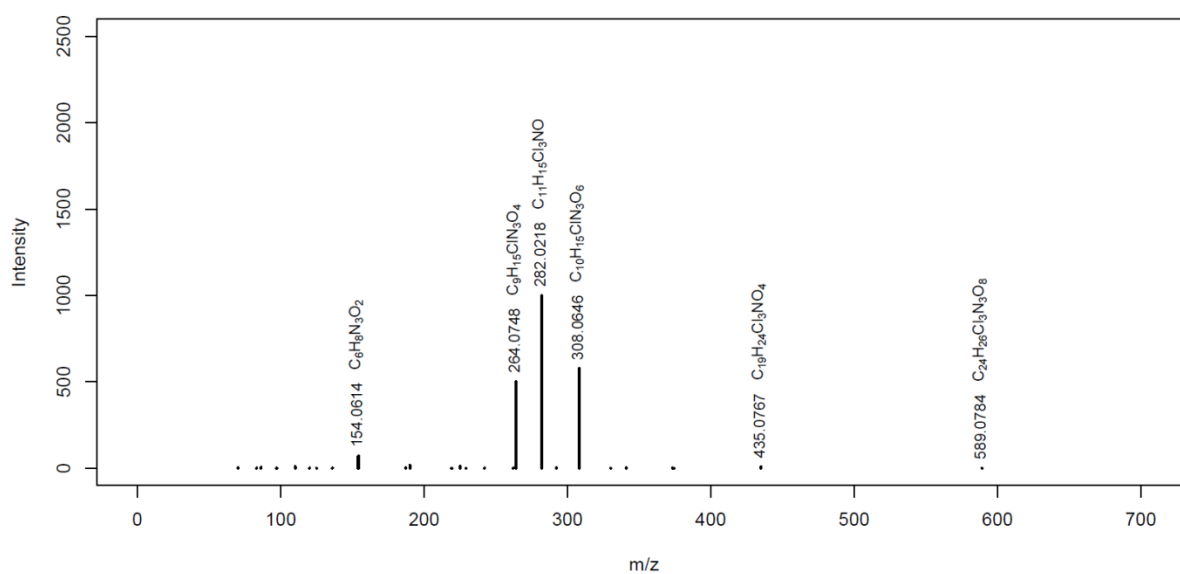
**PRZ\_M392a**

MassBank ID: **ET202101**

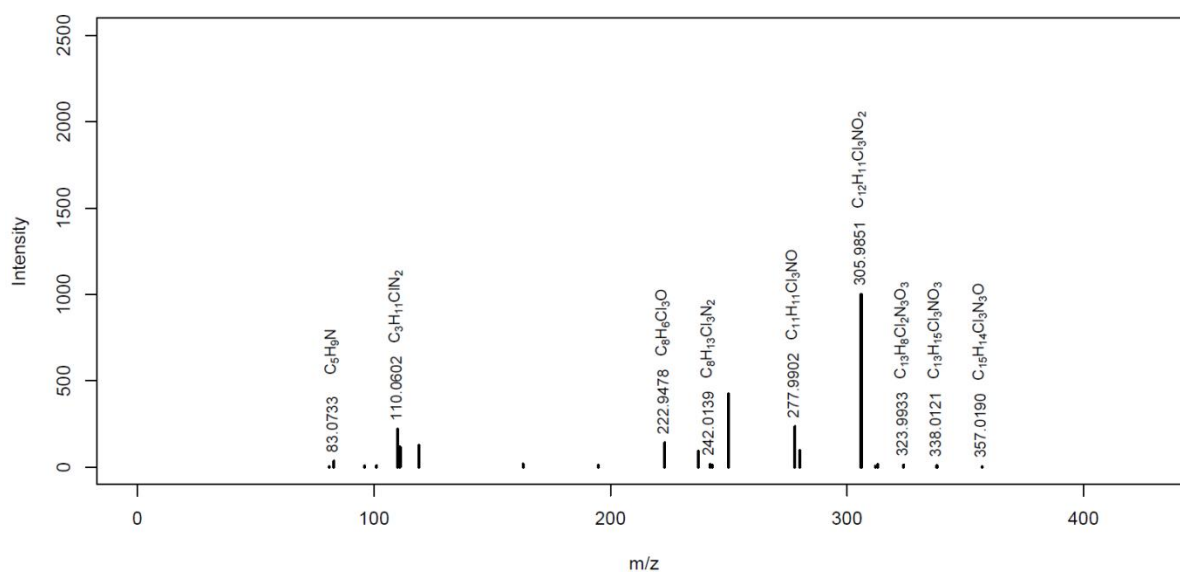
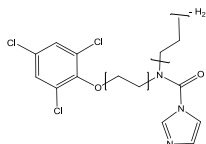


**PRZ\_M589**  
MassBank ID: **ET204001**

*unclear structure*

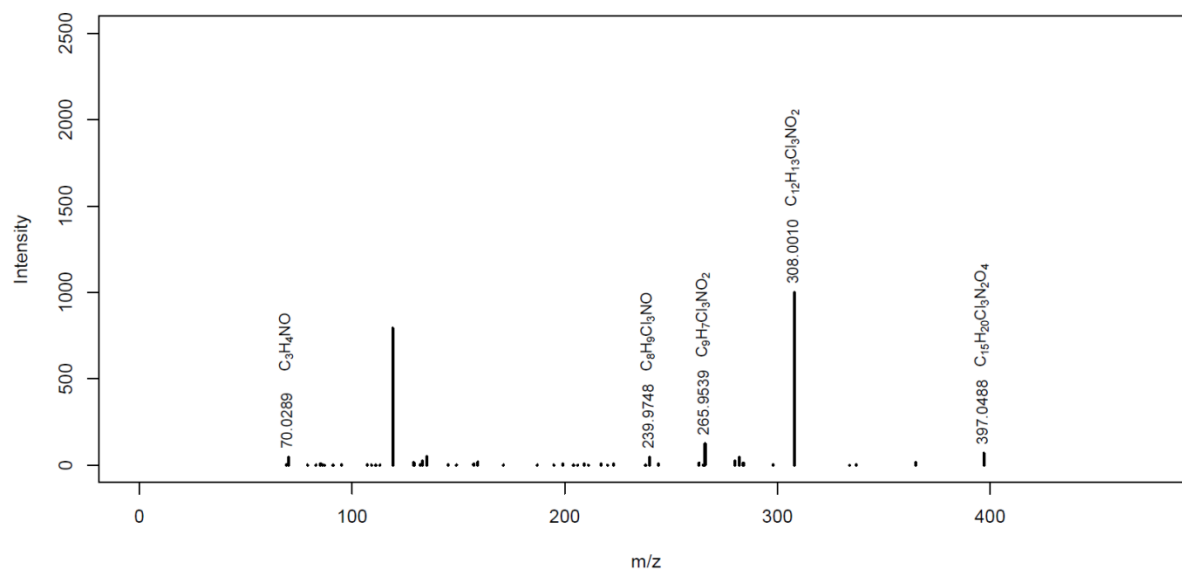
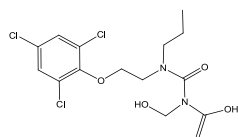


**PRZ\_M374**  
MassBank ID: **ET205001**, ET205002, ET205003, ET205004



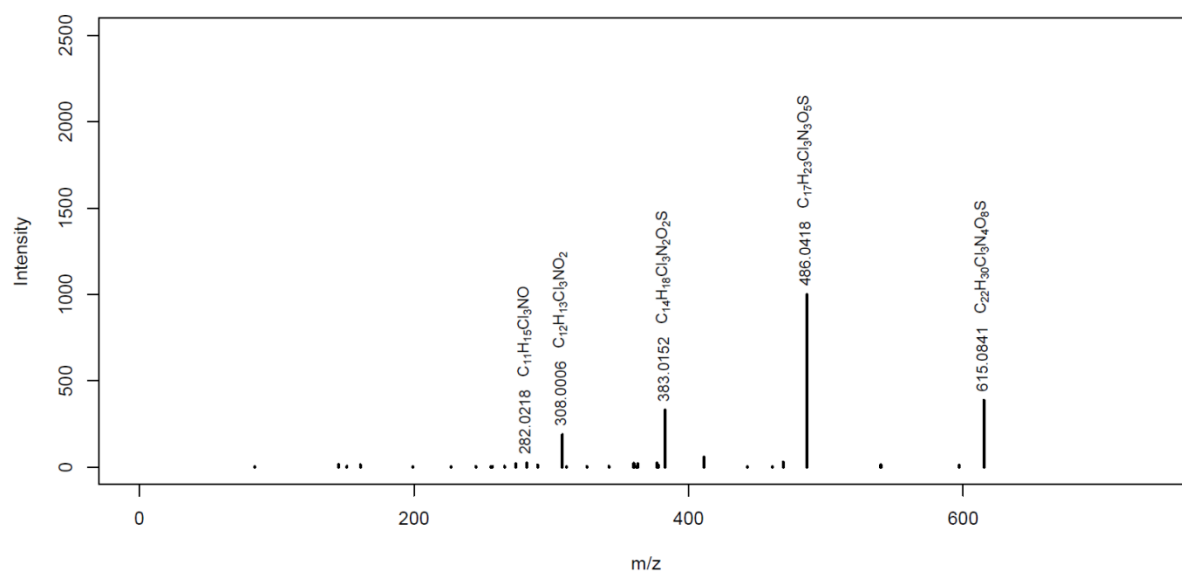
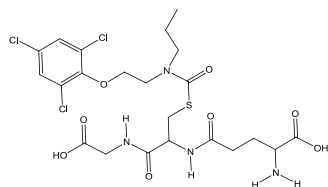
**PRZ\_M397 \***

MassBank ID: **ET204301**

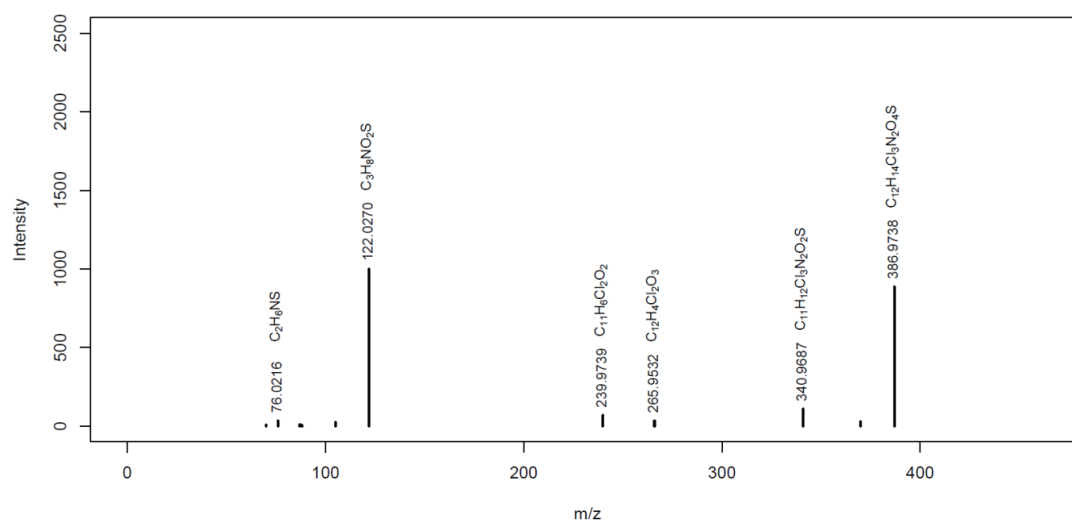
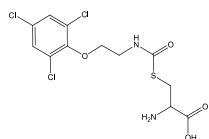


**PRZ\_M615 \***

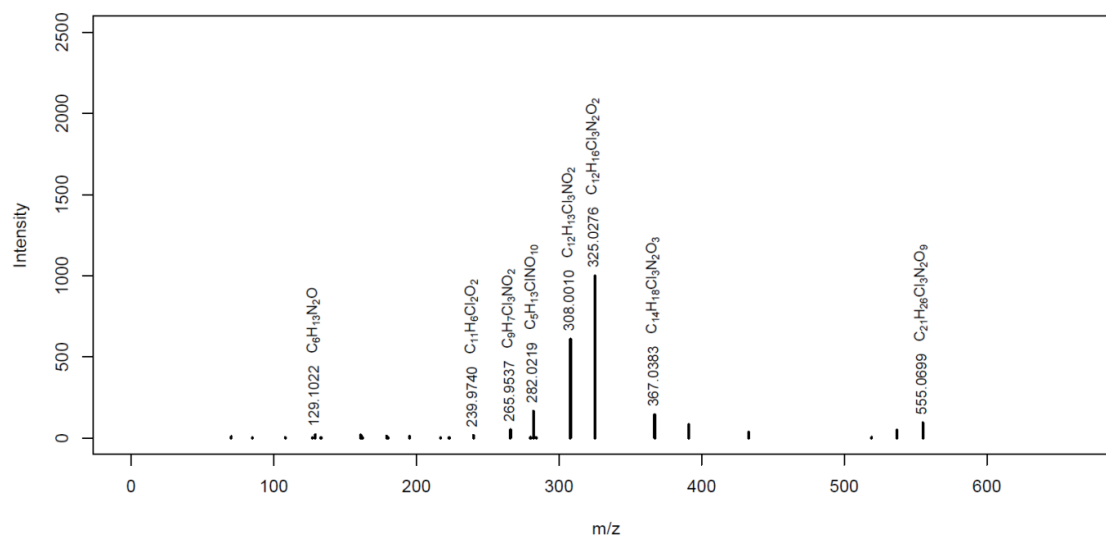
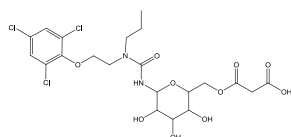
MassBank ID: **ET203701**



**PRZ\_M386 \***  
MassBank ID: **ET201902**

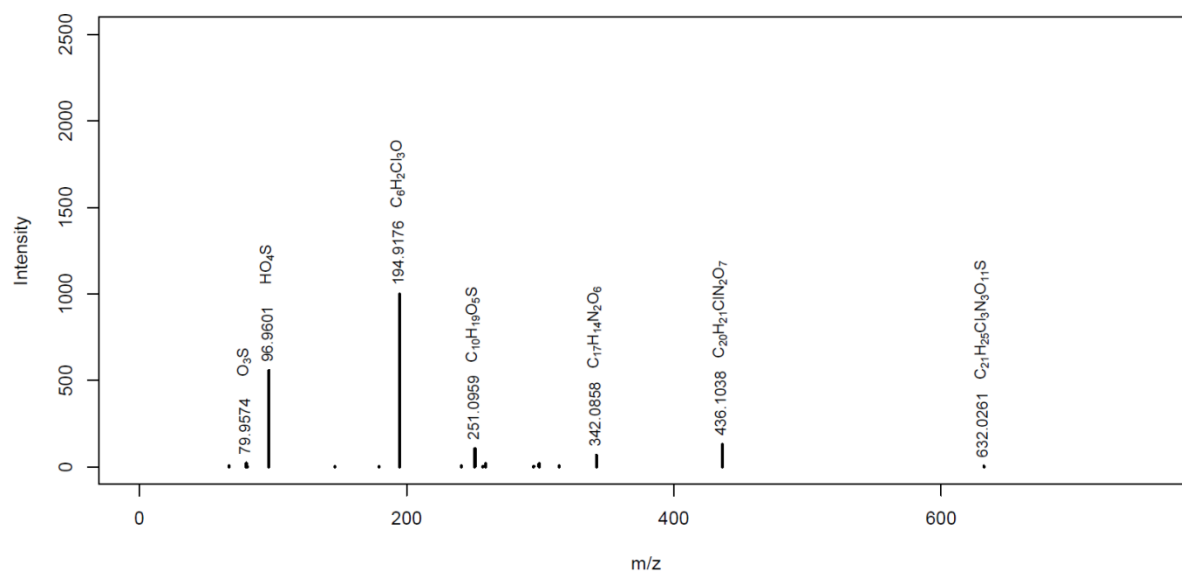


**PRZ\_M573.1 \***  
MassBank ID: **ET204801**



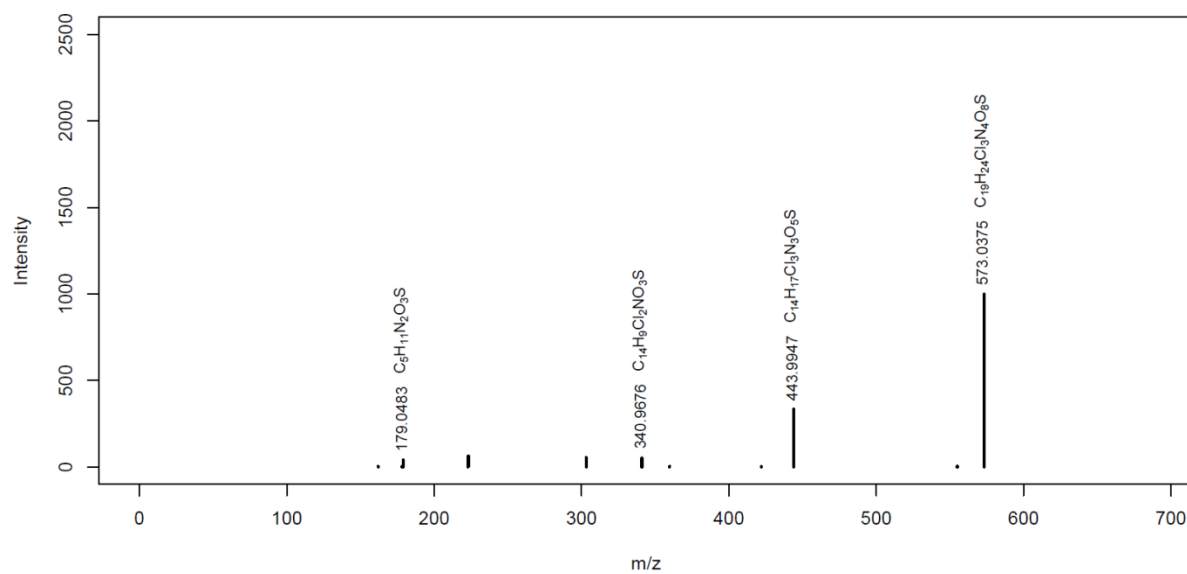
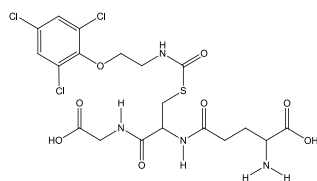
**PRZ\_M632c**

MassBank ID: **ET203152** *unclear structure*

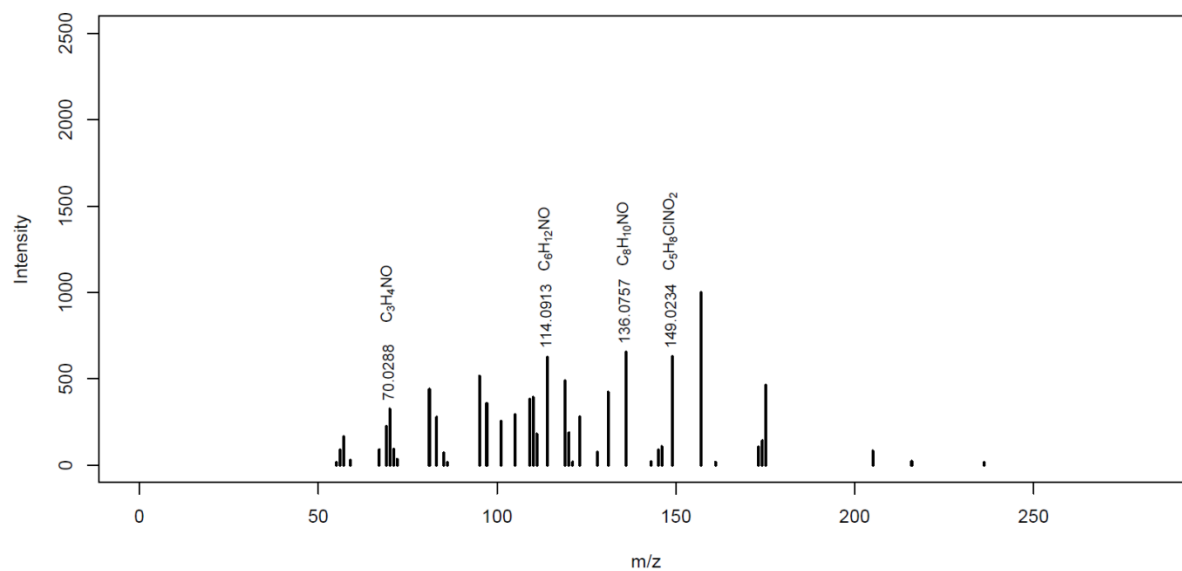
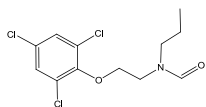


**PRZ\_M573 \***

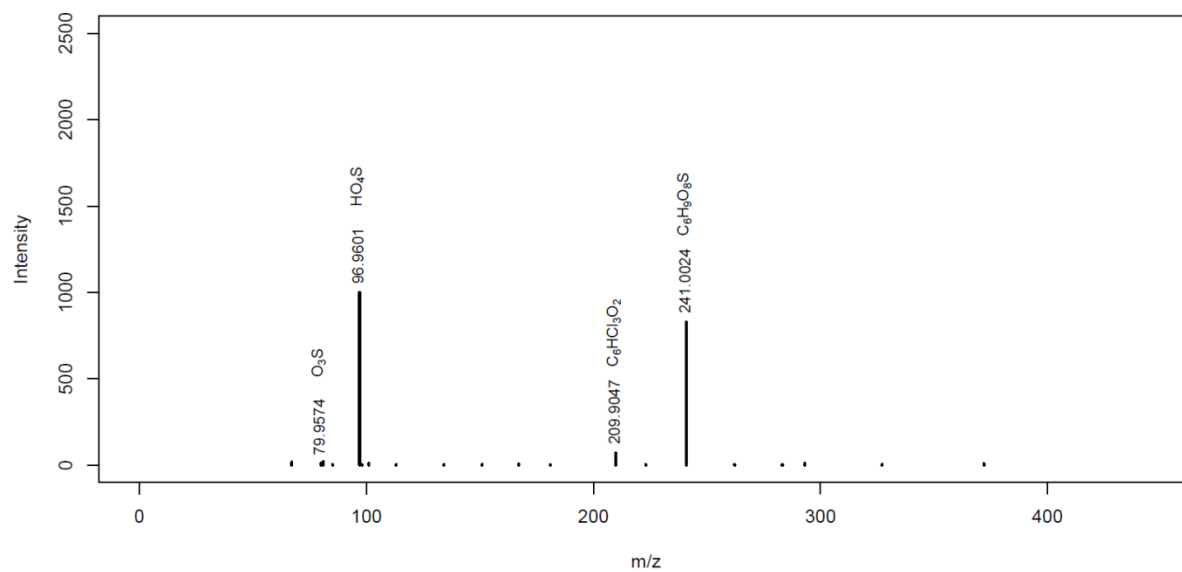
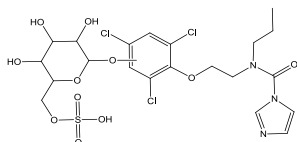
MassBank ID: **ET203502**

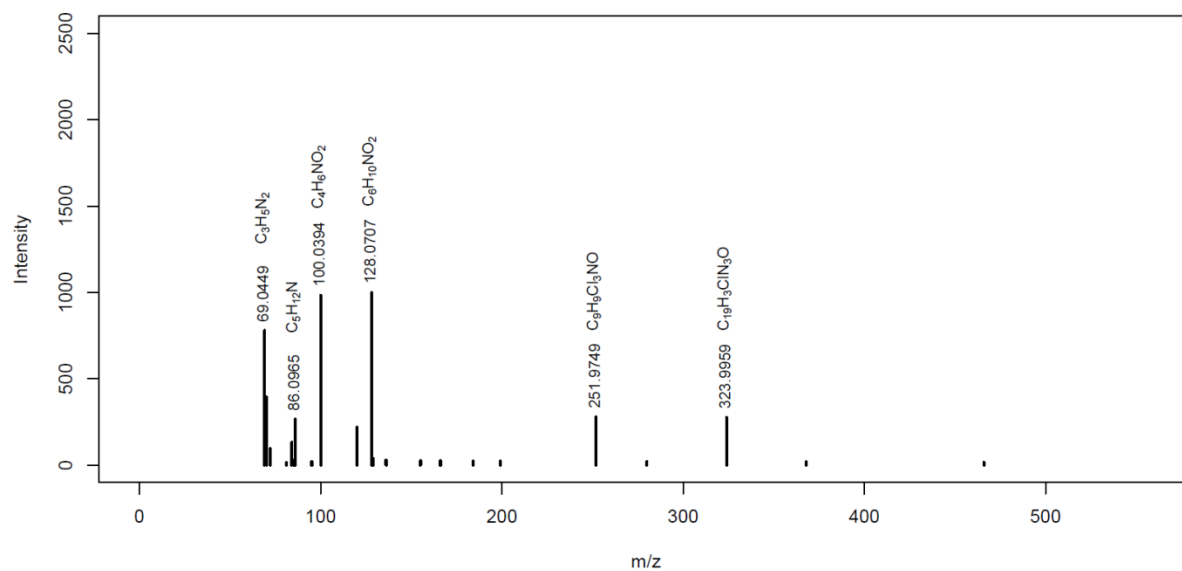
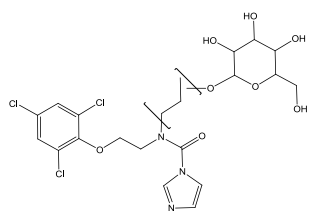
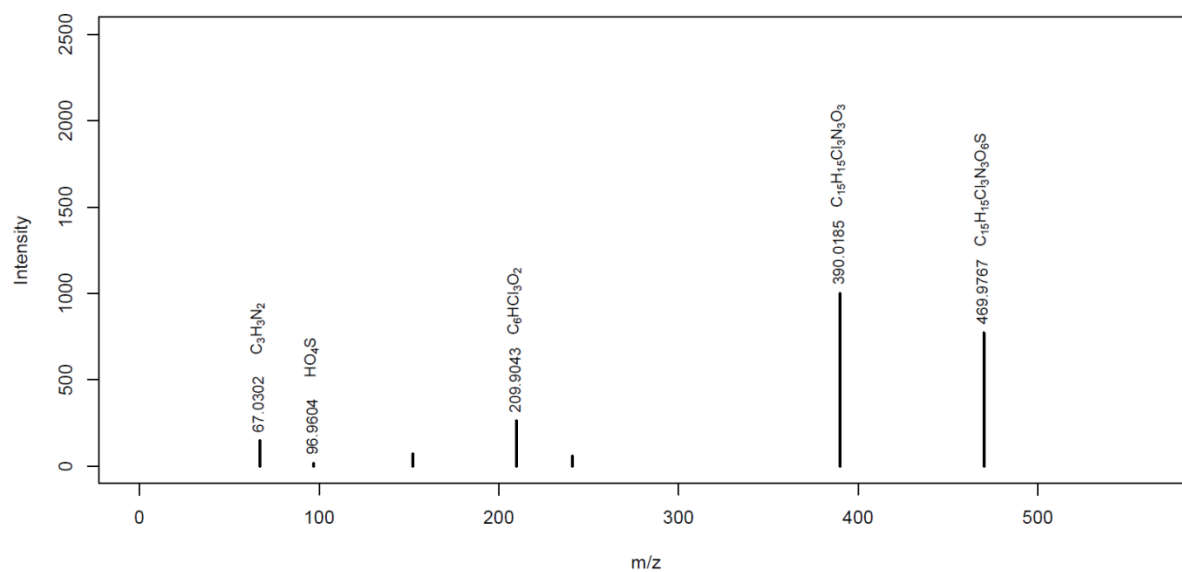
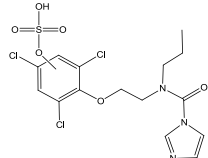


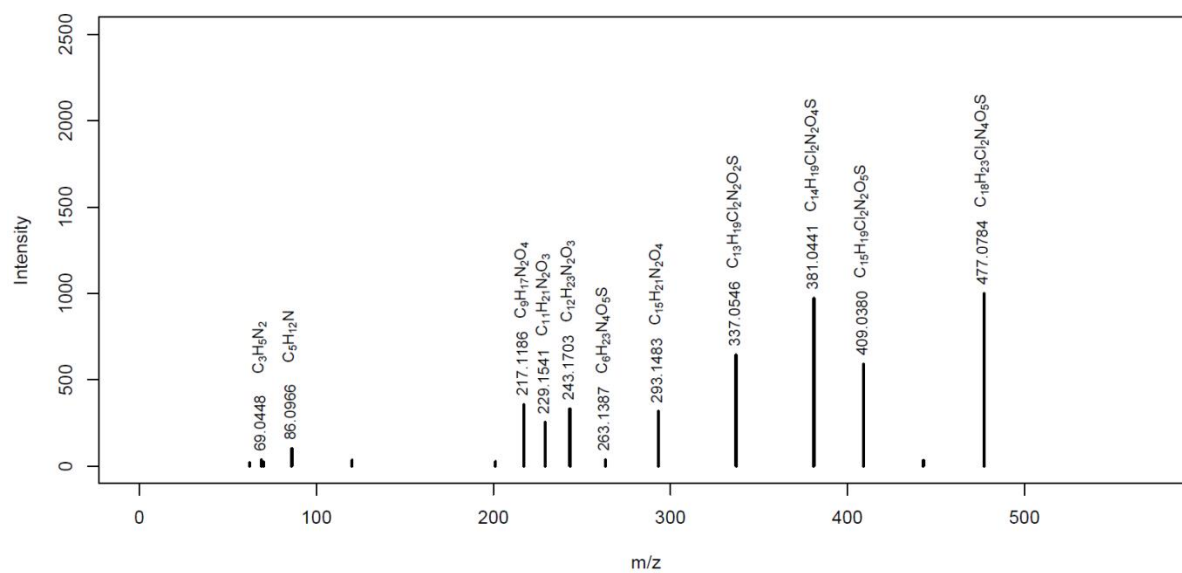
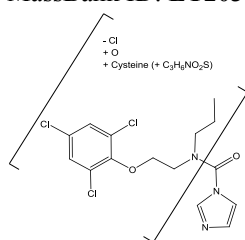
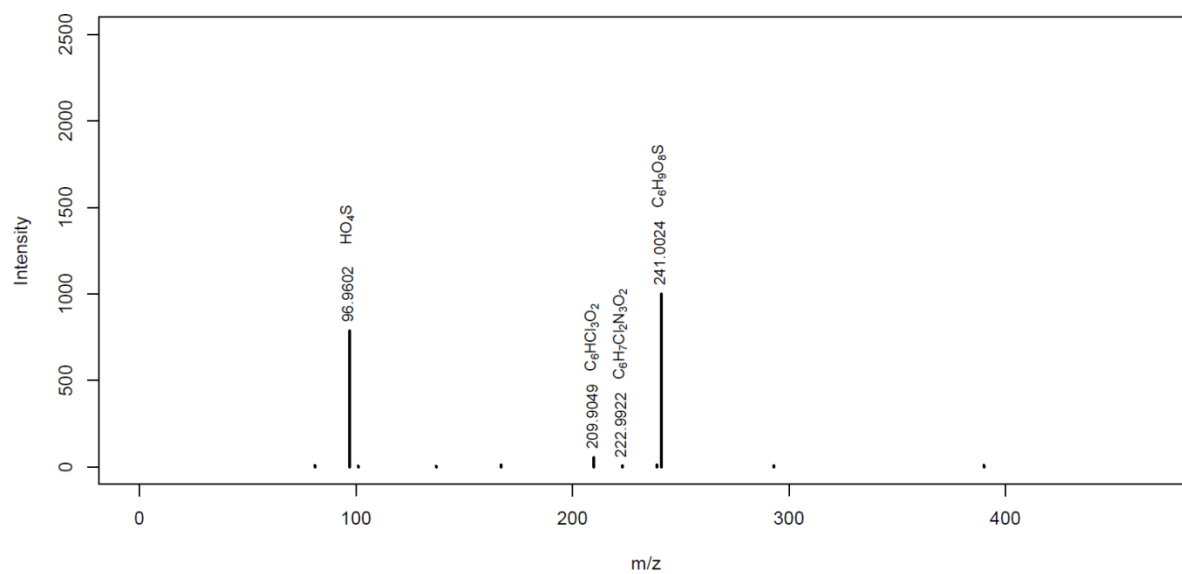
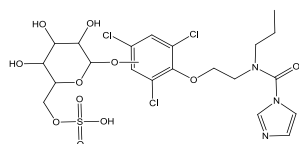
**PRZ\_M310 \***  
MassBank ID: **ET205202**



**PRZ\_M632a**  
MassBank ID: **ET202952**

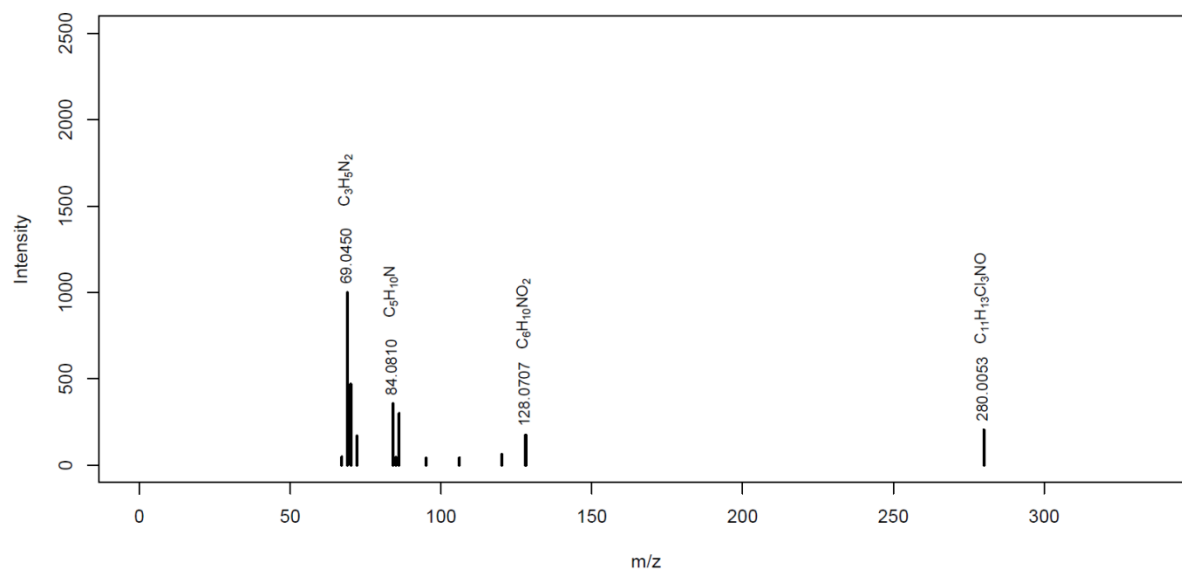
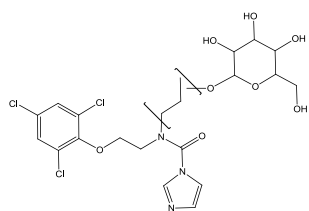


**PRZ\_M554a**MassBank ID: **ET203801****PRZ\_M469**MassBank ID: **ET202051**

**PRZ\_M477**MassBank ID: **ET203601****PRZ\_M632b**MassBank ID: **ET203051**

**PRZ\_M554b**

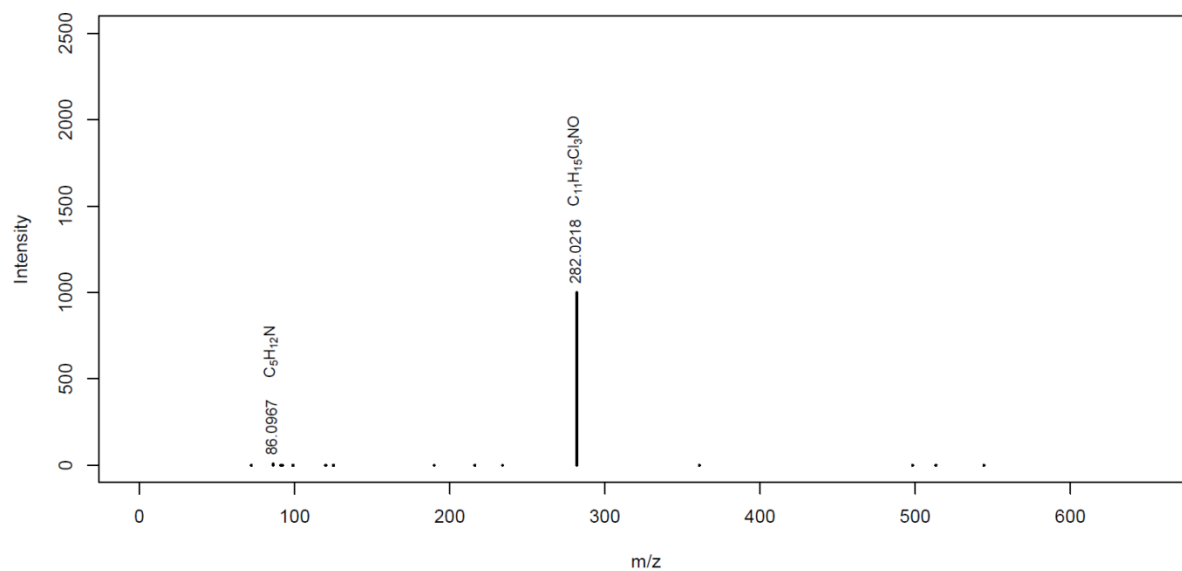
MassBank ID: **ET203901**



**PRZ\_M515**

MassBank ID: **ET204402**

*unclear structure*



## References

- (1) Borgmann, U. Systematic analysis of aqueous ion requirements of *Hyalella azteca*: A standard artificial medium including the essential bromide ion. *Arch. Environ. Contam. Toxicol.* **1996**, *30* (3), 356–363.
- (2) Rösch, A.; Anliker, S.; Hollender, J. How Biotransformation Influences Toxicokinetics of Azole Fungicides in the Aquatic Invertebrate *Gammarus pulex*. *Environ. Sci. Technol.* **2016**, *50* (13), 7175–7188.
- (3) Naylor, C.; Malby, L.; Callow, P. Scope for growth in *Gammarus pulex*, a freshwater detritivore. *Hydrobiologia* **1989**, *188*, 517–523.
- (4) Rösch, A.; Gottardi, M.; Vignet, C.; Cedergreen, N.; Hollender, J. Mechanistic understanding of the synergistic potential of azole fungicides in the aquatic invertebrate *Gammarus pulex*. *Environ. Sci. Technol.* **2017**, *51* (21), 12784–12795.
- (5) Ashauer, R.; Caravatti, I.; Hintermeister, A.; Escher, B. I. Bioaccumulation kinetics of organic xenobiotic pollutants in the freshwater invertebrate *Gammarus pulex* modeled with prediction intervals. *Environ. Toxicol. Chem.* **2010**, *29* (7), 1625–1636.
- (6) Lotufo, G. R.; Landrum, P. F.; Gedeon, M. L.; Tigue, E. A.; Herche, L. R. Comparative toxicity and toxicokinetics of DDT and its major metabolites in freshwater amphipods. *Environ. Toxicol. Chem.* **2000**, *19* (2), 368–379.
- (7) Jager, T.; Øverjordet, I. B.; Nepstad, R.; Hansen, B. H. Dynamic Links between Lipid Storage, Toxicokinetics and Mortality in a Marine Copepod Exposed to Dimethylnaphthalene. *Environ. Sci. Technol.* **2017**, *51* (13), 7707–7713.
- (8) R Core Team. A language and environment for statistical computing, R Foundation for Statistical Computing, 2016.
- (9) Ritz, C.; Streibig, J. C.; Ritz, C. & Streibig, J. C. Bioassay Analysis using R. *J. Stat. Softw.* **2005**, *12* (5), 1–22.
- (10) European Mass Bank Server (NORMAN MassBank) [www.massbank.eu](http://www.massbank.eu).
- (11) Schymanski, E. L.; Jeon, J.; Gulde, R.; Fenner, K.; Ruff, M.; Singer, H. P.; Hollender, J. Identifying small molecules via high resolution mass spectrometry: communicating confidence. *Environ. Sci. Technol.* **2014**, *48*, 2097–2098.
- (12) Debrauwer, L.; Rathahao, E.; Boudry, G.; Baradat, M.; Cravedi, J. P. Identification of the major metabolites of prochloraz in rainbow trout by liquid chromatography and tandem mass spectrometry. *J. Agric. Food Chem.* **2001**, *49* (8), 3821–3826.
- (13) Needham, D.; Challis, I. R. The metabolism and excretion of prochloraz, an imidazole-based fungicide, in the rat. *Xenobiotica* **1991**, *21* (11), 1473–1482.
- (14) Roberts, T. R.; Hutson, D. H.; Lee, P. W.; Nicholls, P. H.; Plimmer, J. R. *Metabolic Pathways of Agrochemicals: Part 2: Insecticides and Fungicides*; Royal Society of Chemistry, 2007.
- (15) Laignelet, L.; Rivière, J. L.; Lhuguenot, J. C. Metabolism of an imidazole fungicide (prochloraz) in the rat after oral administration. *Food Chem. Toxicol.* **1992**, *30* (7), 575–583.